Hydrologic Modeling to Estimate Peak Streamflow for Post-Fire Forest Management

A Thesis
Presented in Partial Fulfillment of the Requirements for the
Degree of Master of Science
with a
Major in Water Resources
in the
College of Graduate Studies
University of Idaho
by
Matthew L. Lesiecki

Approved by:
Major Professor: Erin Brooks, Ph.D.
Committee Members: Peter R. Robichaud, Ph.D.; Elowyn Yeager, Ph.D.
Department Administrator: Timothy Link, Ph.D.

August 2023

Abstract

In forested ecosystems, wildfires often effect changes in a watershed's hydrologic response to precipitation. Elevated runoff causes stream discharge to spike during high intensity, short duration rainfall and snowmelt events. This discharge can damage or destroy road infrastructure such as culverts, and make roads impassable, resulting in expensive repairs. Forest managers use hydrologic models to identify areas of highest risk to this damage and prescribe treatments to mitigate the risk. We measured peak flow at 12 road crossings following five large wildfires in 2017 in Western Montana and used the data to assess the peak flow estimates of four commonly used hydrologic models: Runoff Curve Number, USGS Regression Equations, WEPPcloud-PEP (Post-fire Erosion Prediction), WEPPcloud-Disturbed. Our data showed that annual peak flow in this region occurs primarily during the spring runoff, though small, isolated rainfall events are capable of producing large spikes in streamflow volume. The Runoff Curve Number method tended to greatly over-estimate peak flows generated by rainfall events we observed and is unable to model runoff events caused by snowmelt. USGS Regression equations underpredicted the changes to post-fire hydrology. When detailed soil information was used, WEPPcloud-Disturbed was able to reasonably predict runoff for both rainfall and snowmelt events which is critical in snowmelt dominated watersheds.

Acknowledgments

I would like to acknowledge the USDA Forest Service Burned Area Emergency Response (BAER), program who provided funding via the Lolo National Forest and Rocky Mountain Research Station. This project would not have been possible without field and administrative support from Vince Archer, Traci Sylte, Dave Callery, and Dustin Walters of Region 1 and the Lolo National Forest. Dr. Pete Robichaud, Bob Brown, Sarah Lewis, and countless others from the USFS Rocky Mountain Research Station in Moscow, ID. They were my mentors, inspiration, and guiding light throughout this project. It is impossible to describe how important they were in my development both personally and professionally over the years. Finally, my academic advisor Erin Brooks kept me going throughout this process with constant encouragement and guidance. I learned more from him than I could have ever imagined. He taught me to think in new and unique ways about my research, and his “tips and tricks” when it comes to data management and analysis are truly unmatched. I cannot thank you enough. I learned more from each and every one of you than you will ever know.

Dedication

I would like to dedicate this thesis to my friends, who never failed to ask if I was finished with it yet; to my family, who always knew I would finish it eventually; and to Mary, who held my hand and helped me drag it over the finish line. You all care for me deeply and I feel it every day. I love all of you.

Table of Contents

List of Tables

List of Figures

Introduction

Wildfire and burned landscapes have become an increasingly common throughout forests in the American West (Westerling *et al.*, 2006; Dennison *et al.*, 2014; Parks and Abatzoglou, 2020). Though many ecosystems depend on wildfire for maintaining ecosystem health (Hardesty *et al.*, 2005; Myers, 2006; Collins and Roller, 2013), dramatic shifts in the function of soil, water, and habitat resources can create challenging management decisions for both private and public land managers. Along with ecosystem health, wildfire impacts man-made systems such as road networks, trail systems, and building infrastructure through increased soil erosion, surface runoff, and flooding. After a wildfire occurs, land managers rely heavily on hydrologic models to predict how a watersheds hydrology may change in response to wildfire, and they use the results to prescribe a variety of treatments that can mitigate fire effects. Therefore, it is critical to understand how wildfire effects the physical properties of a watershed, what treatment options are available, and how various hydrologic models can be used to manage a burned landscape.

Part 1 of this thesis uses observed data to assess three different methods of modeling post-fire hydrology, with specific emphasis on peak flow discharges generated by spring snowmelt or summer rainfall events. While all three models are commonly used by forest managers to assess changes in watershed hydrology, this research aims to provide guidance on which techniques will provide the most accurate and reliable results in complex post-fire environments.

Part 2 discusses the impact that wildfire has on in-stream aquatic habitats for fish species such as trout and char. It argues that the ability for fish populations to recover from wildfire depends heavily on both pre-fire and post-fire land management practices, and that some simple strategies can be used proactively to greatly increase the likelihood of fish survival recovery.

1 Post-Fire Hydrologic Modeling

1.1 Soil Properties and Watershed Function

Changes in watershed hydrology can result in some of the most dramatic and potentially dangerous post-fire management concerns. In unburned forests, structures such as tree canopy and a thick duff layer intercept large portions of rainfall and surface runoff (Moody and Martin, 2001; Neary *et al.*, 2005). Wildfire consumes much of this cover causing increased surface runoff and soil erosion which, especially during intense rainfall events, can result in increased peak streamflow, flooding, and can even trigger debris flows. These are exacerbated by soil sealing and fire-induced water repellency which further reduce soil infiltration, increasing surface runoff (DeBano, 1981; Neary *et al.*, 2003; Wagenbrenner *et al.*, 2015).

Water repellency results from the volatilization of organic compounds which are translocated downwards into the soil profile by the heat pulse, then condense on soil particles to form a hydrophobic layer that can inhibit movement of water into the soil (DeBano *et al.*, 1967; Doerr *et al.*, 2009). Even in areas where the soils are naturally water repellent, such as the ash-cap soils found in Western Montana (Kawamoto *et al.*, 2007), fire can alter or enhance the repellent characteristics of this layer (Doerr *et al.*, 2006; Robichaud *et al.*, 2016). Though water repellency is difficult to quantify (Robichaud *et al.*, 2008) and is often not homogeneous throughout a burned watershed (Lewis *et al.*, 2008), it can be a significant factor in elevated runoff and soil erosion (Robichaud, 2000; Cerda and Robichaud, 2009) and may persist anywhere from days/weeks to several months after the fire (Larsen *et al.*, 2009).

1.2 Culverts and Forest Roads

Fire induced changes to watershed hydrology generally lead to higher annual water yield as well as increased peak streamflow during rainfall and runoff events (Saxe et al., 2016; Hallema et al., 2017; Rust et al., 2019; Niemeyer et al., 2020). The magnitude of peak streamflow events can often be several orders of magnitude greater compared to pre-fire conditions (Anderson, 1976; Neary *et al.*, 2010), with the greatest effect occurring in small watersheds (Gartner *et al.*, 2004; Neary *et al.*, 2005). Because of this, infrastructure such as

bridges and culverts commonly used in forest road networks are often undersized and have the potential to fail during large peak flow events (Foltz *et al.*, 2009).

During a post-fire peak flow event, streamflow combines with sediment and debris moving in a stream channel. Culverts need to be large enough to pass not only the clean-water discharge (i.e. “flood-flow”), but the sediment and woody debris that is mobilized during a runoff event as well. The effect of sediment and debris moving in the stream channel is referred to as a “bulking factor”, the idea being that discharge is increased by some amount relative to the volume of sediment and debris present in the stream (Gusman *et al.*, 2009; Kean *et al.*, 2016). Bulked streamflow may cause a culvert to fail by simply exceed the culvert capacity and begin to flow over the road surface, but more often woody debris and sediment will completely plug the culvert and cause the entirety of the streamflow to be redirected onto and over the road surface (Figure 1). Following wildfires in Oregon, Washington, and Northern California, Furniss et al. (1998) found that only 6 percent of culvert failures were a result of simply exceeding hydraulic capacity. The majority of failures occurred due to the culvert becoming plugged by large amounts of sediment and woody debris moving in the stream and resulted in more substantial and destructive failures. Bulked peak flow during the largest events have been estimated to be up to 50 times greater than the peak flow during normal flooding (VanDine, 1985; Kean *et al.*, 2016), while other attempts to quantify sediment bulking resulted in a bulking factor of just 2-3 times the stream discharge for debris-laden flows (Gusman *et al.*, 2009).

At some point, bulked streamflow transitions from otherwise “normal” streamflow laden with debris to what would be considered debris flow (Slaymaker, 1988; Iverson, 1997; Parise and Cannon, 2012). Debris flows are one of the most hazardous consequences of wildfire both for infrastructure and property, as well as for public safety (Parrett, 1987; Cannon, 2001; Parrett *et al.*, 2004). Though considerable advances have been made in both their modeling and prediction (Cannon *et al.*, 2010; Staley *et al.*, 2016; Kean and Staley, 2021), debris flows remain challenging to predict due to limitations of weather forecasting as well as our still incomplete understanding of the hydrologic controls on debris flow initiation, and how those controls change over time (Parise and Cannon, 2012; Staley *et al.*, 2015, 2018; Rengers *et al.*, 2016; McGuire *et al.*, 2017).

Figure 1: Debris flow at Spruce Creek following the 2017 Rice Ridge fire on the Lolo National Forest in Montana. Notice the large amount of woody debris on the upstream side of the road which blocked the culvert and redirected the flow onto the road surface.

Debris laden flows are the most common cause of culvert/road failure following wildfire (Best *et al.*, 1995; Furniss *et al.*, 1998), and because road treatments account for over 20 percent of the total expenditures for post-fire mitigation treatment (Robichaud *et al.*, 2014), considering the risk of such events is crucial in burned watersheds.

1.3 Post-Fire Assessment

As the scale of wildfire grows, so does the cost of mitigating post-fire damage (Robichaud *et al.*, 2014). In the wake of any large (>500 acres [200 ha]) wildfire, post-fire assessment teams such as Burned Area Emergency Response (BAER) teams are deployed assess watersheds affected by the fire. The goal of these teams is to describe the degree to which watershed resources such as soil health and hydrologic function were affected by the fire. The teams evaluate the risk of undesirable outcomes (e.g. infrastructure damage), and to prescribe mitigation treatments to reduce the risk and minimize the impact of the fire on overall watershed/forest health (USFS, 2018a).

BAER teams are multidisciplinary, made up of experts in hydrology, soils, fisheries, engineering, forestry/weed control, GIS, and other pertinent fields. Teams survey the burned area immediately after fire containment and attempt to quantify the severity of both the direct and indirect fire effects (Robichaud and Ashmun, 2013). The result of a BAER assessment is a Burned Area Report which describes the severity of the fire and its impact on public

safety, private property, infrastructure, and watershed resources. The report also outlines a treatment plan to mitigate post-fire effects (Napper, 2006).

One of the most important measures used to describe fire effects is soil burn severity (Parsons *et al.*, 2010). Soil burn severity can be defined based on the degree to which five primary factors are observed at or near the soil surface: loss of groundcover due to consumption by the fire, changes in the color of the soil surface due to charring or ash deposits, loss of soil structure due to the consumption of soil organic matter, consumption of fine roots in the topsoil, and the formation of a water repellent layer that reduces water infiltration (Keeley, 2009; Parsons *et al.*, 2010).

Field observations gathered during the post-fire assessment are combined with multispectral satellite indices (Tucker, 1979; Key and Benson, 2006; Lutes *et al.*, 2006) to create a Soil Burn Severity (SBS) map. Areas within the fire perimeter are designated as either unburned, low burn severity, moderate burn severity, or high burn severity, with the idea that areas of high burn severity experienced a greatest degree of fire effects (Robichaud and Ashmun, 2013). Spectral indices such as the Normalized Difference Vegetation Index (NDVI) (Tucker, 1979) and Normalized Burn Ratio (NBR) (Key and Benson, 2006; Lutes *et al.*, 2006) are calculated using multi-spectral satellite imagery and used to produce a Burned Area Reflectance Classification (BARC) map. The BARC map is then updated using field observations gathered by the BAER team during their post-fire assessment, and a finalized Soil Burn Severity (SBS) map is produced which delineates areas within the fire that burned at low, moderate, or high severity.

Post-fire treatments are often divided into four treatment categories: hillslope, road, channel, and protection of public safety. Hillslope treatments are aimed at minimizing excessive runoff and erosion from burned hillslopes. Road treatments improve drainage of water on and through forest road networks. Channel treatments attempt to maintain the functionality of the stream channel itself, which can be affected by high flows, sediment, and debris. Public Safety treatments consist of more administrative tasks such as closing hazardous roads and improving signage in an effort to protect the public from unknowingly entering a dangerous situation (Robichaud *et al.*, 2014).

This thesis focuses on post-fire road treatments. From 1972-2009, road treatments ranked second in terms of total monetary expenditures from post-fire treatments (Robichaud *et al.*, 2014). Most road treatments involve upgrades to drainage structures such as culverts, as well as upgrades to the road prism itself including rolling dips (i.e. water bars), roadside ditches, and road surface treatments (i.e. adding surface gravel). For the purposes of discussion, the term “upgrade” generally means increasing the size of the given drainage structure to accommodate the expected increases in runoff and sediment moving through a watershed after a wildfire (Figure 2).

Figure 2: Example of undersized culvert (left) and post-fire upgraded culvert (right).

Before making culvert treatment recommendations, managers use a variety of methods to simulate and quantify the increased peak flows in response to a wildfire. Foltz et al. (2009) conducted interviews with forest managers in the early 2000’s and found that the methods most often used for this estimation were 1) the USGS Regression method, 2) the Curve Number method, 3) the Rule of Thumb method developed by Kuymjian in 2007, 4) the Water Erosion Prediction Project (WEPP) model, and 5) the Fire-Enhanced Runoff and Gully Initiation (FERGI) model. Though the proportion of managers using each of these methods has likely changed since the time of the interviews, this list still represents the most common approaches in modeling post-fire hydrology. This study will focus on three of the

above methods: USGS Regression method, Curve Number method, and WEPP model. A brief description of these three methods is provided below.

1.4 USGS Regression

The USGS Regression method uses observed discharge records to develop empirical equations unique to individual hydrologic regions/states across the country. These equations are a result of cooperation between the US Geological Survey (USGS) and state scientists who developed empirical equations for predicting streamflow based on characteristics unique to their state or region. To develop Montana StreamStats, basin characteristics and streamflow data through water year 2009 were analyzed from 755 gauging stations throughout the state (McCarthy *et al.*, 2016a). Of the 40 basin characteristics used in the analysis, three were identified as the most significant for predicting discharge: watershed area, mean annual precipitation, and percent of watershed with slopes greater than 50 percent (McCarthy *et al.*, 2016b).

USGS Regression equations are most commonly accessed through the StreamStats online application tool (USGS, 2016a). With this interface users can identify watersheds of concern by locating and selecting a channel-outlet. The application then delineates the watershed boundary and gathers the necessary inputs such as watershed area, elevation and slope, average monthly temperature and precipitation automatically. Using the regionalized regression equations, StreamStats calculates various streamflow statistics such as peak flow return periods, mean annual flow, and monthly flows (McCarthy *et al.*, 2016a).

Because this method returns statistics for natural (i.e. unburned) conditions in the watershed, the values need to be adjusted when being applied in a post-fire environment. A method for doing these adjustments is presented by Foltz et al. (2009). Once the pre-fire values are calculated, the user manually estimates the percent runoff increase in the high and moderate soil burn severity areas. This is a subjective endeavor; thus, managers tend to use a general assumption about the magnitude of runoff increase. For example, Forest Service managers tend to assume that runoff in moderate and high severity burned areas will double for the year after the fire. Assumptions also need to be made about level of water repellency present in the burned watershed.

Once the runoff increase has been decided, a *modifier* can be calculated using equation 1:

$$modifier = 1 + \frac{Percent\ runoff\ increase}{100\%} \times \frac{(A_h + A_m)}{A_T} \quad (1)$$

where

A_h = high severity burn area within watershed (acre or mi^2)

A_m = moderate burn severity area within watershed (acre or mi^2)

A_T = total watershed area (acre or mi^2)

To estimate the post-fire runoff, multiply the pre-fire runoff values by the modifier.

1.5 NRCS Curve Number

NRCS Curve Number method was developed by the USDA Natural Resources Conservation Service (NRCS) in the early 1970s. The basic equation calculates a runoff depth and essentially relies entirely on the Curve Number (CN) as the explanatory variable that describes the runoff characteristics for a given rainfall event. The basic curve number equation can be found in Technical Report-55 from the NRCS (1986):

$$Q = \frac{(P - 0.2S)^2}{(P + 0.8S)} \quad (2)$$

where

Q = runoff (in)

$S = \frac{1000}{CN} - 10$

CN = Curve Number

P = rainfall (in)

One program developed to conduct Curve Number calculations in an Excel spreadsheet is called FireHydro (Cerrelli, 2005). FireHydro allows users to calculate the runoff from a watershed under both unburned and burned conditions. The program expands on the basic Curve Number equation and takes inputs such as watershed area, basin slope, and 6- and 24-hour rainfall return period intervals to calculate runoff.

To obtain realistic predictions, it is critical that a proper Curve Number needs to be selected. Curve numbers can range anywhere from 1-100, depending on soil and landuse characteristics. Hypothetically, a curve number of 1 might represent flat area of deep, loosely packed sands that have the capacity to immediately infiltrate any water/precipitation that is applied. A value of 100 might represent a paved surface, such as a parking lot. Practically speaking, curve numbers tend to range between the 30s and the 80s for healthy forests (USDA-NRCS, 1989, 1991), and will tend to be higher in a burned forest. Most tables used for Curve Number selection are based on subjective judgements, such as whether the watershed is in “good”, “fair”, or “poor” condition (USDA-NRCS, 1986). These tables serve as guidelines for selecting a proper Curve Number, but managers often adjust this value based on an understanding of site-specific situations. Choosing a curve number to represent a burned watershed can be difficult, but regional recommendations do exist (Cerrelli, 2005; USDA-NRCS, 2016).

Using an NRCS Curve Number method such as FireHydro provides managers with a relatively quick and simple method of estimating runoff volumes after a wildfire. While this technique can provide a reasonable estimate of runoff to an experienced user, the necessity of assumptions and subjective judgment make it vulnerable to significant user error (Foltz *et al.*, 2009). As a side note, another commonly used modeling interface applying the Curve Number method is WILDCAT5 (Hawkins and Barreto-Munoz, 2016). Like FireHydro, this is an excel spreadsheet that allows users to model a watershed under a single-storm scenario, and outputs predicted peak flow and runoff volumes. FireHydro and WILDCAT5 are essentially interchangeable, and both used often by forest managers.

1.6 Watershed Erosion Prediction Project (WEPP)

The physically-based Watershed Erosion Prediction Project (WEPP) was developed and first released by the USDA Agricultural Research Service (ARS) in 1995. The primary goal of the project was to generate process-based model to replace the Universal Soil Loss Equation (USLE), an empirical model widely used to predict long term soil erosion (Flanagan *et al.*, 2007). Though the model was originally developed for use in agricultural lands, WEPP was adapted to be used in harvested and burned forested environments, forest roads, and other disturbed forest conditions. It has proven to be accurate for these applications (Elliot and Hall, 1997; Covert *et al.*, 2005; Robichaud *et al.*, 2007; Elliot, 2013; Chandramohan *et al.*, 2015; Brooks *et al.*, 2016; Srivastava *et al.*, 2017, 2020).

WEPP can be run in either a “hillslope” or a “watershed” version. The WEPP Hillslope version allows users to run the WEPP model on a single hillslope with a given hillslope profile. The model uses climate, soil, and land management characteristics to make predictions about the aspects of the surface and subsurface hydrology, as well as about soil erosion and deposition on the hillslope. WEPP Watershed uses similar modeling processes as the hillslope version but allows the model to be applied across a watershed versus a single hillslope. The watershed structure is composed of multiple hillslopes which then drain to downstream channels. Each channel network is defined using the TOPAZ model (Garbrecht and Martz, 1999) based on user defined critical upslope catchment areas and minimum stream channel length. With a channel network, hillslopes are fixed for each site of the stream channel assuming the width of the hillslope is equal to the average stream reach length. Recent modifications to the model now limit the slope length to 300 m and in this case the width is assumed to be the hillslope area divided by 300 m. The model simulates the hydrology of each hillslope and then routes the water draining off the hillslopes through the stream channel network to the watershed outlet. Further information about WEPP can be found in the model documentation (Elliot *et al.*, 1995; USDA-NRCS, 1995; Elliot and Hall, 1997; Flanagan *et al.*, 2001, 2012; Dun *et al.*, 2009; Dobre *et al.*, 2022; Lew *et al.*, 2022).

Modern advances in WEPP technology have provided user-friendly interfaces that allow users to access the WEPP model via an online portal to use a suite of Forest Service (FSWEPP) interfaces (https://forest.moscowfsl.wsu.edu/fswepp/). The Erosion Risk Management Tool (ERMiT) and Disturbed WEPP allow users to predict hydrology and soil erosion at the hillslope scale while WEPPcloud-PEP and WEPPcloud-Disturbed (Dobre *et al.*, 2022; Lew *et al.*, 2022) can model post-fire conditions at the watershed scale. The WEPPcloud-PEP interface was primarily developed to match runoff and erosion from summer rainfall events and was not meant to represent spring runoff or snowmelt conditions. It sets key soil properties such as effective hydraulic conductivity (K_{eff}), soil depth, and erodibility based on burn severity and soil texture (Table 1).

WEPPcloud-Disturbed is an online version of the WEPP model which uses the STATSGO and SSURGO soil databases to define soil depth, bulk density, rock content and other properties (Boll *et al.*, 2015). A Soil Burn Severity (SBS) map is used to identify areas of low, moderate, and high burn severity. The model then modifies surface erodibility, critical shear

stress, and effective hydraulic conductivity to represent burned conditions using the values in Table 1.

WEPPcloud-Disturbed has been shown to be effective in modeling streamflow in undisturbed forests (Dobre *et al.*, 2022), but has only been rigorously assessed under burned conditions by Quinn (2018) who used a stepwise calibration to find that, after a large 2011 wildfire in Eastern Arizona and Western New Mexico, the effective hydraulic conductivity of the soil surface needed to be significantly reduced to accurately represent observed streamflow. Those reduced K_{eff} values were used to modify the soil input files for this study and are described with more detail in the methods section.

Table 1: Key soil parameters used by WEPPcloud-PEP, based on soil texture and burn severity.

Burn Severity	Soil Depth		Texture	Effective Hydraulic Conductivity		% Sand	% Clay	% Organic	% Rock	Albedo	Initial Saturation (m/m)	Interrill Erodibility (kg*s/m4)	Rill Erodibility (s/m)	Critical Shear (N/m2)	Cation Exchange Capacity (meq/100g)
	in	mm		in/hr	mm/hr										
Unburned	32	800	Clay Loam	1.4	35	25	30	5	15	0.06	0.5	400000	0.00002	0.5	25
			Silt Loam	1.6	40	25	15	5	15	0.06	0.5	1000000	0.00005	1.5	15
			Loam	2.0	50	45	20	5	20	0.06	0.5	400000	0.00003	1	20
			Sandy Loam	2.4	60	65	10	5	25	0.06	0.5	400000	0.00008	2	15
Low	15	400	Clay Loam	0.7	18	25	30	5	15	0.15	0.75	1500000	0.00005	0.5	25
			Silt Loam	0.5	13	25	15	5	15	0.15	0.75	1000000	0.0001	1.5	15
			Loam	0.8	20	45	20	5	20	0.15	0.75	1000000	0.00008	1	20
			Sandy Loam	0.8	20	65	10	5	25	0.15	0.75	400000	0.00012	2	15
Moderate	15	400	Clay Loam	0.7	18	25	30	5	15	0.15	0.75	1500000	0.00005	0.5	25
			Silt Loam	0.5	13	25	15	5	15	0.15	0.75	1000000	0.0001	1.5	15
			Loam	0.8	20	45	20	5	20	0.15	0.75	1000000	0.00008	1	20
			Sandy Loam	0.8	20	65	10	5	25	0.15	0.75	400000	0.00012	2	15
High	15	400	Clay Loam	0.6	14	25	30	5	15	0.1	0.75	1500000	0.00006	0.5	25
			Silt Loam	0.4	10	25	15	5	15	0.1	0.75	1000000	0.00012	1.5	15
			Loam	0.6	15	45	20	5	20	0.1	0.75	1000000	0.0001	1	20
			Sandy Loam	0.6	15	65	10	5	25	0.1	0.75	400000	0.00014	2	15

2 Objective

The goal of this research is to assess the predictive ability of post-fire hydrologic models based on observed streamflow at road crossings in small, recently burned watersheds.

3 Methods

3.1 Site Description

In 2017, the Lolo National Forest had several large fire incidents that burned across 182,455 acres (73,837 ha) with roughly 50% in moderate and high soil burn severity. BAER teams found many unacceptable risks to road and trail infrastructure, water quality, and native plant and animal communities (USFS, 2018b). As part of their effort to reduce the risk of excessive erosion and road failure, various road treatments were proposed throughout the region. Primarily prescribed treatments included upsizing and removing culverts, installing drain dips, and reshaping roadbeds. Proposed road treatments within the burned areas totaled >$1,000,000. This information can be found in the Burned Area Reports from the Lolo Peak Fire, Highway 200/Moose Peak Fire complex, Sunrise Fire, Liberty Fire, and Rice Ridge Fire (USFS, 2017a, 2017b, 2017c, 2017d, 2018b).

After site visits in Spring 2018, 17 high priority culvert locations were identified by Lolo National Forest personnel for the study. The locations were based on both the managers' priority ranking as well has how accurately they represented the variability of aspect, elevation, slope, and burn severity throughout the burned areas. These 17 culvert locations were spread across 5 separate fires to expand the study area over a wide geographic region with different precipitation patterns, thus increasing the likelihood of capturing rainfall/runoff events (Figure 3).

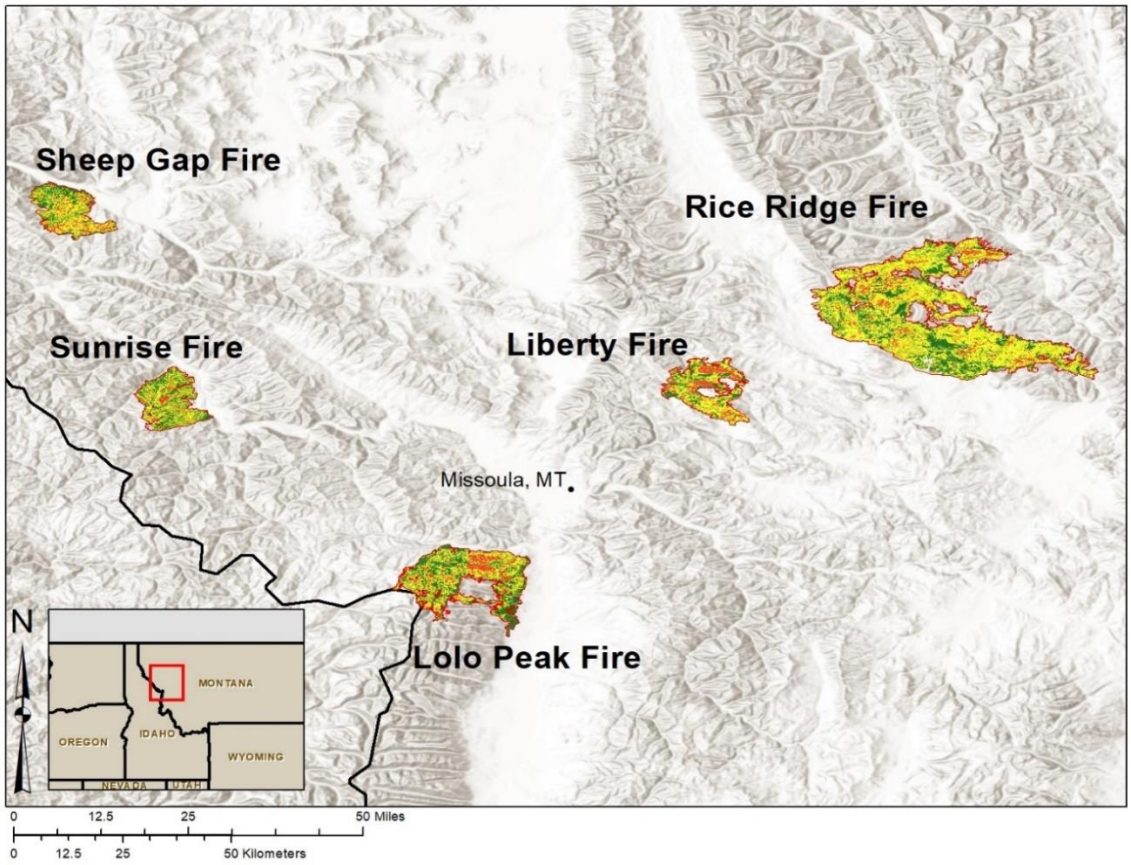

Figure 3: Overview of the 5 wildfires used in this study. The fires occurred in 2017 on the Lolo National Forest in Northwest Montana. The incidents were generally centered around the city Missoula, MT.

Vegetation regimes in this region range from low-elevation ponderosa pine (*Pinus ponderosa*) dominated forests to high-elevation subalpine fir (*Abies lasiocarpa*) forests. The sites in this study are almost exclusively in mid-elevation to high-elevation forests dominated by lodgepole pine (*Pinus contorta*), Douglas fir (*Pseudotsuga menziesii*), and subalpine fir (*Abies lasiocarpa*) (USFS, 2016). Fire history in these forest types tends to be mixed, and includes relatively frequent (5-25 years) low-intensity wildfires combined with infrequent (100+ years) high-severity “stand replacing” wildfires (Arno, 1980; Brown *et al.*, 1999; Odion *et al.*, 2014).

Volcanic ash-capped soils dominate (USDA-NRCS, 2020), which tend to exhibit some level of natural water repellency at the soil surface (Kawamoto *et al.*, 2007). Soil texture is generally silt-loam (25% sand, 65% silt, and 10% clay), except for soils at the Lolo Peak fire which are sandy-loam (50% sand, 40% silt, and 10% clay). Geology throughout the region is

made up primarily of quartzite and meta-argillite, metamorphosed sedimentary rock from the Mid-Proterozoic (Raines and Johnson, 1996).

The selected watersheds range in size from 30 ac (12 ha) to 3500 ac (1400 ha) at the largest. As a result of regional topography, the elevation of the watershed outlets (i.e. monitoring locations) tend to be lower on the easter half of the forest, between 3500-4500 ft (1000-1400 m) (Lolo Peak Fire: Figure A1, Sheep Gap Fire: Figure A2, Sunrise Fire: Figure A3) and higher on the western half of the forest, between 4300-5800 ft (1300-1800 m) (Liberty Fire and Rice Ridge Fire: Figure A4-Figure A6). Burn severities vary between watersheds, from roughly 10% moderate and high burn severity to 100%. A summary of the watershed characteristics can be found in Table 2 below.

Table 2: Characteristics of study watersheds.

Watershed Characteristic	Rice Ridge Fire							Liberty Fire		
	Spruce 1	Spruce 2	Nome Creek	Dunham East	Dunham West	Swamp Main	Swamp Upper	East Liberty	West Liberty 1	West Liberty 2
Contributing Area (acres) [ha]	717 [290]	434 [176]	1308 [529]	117 [47]	30 [12]	2400 [971]	425 [172]	839 [340]	294 [119]	66 [27]
Mean Basin Slope (%)	33	26	37	45	45	35	55	36	27	26
Elevation of Staff Gauge (ft) [m]	5191 [1582]	5191 [1582]	4868 [1484]	4692 [1430]	4388 [1337]	4331 [1320]	5415 [1650]	4829 [1472]	5790 [1765]	5567 [1697]
Latitude	47.21132	47.21225	47.19191	47.17866	47.1614	47.18888	47.2009	47.03625	47.0653	47.057834
Longitude	-113.2064	-113.2035	-113.20729	-113.1965	-113.1956	-113.4225	-113.3825	-113.701	-113.7621	-113.7531
% Unburned	0	0	11	26	0	30	44	7	15	78
% Low Burn	3	0	11	32	50	28	22	4	14	13
% Mod. Burn	82	100	71	37	50	41	31	61	50	9
% High Burn	15	0	7	4	0	2	1	28	20	0

Watershed Characteristic	Lolo Peak Fire		Sunrise Fire	Sheep Gap Fire				
	John Creek	Mormon Creek	Sunrise	East Bemish Lower	East Bemish Middle	East Bemish Upper	West Bemish 1	West Bemish 2
Contributing Area (acres) [ha]	480 [194]	3478 [1408]	260 [105]	2561 [1036]	890 [360]	209 [85]	43 [17]	78 [32]
Mean Basin Slope (%)	37	40	48	40	39	30	36	34
Elevation of Staff Gauge (ft) [m]	4506 [1373]	4102 [1250]	3633 [1107]	3465 [1056]	3766 [1148]	3998 [1219]	4036 [1230]	4235 [1291]
Latitude	46.72674	46.71658	47.07219	47.44304	47.43375	47.43906	47.44131	47.43199
Longitude	-114.1976	-114.1438	-114.8253	-115.0478	-115.0451	-115.0366	-115.0581	-115.0555
% Unburned	5	11	9	34	31	19	0	0
% Low Burn	11	19	37	11	21	4	0	0
% Mod. Burn	23	38	34	35	32	50	72	81
% High Burn	60	33	20	18	16	27	28	19

3.2 Peak Flows

To measure peak streamflow, standard USGS crest-stage gauges were installed a short distance above the inlet of each culvert. These gauges are designed to record the crest, or peak flow in the channel during a runoff event. The gauge itself consists of a wooden stake housed in a steel pipe (3 in [75 mm] diameter by roughly 3 feet [1 m] long). The pipe has holes drilled in its base allowing runoff to flow into and fill the pipe. As the water level rises in the pipe, a small amount of ground cork floats on the water surface and clings to the wooden stake. As the water level drops, the cork remains stuck to the stake thus recording the maximum height experienced during the runoff event. This is similar to a design described by Friday (1965). These gauges need to be visited immediately following a runoff event in order to record the peak flow reading. They then need to be "reset" in preparation for the next storm (Figure 4).

Figure 4: (left) Crest gauge and e-tape installation, (right) high water marked by cork on wooden stake.

Additionally, 10 of the locations were instrumented with e-tapes (Milone Technologies, Continuous Fluid Level Sensor, #PN-12110215TC-X). E-tapes use electrical resistance to continuously measure flow depth in the stream. This allowed us to capture minor changes in

stream discharge and intermediate peak flow events that may have otherwise been missed by the crest gauges. Peak flows from spring 2018 were estimated based on measurements from high water in the stream channel.

3.2.1 Streamflow Rating Curve Calibration

Using the observed streamflow measurements described above, unique rating curves were developed to represent streamflow in each watershed. A rating curve is a mathematical relationship that equates stream depth (also known as stream "stage") to discharge. These stage-discharge relationships are commonly used by the U.S. Geologic Survey (USGS) to record river discharge at gauging stations throughout the country. Generating a rating curve is a three step process consisting of 1) measuring stream stage, 2) measuring stream discharge, and 3) creating a stage-discharge relationship (Rantz, 1982a, 1982b).

3.2.2 Measuring Discharge

Two methods for measuring stream discharge were used in this study. Initially the velocity-area was used during early 2018 summer runoff. The velocity-area method (Turnipseed & Sauer, 2010) involves dividing the stream cross-section into segments of equal area and measuring the average velocity in each segment. The summation of these values is the total stream discharge (Q).

While this method is relatively simple and practical to use in low gradient streams (slope < ~5%), it becomes less effective in high gradient streams. In steep snowmelt dominated watersheds such as those in this study, summer water levels may be so low that it becomes impossible to measure cross section dimensions or water velocity accurately. During high flow, non-logarithmic velocity profiles and aeration make it difficult to find a representative average velocity using a standard velocity probe (Byrd *et al.*, 2000; Wilcox and Wohl, 2007; Nitsche *et al.*, 2012). Because of these issues, we measured discharge using the salt dilution method.

The salt dilution method (Ostrem, 1964) calculates discharge based on the relative dilution of a known salt solution, and is highly effective in highly turbid mountain streams (Kilpatrick and Cobb, 1985; Hongve, 1987). The method works on the principle of the conservation of

mass and applies the following equation from Sappa et al. (2015). The equation can be easily converted from metric to English units, which is how it is presented here:

$$Q = C_s \times \frac{V_s}{\int_{t_0}^{t_0+t_p}[C(t)-C_b]\times dt} \quad (3)$$

where

$Q =$ Stream Discharge (cms)

$V_s =$ Volume of salt solution (m^3)

$C_s =$ Electrical conductivity of salt solution (µS/cm)

$C_b =$ Background conductivity of stream (µS/cm)

$C(t) =$ Stream electrical conductivity at time (t)

$t_0 =$ Elapsed time (s)

$t_p =$ Time of "arrival" of salt solution at downstream measurement location (s)

To conduct salt dilution measurements, a known volume of tracer solution with a known electrical conductivity (EC) is added instantaneously to the stream. An EC meter is positioned in the stream at a location far enough downstream so that the salt solution has time to mix evenly through the water column (generally 5-10x the stream width). The EC meter measures the conductivity of the stream as the salt "pulse" passes. By integrating the area under the pulse curve, the volume of water in the stream (i.e. discharge) can be calculated based on how much it diluted the salt solution.

3.2.2.1 Generating Rating Curves

Using the measured discharge data, a unique rating curve was created for each location, where sufficient data was available (Figure 5). Multiple discharge measurements were taken at or near peak flow and at or near low flow to capture the full range of possible discharges throughout the year. The fitted equations from these relationships were used to convert the stage data, recorded by the crest gauges and/or e-tapes, to discharge data. By plotting the points on using logarithmic scales, the data are well represented with the following power fit equation $y = ax^b$ where a and b are fitting coefficients, x is stream depth, and y is the stream discharge.

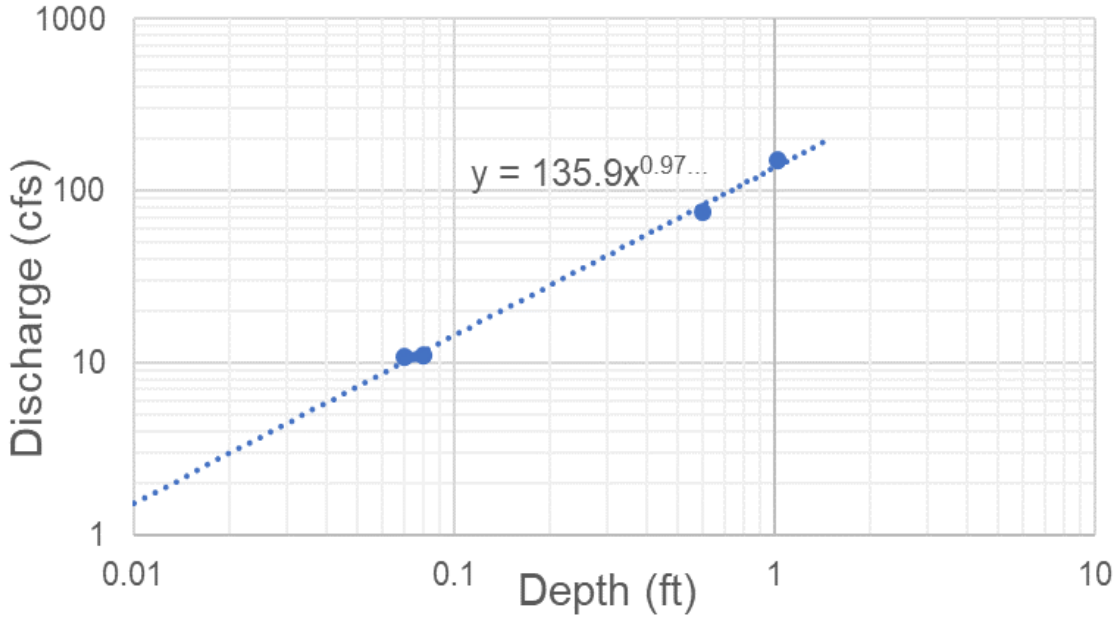

Figure 5: Example of rating curve, used at Nome Creek

3.3 Precipitation

Tipping bucket rain gauges (Rainwise Inc., Wired Rain Gauge, RAINEW 111) were positioned at or near the top of the instrumented watersheds. A total of 13 rain gauges were initially installed across all the study areas, with some watersheds sharing a single gauge. These rain gauges have a measurement resolution of 0.1 in (0.254 mm), do not include wind-shields, and are unable to measure snowfall (Figure 6).

Figure 6: (left) Rain gauge installed at the Rice Ridge Fire, (right) Rain gauge installed at the Sheep Gap Fire.

Individual rainfall events were defined as having at least a 5-minute duration and were separated by at least 6-hours with no rainfall. Three different “storm characteristics” were calculated for each event: duration and rainfall total, maximum 10-minute rainfall intensity (I_{10}), and maximum 30-minute rainfall intensity (I_{30}). Each storm characteristic was categorized as either <2, 2, 5, 10, 25, 50, or 100-year return period intensities relative to precipitation intensity return periods derived for each location from the Volume 1 of the NOAA Atlas 2 (Miller *et al.*, 1973; Arkell and Richards, 1986). Using event duration and total rainfall, the storm total return period was calculated via an Intensity-Duration-Frequency (IDF) analysis (Schwab *et al.*, 1992). Rainfall events with at least one storm characteristic that exceeded a 2-year return period were considered significant and included as part of this analysis.

Data from nearby SNOTEL sites (Table 3) were analyzed to characterize regional precipitation trends. Total summer precipitation (May-October) and total annual precipitation during years 2018-2020 were compared to averages over the period of record at each SNOTEL site.

Table 3: SNOTEL sites used to characterize regional precipitation trends. See Table 8 and Table 9 for results.

Fire	SNOTEL Site	Lat°, Long°	Period of Record
Rice Ridge Fire	North Fork Jocko (667)	47.27, -113.75	1989-Present
Lolo Peak Fire	Lolo Pass (588)	46.63, -114.58	1983-Present
Sunrise Fire	Hoodoo Basin (530)	46.98, -115.03	1981-Present
Sheep Gap Fire	Sleeping Woman (783)	47.18, -114.33	1993-Present
Liberty Fire	Stuart Mountain (901)	47.00, -113.93	1995-Present

3.4 Ground Cover

Groundcover measurements were conducted at plots randomly identified using combinations of soil burn severity (high, moderate, low), hillslope aspect (NE, SW), and elevation (above/below 5500 ft [1700 m]), during peak growing season (July-August). A minimum of 3 replications of each combination were spread randomly across the five fires. Percent ground cover was estimated using a 3 ft (1 m), 100 point sampling grid (Chambers and Brown, 1983). Points categorized as mineral soil, gravel, or ash were grouped together as “bare soil” while points categorized as litter, moss, rock, wood, live vegetation, or tree

were grouped together as “ground cover”. These measurements were used to characterize burn severity and recovery relative to the soil burn severity map generated during post-fire assessment (Lewis *et al.*, 2017).

3.5 Watershed Modeling

3.5.1 Runoff Curve Number – FireHydro

Because there are not curve numbers explicitly defined for burned areas, many researchers and forest managers have attempted to come up with their own guidelines. In this case the curve number associated with each burn severity (low, moderate, high) was chosen based on a consensus of several engineers at the Natural Resources Conservation Service to represent burned areas in this region of Montana (Figure 7). The actual CN value used by the model is a simple weighted average based on the coverage of each burn severity within the watershed (Table 4).

For High Severity Burn Areas*-	HSG A soils = RCN 64 HSG B soils = RCN 78 HSG C soils = RCN 85 HSG D soils = RCN 88
For Moderate Severity Burn Areas-Use Cover Type in FAIR Condition	
For Low and Unburned Areas-	Use Cover Type in GOOD Condition for North & East facing slopes Use Cover Type between FAIR & GOOD for South & West facing slopes

Figure 7: RCN guidelines taken from Cerrelli (2005). The cover type and condition are in reference to the descriptions used in the NRCS National Engineering Handbook (USDA-NRCS, 1991).

Watershed area and slope were calculated using ESRI ArcMap software. Percent coverage of low, moderate, and high burn severities were calculated using the soil burn severity maps. Rainfall inputs for FireHydro were derived from Volume 1 of the NOAA Atlas 2 (Miller *et al.*, 1973), which provides maps of isohyets (i.e. lines of equal precipitation) for the state of Montana (Table A1). These data were then used to calculate the short-duration rainfall intensity return periods used in the precipitation analysis (Table A2).

Table 4: Pre fire and post fire runoff curve number (RCN) values used in FireHydro analysis.

Site	CN-Pre Fire	CN-Post Fire
Spruce 1	60	82
Spruce 2	60	82
Nome Creek	60	79
East Dunham	60	68
West Dunham	60	82
Swamp Main	60	76
Swamp Upper	60	72
East Liberty	60	82
West Liberty 1	60	80
West Liberty 2	60	63
John Creek	60	87
Mormon Creek	60	80
Sunrise	60	88
East Bemish Lower	66	75
East Bemish Mid	66	75
East Bemish Upper	60	74
West Bemish 1	66	72
West Bemish 2	60	82

3.5.2 Montana StreamStats

Montana StreamStats was accessed through the USGS StreamStats web application (USGS, 2016b). After running the model on each watershed, the results were modified to represent burned conditions using Equation 1. A runoff increase of 100% (double the pre-fire amount) was assumed for moderate and high burn severity conditions (Story *et al.*, 2006). The pre-fire peak flow magnitude for each watershed was simply multiplied by the corresponding modifier (Table 5) to estimate post-fire flow.

Table 5: Modifiers applied for each site in StreamStats analysis.

Site	Modifier
Spruce 1	2.0
Spruce 2	2.0
Nome Creek	1.8
East Dunham	1.4
West Dunham	1.5
Swamp Main	1.4
Swamp Upper	1.3
East Liberty	1.9
West Liberty 1	1.7
West Liberty 2	1.2
John Creek	1.8
Mormon Creek	1.7
Sunrise	1.9
East Bemish Lower	1.5
East Bemish Mid	1.5
East Bemish Upper	1.8
West Bemish 1	2.0
West Bemish 2	2.0

3.5.3 WEPPcloud-PEP

The WEPPcloud-PEP interface was used to setup and run each watershed for a 100-year simulation in both burned and unburned conditions. The watersheds were delineated using TOPAZ (Garbrecht and Martz, 1999) with the default minimum channel length and critical source area values of 330 ft (100 m) and 25 acres (10 ha), respectively.

Using long-term monthly averages from nearby weather stations (Table 6) unique daily weather files were generated for each hillslope with CLIGEN (Nicks *et al.*, 1995). The files were then adjusted with scaling factors calculated from 30-year monthly average PRISM raster maps of precipitation and temperature (http://prism.oregonstate.edu). The same weather files were used for both the burned and unburned simulations.

Table 6: Weather stations used to build 100-year CLIGEN climate files.

Fire	Weather Station	Lat., Long.
Rice Ridge	Seeley Lake, MT	47.22, -113.52
Liberty	Seeley Lake, MT	47.22, -113.52
Sheep Gap	Superior, MT	47.18, -114.87
Lolo Peak	Stevensville, MT	46.52, -114.10
Sunrise	Superior, MT	47.18, -114.87

Soil Burn Severity (SBS) maps were used to define the landuse parameters of each watershed. Landuse options included unburned, low severity burn, moderate severity burn, or high severity burn. Then based on the landuse and soil texture, soil parameter files were assigned to each hillslope (Table 1). The model generates peak flows at a sub-daily timestep using the Muskingum-Cunge method (Wang *et al.*, 2010). This output was used to calculate 2, 5, 10, and 25-year return period annual peak flows for each watershed, in both the unburned and burned condition.

3.5.4 WEPPcloud-Disturbed

WEPPcloud-Disturbed was run using two different sets of soil parameters. First, the model was run using the default soil parameters for both burned and unburned soils. Second, they were modified by significantly reducing the effective hydraulic conductivity (K_{eff}) of the soil surface on burned hillslopes. Because our observed dataset is relatively short (~3 years), it lacks the extent traditionally required to conduct a true calibration, which requires a calibration period and a separate validation period. Instead, the results from Quinn (2018) were used as our modified K_{eff} values (Table 7).

Table 7: Modified K_{eff} values adopted from Quinn (2018). The modified values were applied to the surface layer of all burned soils.

Burn Severity	**Default K_{eff}**		**Modified K_{eff}**	
	in/hr	mm/hr	in/hr	mm/hr
Low	0.5-0.8	13-20	default	default
Moderate	0.5-0.8	13-20	0.04	1
High	0.4-0.6	10-15	0.004	0.1

3.6 Analysis

The primary model assessment was based on the ability of WEPPcloud-Disturbed to simulate the timing and magnitude of observed annual peak streamflow. The Nash-Sutcliffe Efficiency (NSE) (Nash & Sutcliffe, 1970), is a commonly used dimensionless statistic comparing the magnitude of residual variance with the magnitude of variance within the observed data itself. NSE has a range from -∞ to +1. The closer the NSE value is to 1, the better the model can be said to have performed. The equation for NSE is as follows:

$$NSE = 1 - \left[\frac{\sum_{i=1}^{n}(Y_i^{obs} - Y_i^{sim})^2}{\sum_{i=1}^{n}(Y_i^{obs} - Y^{mean})^2}\right] \quad (4)$$

Where

Y_i^{obs} = i[th] observed value

Y_i^{sim} = i[th] simulated value

Y^{mean} = mean of observed values

Percent Bias (PBIAS) (Gupta *et al.*, 1999) was used to assess whether the model over-predicted or under-predicted the observed data. Negative PBIAS values indicate that the model is overestimating, while positive PBIAS values indicate that the model is underestimating. PBIAS is calculated by:

$$PBIAS = \frac{\sum_{i=1}^{n}(Y_i^{obs} - Y_i^{sim}) \times 100}{\sum_{i=1}^{n}(Y_i^{obs})} \quad (5)$$

where

Y_i^{obs} = i[th] observed value

Y_i^{sim} = i[th] simulated value

Root mean square error (RMSE) (Chu and Shirmohammadi, 2004; Moriasi *et al.*, 2007) was also used as an index for goodness of fit. Similar to the standard deviation of the model error, values closer to 0 indicate better model performance. It is calculated by:

$$RMSE = \sqrt{\frac{\sum_{i=1}^{n}(Y_i^{obs} - Y_i^{sim})^2}{n}} \quad (6)$$

where

Y_i^{obs} = i[th] observed value

Y_i^{sim} = i[th] simulated value

n = number of data points

4 Results

4.1 Precipitation

4.1.1 Regional Precipitation Trends

SNOTEL data from across the region indicated that summer precipitation was below average in 2018 (90%), about average in 2019 (99%), and above average in 2020 (125%) (Table 8). Total water year precipitation was above average in 2018 (112%), and just below average in 2019 and 2020 (97% and 95%, respectively) (Table 9). These trends suggest that while total precipitation was about average in 2018, it was a relatively dry summer compared to normal. The opposite is true for 2020, when more rainfall came during the summer compared to normal.

Table 8: Total **summer** precipitation (May-October) as a percentage of long-term average. Long-term average includes data from the beginning of the period of record through 2017.

Snotel Site	Long Term Average		2018			2019			2020		
	in	mm	in	mm	%	in	mm	%	in	mm	%
North Fork Jocko (667)	16.7	424	14.6	371	87%	16.9	429	101%	20.2	513	121%
Lolo Pass (588)	14.6	371	13.9	353	95%	13.5	343	92%	21.6	549	148%
Hoodoo Basin (530)	18.5	470	15.8	401	85%	15.2	386	82%	20.9	531	113%
Sleeping Woman (783)	14.4	366	13.1	333	91%	17	432	118%	18	457	125%
Stuart Mountain (901)	16.5	419	15	381	91%	16.7	424	101%	19.7	500	119%

Table 9: Total **water year** (1 Oct – 30 Sept) precipitation as a percentage of long-term average. Long-term average includes data from the beginning of the period of record through 2017.

Snotel Site	Long Term Average		2018			2019			2020		
	in	mm	in	mm	%	in	mm	%	in	mm	%
North Fork Jocko (667)	68.1	1730	85.6	2174	126%	60.8	1544	89%	72.2	1834	106%
Lolo Pass (588)	47.2	1199	51.8	1316	110%	46.8	1189	99%	46.2	1173	98%
Hoodoo Basin (530)	64.5	1638	65.3	1659	101%	55.6	1412	86%	53.5	1359	83%
Sleeping Woman (783)	35.6	904	39	991	110%	40.2	1021	113%	37	940	104%
Stuart Mountain (901)	48.9	1242	55.1	1400	113%	47.1	1196	96%	48.6	1234	99%

4.1.2 Rainfall Data

Total annual summer rainfall recorded by our rain gauges, listed in Table 10 below, tended to be below the long-term averages based on SNOTEL data. This may be due to under-catch, which can be significant (10-35%) when wind shields are not installed (Hanson *et al.*, 2004).

Table 10: Total summer rainfall (May-Oct) recorded by our rain gauges.

Fire	Total Summer Rainfall					
	2018		2019		2020	
	in	mm	in	mm	in	mm
Rice Ridge	6.4	161	11.0	279	8.7	222
Lolo Peak	7.2	182	9.4	239	9.0	227
Sheep Gap	6.1	156	12.9	329	7.1	181
Liberty	-	-	9.2	234	3.8	96

Most recorded rainfall events were relatively long-duration, low-intensity storms. The average storm duration was 20 hours, with an average intensity of 0.3 in/hr (7.6 mm/hr). Events with at least one rainfall characteristic (storm total, I_{10}, I_{30}) that met or exceeded a 2-year return interval are listed in Table 11 below. The return intervals used to categorize the events can be found in Table A1 and Table A2.

Table 11: Rainfall events with at least one storm characteristic that meets or exceeds a 2-year return period. All three storm characteristics (storm total, maximum 10-minute rainfall intensity [I_{10}], maximum 30-minute rainfall intensity [I_{30}]) are listed for each event.

Fire	Date	Duration		Rainfall Depth		Return Period	I_{10}		Return Period	I_{30}		Return Period
		min	hrs	in	mm		in/hr	mm/hr		in/hr	mm/hr	
Sheep Gap	25-Oct-18	**1725**	**28.8**	**1.4**	**35**	**2-year**	0.5	14	<2-year	0.3	8	<2-year
	16-May-19	**3432**	**57.2**	**2.4**	**61**	**10-year**	0.8	19	<2-year	0.5	14	<2-year
	15-Aug-19	112	1.9	0.3	7	<2-year	**2.0**	**50**	**2-year**	0.7	17	<2-year
	28-Jun-20	**2831**	**47.2**	**1.5**	**38**	**2-year**	0.3	8	<2-year	0.2	5	<2-year
Lolo Peak	3-Jul-19	**31**	**0.5**	**0.3**	**7**	**2-year**	1.0	24	<2-year	0.5	13	<2-year
	15-Aug-19	300	5.0	0.8	20	<2-year	**1.8**	**44**	**5-year**	**1.2**	**30**	**5-year**
	28-Jun-20	**2846**	**47.4**	**3.0**	**70**	**5-year**	0.5	12	<2-year	0.2	6	<2-year
Rice Ridge - Dunham Creek	14-Jul-19	**15**	**0.3**	**0.1**	**2**	**5-year**	0.4	11	<2-year	0.4	5	<2-year
	23-Jul-19	**23**	**0.4**	**0.6**	**16**	**100-year**	**2.2**	**55**	**2-year**	**1.3**	**33**	**10-year**
	23-Jul-20	**21**	**0.4**	**0.4**	**10**	**10-year**	**1.7**	**43**	**2-year**	**0.8**	**19**	**2-year**
	16-Oct-20	**992**	**16.5**	**1.9**	**49**	**2-year**	0.3	8	<2-year	0.3	7	<2-year
Rice Ridge - Swamp Creek	14-Jul-19	280	4.7	0.4	11	<2-year	**1.9**	**49**	**2-year**	0.7	17	<2-year
	8-Sep-19	**1275**	**21.3**	**2.6**	**66**	**5-year**	**1.9**	**47**	**2-year**	**1.2**	**30**	**5-year**
	28-Jun-20	**3127**	**52.1**	**2.2**	**55**	**2-year**	0.6	15	<2-year	0.4	9	<2-year
Liberty	8-Sep-19	**844**	**14.1**	**1.5**	**38**	**2-year**	1.3	34	<2-year	0.9	24	<2-year

The longest events occurred over nearly two days (48 hrs) and had a mean total storm intensity of under 0.05 in/hr (1 mm/hr), while the shortest storms lasted less than 30 minutes and a total storm intensity of over 1.0 in/hr (25 mm/hr). Both the highest 10-minute rainfall intensity (I_{10}) of 2.2 in/hr (55 mm/hr) and the highest 30-minute rainfall intensity (I_{30}) of 1.3 in/hr (33 mm/hr) were recorded during the same event, on 23 July 2019 at the Rice Ridge

fire. The storm was among the shortest recorded at just 23 minutes long. It triggered a large debris flow in the Spruce 1 watershed and caused large peak flows in Nome Creek and Spruce 2. This rainfall event will be analyzed with greater detail in the next section.

4.2 Peak Flows

At all but three watersheds, maximum annual peak flow occurred during spring snowmelt throughout the three year period of study. The only exceptions were the 2019 maximum annual peak flows at Spruce 1, Spruce 2, and Nome Creek which were a result of the 23 July rainfall event (Table 12).

Table 12: Maximum annual discharge recorded at each study site. All peak flows occurred during spring runoff except those highlighted in yellow, which were a result of a summer 2019 rainfall event. The 2019 peak flow in Spruce 1 was estimated based on field measurements taken after peak flow had occurred.

Maximum Annual Peak Discharge

	2018				2019				2020			
Rice Ridge Fire	cfs	in/day	cms	mm/day	cfs	in/day	cms	mm/day	cfs	in/day	cms	mm/day
Spruce 2	45	2.7	1.27	68	24	1.4	0.68	36	18	1.1	0.51	27
Spruce 1	80	2.8	2.27	71	515	18.1	14.58	460	46	1.6	1.30	41
Nome Creek	160	2.9	4.53	74	214	3.9	6.06	99	140	2.5	3.96	65
Dunham East	15	3.2	0.42	82	10	2.1	0.28	54	10	2.1	0.28	54
Dunham West	10	7.7	0.28	196	5	3.8	0.14	98	5	3.8	0.14	98
Swamp Main	-	-	-	-	45	0.5	1.27	12	56	0.6	1.59	15
Swamp Upper	-	-	-	-	15	0.9	0.42	22	20	1.2	0.57	29
Sheep Gap Fire												
East Bemish Lower	50	0.5	1.42	12	35	0.3	0.99	9	40	0.4	1.13	10
East Bemish Mid	15	0.4	0.42	11	13	0.4	0.37	9	14	0.4	0.40	10
East Bemish Upper	10	1.2	0.28	30	10	1.2	0.28	30	10	1.2	0.28	30
West Bemish 1	10	6.3	0.28	161	10	6.3	0.28	161	8	5.1	0.23	129
West Bemish 2	15	5.0	0.42	127	11	3.7	0.31	93	5	1.7	0.14	42
Liberty Fire												
East Liberty	-	-	-	-	20	0.6	0.57	15	15	0.4	0.42	11
West Liberty 1	-	-	-	-	25	2.1	0.71	55	20	1.7	0.57	44
West Liberty 2	-	-	-	-	10	2.2	0.28	55	12	2.6	0.34	66
Sunrise Fire												
Sunrise	-	-	-	-	1	0.1	0.03	2	1	0.1	0.03	2

Throughout the study period, the highest peak discharges per unit area (discharge in cfs of cms divided by the area of the watershed) occurred in the smallest watersheds. In 2018, peak discharge at West Bemish 1, West Bemish 2, and Dunham West were estimated to have been over 5 in/day (125 mm/day), the highest of all sites. These were also the three smallest watersheds in the study, at <100 acres (40 hectares). In contrast, the lowest peak discharges per unit area tended to occur in the largest watersheds. The East Bemish Lower and Swamp Main watersheds are each >2200 acres (900 hectares), and consistently had

unit peak discharges below 0.6 in/day (15 mm/day). The following is a summary of rainfall and peak flow observed at each study site.

4.2.1 Rice Ridge Fire

Our study sites at the Rice Ridge Fire are split between two larger watersheds: Swamp Creek and Dunham Creek. At the Swamp Creek watershed, we recorded 3 significant rainfall events, all of which caused a measurable spike in streamflow (Figure 8). The first event was on 14 July 2019 and caused a small spike in streamflow of roughly 1 mm/day. The storm produced a 2-year rainfall event with an I_{10} of 1.9 in/hr (49 mm/hr). Two smaller rainfall events were recorded on 3 July and 8 July which also caused small spikes in streamflow, but these events were not severe enough to exceed a 2-year return period.

On 8 September 2019, a large weather system moved across western Montana. Though the event produced some amount of rainfall at all study areas, Swamp Creek and the Liberty Fire were the only areas where the event exceeded a 2-year return period. At Swamp Creek the storm produced 2-year I_{10} of 1.9 in/hr (47 mm/hr), a 5-year I_{30} of 1.2 in/hr (30 mm/hr), and a 5-year storm total with 2.6 in (66 mm) of rainfall in 21 hrs. The event caused a 3 mm/day spike in stream discharge at Swamp Creek (Figure 8).

The last event at Swamp Creek occurred on 28 June 2020 where 2.2 in (55 mm) of rainfall were produced over 2 days, resulting in a 2-year storm total. Neither the I_{10} nor the I_{30} exceeded a 2-year return period. It occurred on the falling-limb of the hydrograph and was likely a partial rain-on-snow event in the upper portions of the watershed.

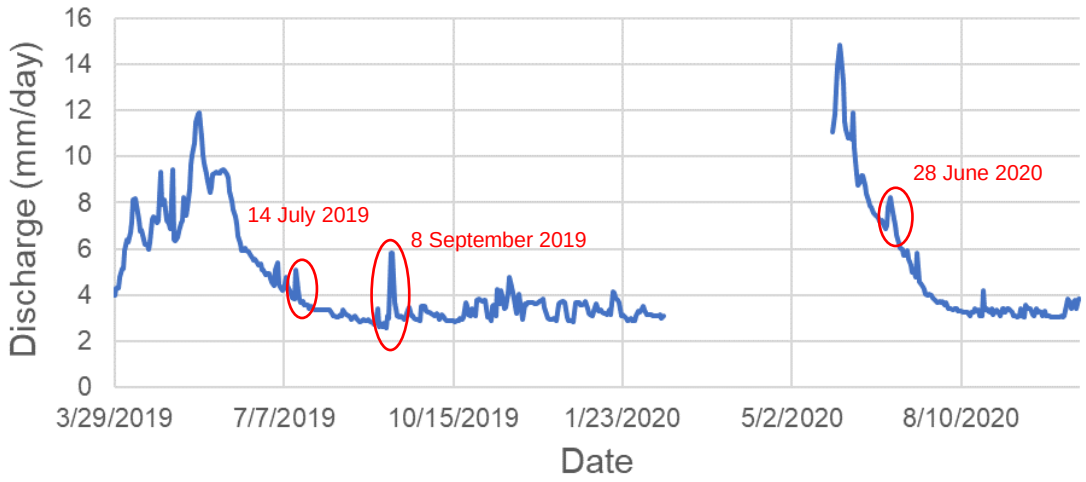

Figure 8: Hydrograph at the Swamp Main crest gauge. Roughly 3-months of data are missing between 16 February 2020 and 26 May 2020 due to power loss at the datalogger.

At Dunham Creek the first significant storm was recorded on 14 July 2019. It was a short, 15-minute rainfall event that did not produce any noticeable spike in streamflow at Nome Creek (Figure 9). It was a 5-year storm total, producing 0.1 in (2 mm) of rainfall in 15 minutes. Based on data from the individual rain gauges, the storm was more intense in the lower portion of Dunham Creek, near the Dunham East and Dunham West crest gauges. No peak flow was recorded at either of these crest gauges.

Just over a week later, on 23 July 2019, a rainfall event occurred that produced the highest rainfall intensity recorded during the three-year study period. While the I_{10} and I_{30} calculated from this event are 2-year and 10-year return periods, respectively, it was a 100-year event based on the storm total (Table 11). In Nome Creek, streamflow spiked to 3.9 in/day (99 mm/day) (Figure 9). A similar spike was recorded at Spruce 2 where streamflow spiked to 1.4 in/day (36 mm/day). This storm triggered several debris flows in the vicinity of Nome Creek and Spruce Creek which are described in detail by Walters et al. (2019) (Figure 9).

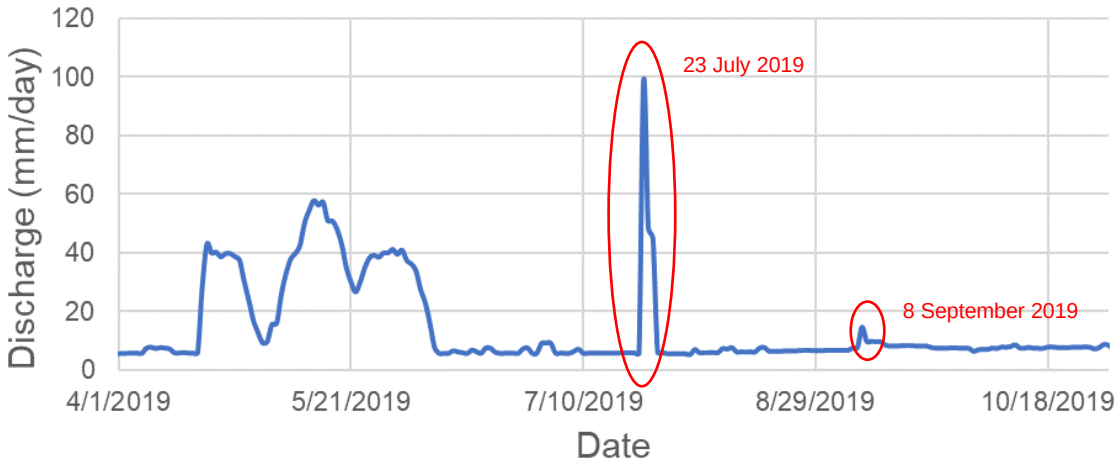

Figure 9: Peak Flow hydrograph at the Nome Creek crest gauge. Technical issues with the datalogger began spring 2020. Data from spring-fall 2019 is shown here.

The crest gauge at Spruce 1 was lost in the debris flow, thus no Spruce 1 data was recovered from the event. In an attempt to recreate the runoff from the rainfall event, hydrologists from the Lolo National Forest surveyed the scar for high water marks and used procedures outlined in the final debris flow report (Walters *et al.*, 2019) to determine that the discharge in Spruce Creek just before the debris flow initiated was near 515 cfs (14 cms). Normalized for watershed area that is equivalent to 18 in/day (460 mm/day).

On 30 August 2020 University of Montana collaborators acquired arial imagery of a lower section of the Spruce 1 watershed with a DJI Inspire UAV. Photogrammetric techniques were used to generated a digital elevation model (DEM) of the ground surface following the debris flow (see Adams *et al.*, 2016). By comparing the post-debris flow DEM to one captured by the Lolo National Forest in the years before the fire, we estimated that roughly 120,000ft^3 (3,500 m^3) of sediment and debris was deposited in this section of Spruce 1 during the event on 23 July 2019.

The drone imagery only covers a portion of the Spruce 1 watershed, and because the debris flow scar continues for another ~3 km upstream of the region covered by the analysis, 3,500 m^3 is likely below the total volume of mobilized and/or deposited debris during the event. A larger DEM gathered post-debris flow that covers the entirety of the watershed would be necessary to calculate the total debris flow volume for the entire watershed.

A)

B)

C)

Figure 10: A) First hillslope debris flow. B) Second hillslope debris flow. *Note the road surface is completely covered with debris, but extends straight forward from the bottom of the frame curving slightly to the right. C) View of the channelized Spruce Creek debris flow. The image shows significant sediment and large woody debris deposited on the upstream side of the culvert. Out of frame, the downstream portion of the creek was scoured down to bedrock.

As mentioned previously, the weather system on 8 September 2019 produced rainfall at Dunham Creek as well, though it was not recorded as a 2^{+}-year event based on any of the three storm characteristics. While it produced 2.6 in (66 mm) of rainfall at Swamp Creek, about half that amount that occurred at Dunham Creek (1.5 in [35 mm]). Still, the precipitation did cause a small spike in streamflow at both Nome Creek (Figure 9) and Spruce 2.

Exactly one year after the 2019 debris flows, another relatively high-intensity rainfall event hit the Dunham Creek watershed. On 23 July 2020, a 21-minute rainfall event produced 0.4 in (10 mm) of precipitation. This event was less intense than the 2019 event with an I_{10} and I_{30} of 1.7 in/hr (43 mm/hr) and 0.8 in/hr (19 mm/hr). While a peak flow was recorded at the

crest gauge, the entire gauge itself had shifted, now leaning in the downstream direction, essentially rendering the crest gauge “un-calibrated”.

Based on the peak measurement of the shifted crest gauge, the rainfall event caused a roughly 5 in (13 cm) increase in flow depth relative to what the gauge was later reading at low flow. Assuming the depth-discharge relationship did not change significantly, we can estimate that discharge during the event increased by roughly 1 in/day (25 mm/day).

4.2.2 Sheep Gap Fire

Four significant rainfall events were recorded at Sheep Gap. Three out of these four events were long duration, lasting >24-hours, and one was a 2-hour event. The first event, on 15 October 2018, was a 2-year return period event based on the storm total only. No peak flow was recorded from this event.

An event beginning on 16 May 2019 and lasting over two days produced 2.4 in (61mm) of total rainfall. It occurred on the falling limb of the hydrograph and produced a small spike in flow at East Bemish Mid. In West Bemish 1 the event caused flow to spike to 6.3 in/day (161 mm/day), the highest level recorded at the site in 2019. This may have been a rain on snow event.

On 15 August 2019, a rainfall event produced 0.3 in (7 mm) in just under 2 hours. The event had an I_{10} of 2 in/day (50 mm/day) and produced a small spike in flow at East Bemish Mid but did not produce a peak flow at East Bemish Upper, West Bemish 1, or West Bemish 2. The crest gauge at East Bemish Lower had been removed during this time by a construction crew working on the culvert.

4.2.3 Lolo Peak Fire

Our rain gauge at the Lolo Peak Fire was in the John Creek watershed where it recorded 3 significant rainfall events during the study period. The site was only visited once during 2019 and once during 2020 due to challenging road access conditions. We were not able to generate a rating curve for this stream and were thus unable to estimate streamflow during these events.

4.2.4 Liberty Fire

One significant rainfall event was recorded in the Liberty Fire burn during the study period, on 8 September 2019. Compared to the data from the same event at Swamp Creek, the event at Liberty was shorter duration (14 hrs) and produced less rainfall (1.5 in [38 mm]). We did not record any measurable peak flow from this event.

4.2.5 Sunrise Fire

The rain gauge installed at Sunrise malfunctioned initially and was then destroyed during salvage logging. No rainfall data was recorded here. This site produced the smallest peak flows during the study period. Rarely was there any measurable peak flow recorded, even after spring runoff. It is possible that a section of unburned forest between the crest gauge and the burned area buffered the peak flow response.

4.3 Ground Cover

Total percent ground cover was lowest at all sites in July 2018 and showed continual recovery in both 2019 and 2020 (Figure 11). The most rapid recovery was seen at the high burn severity sites where total percent ground cover increased from 40% in 2018, 69% in 2019, and 73% in 2020. Total percent ground cover at the moderate and low burn severity sites recovered from 59% in 2018 to 77% in 2020, and from 77% in 2018 to 90% in 2020, respectively.

At both high and low burn severities, sites with a North-East aspect had more ground cover than those with a South-West aspect across all three years (Figure 12). There is an opposite relationship at the moderate burn severity sites, where the South-West aspect had more ground cover than the North-East aspect. Within each burn severity, the differences between North-East and South-West aspect are significant across all three years ($p=0.05$, using a student t-test).

The data was also separated by low and high elevation. Throughout the study, ground cover was greater at low elevation sites than at high elevation sites (Figure 13). The difference between elevations was significant at high burn severity sites, but not significant at moderate burn severity sites ($p=0.05$, using a student t-test).

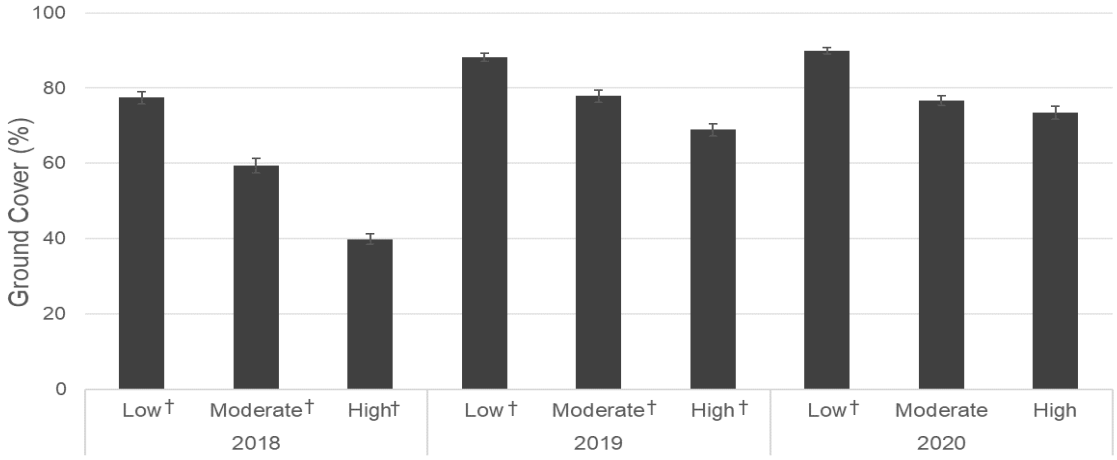

Figure 11: Percent ground cover based on burn severity (low, moderate, high). Ground cover was significantly different at all burn severities in 2018 and 2019 (marked with †). In 2020 the low burn severity sites were significantly different, while the moderate and high burn severity sites were not significantly different from one another.

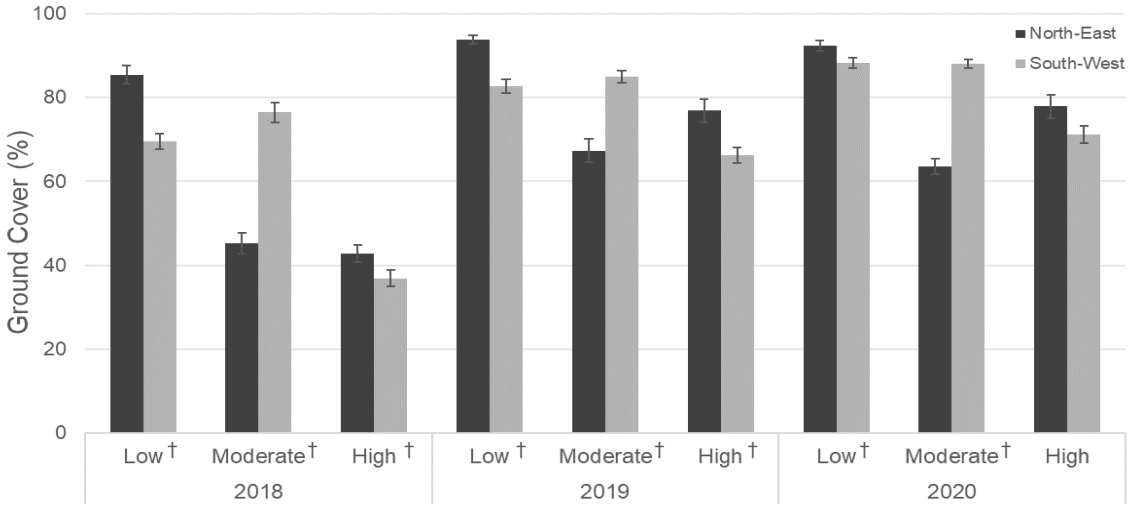

Figure 12: Percent ground cover, separated by aspect (north-east or south-west). Sites were ground cover varied significantly based on aspect are marked with †.

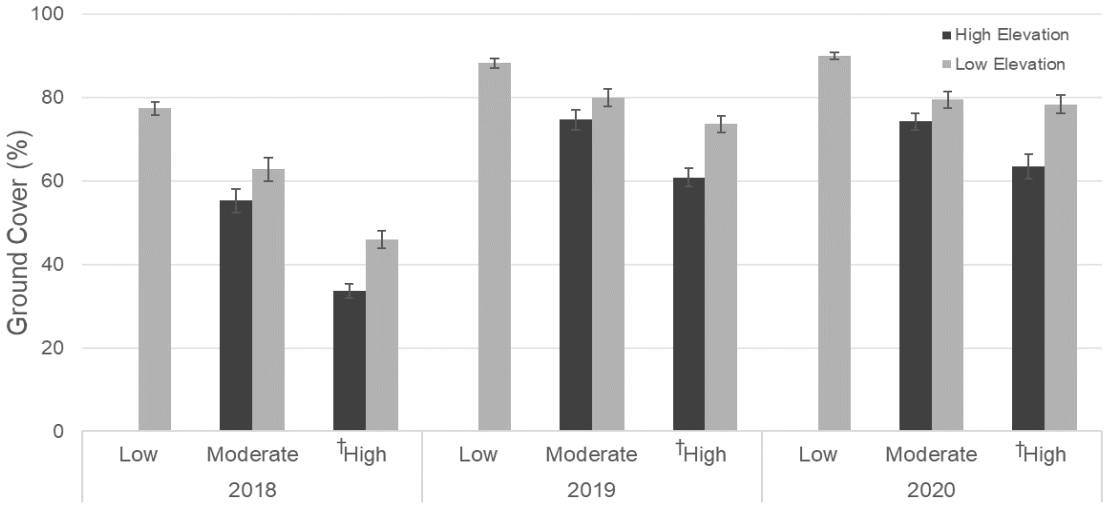

Figure 13: Ground cover data, separated by elevation. High elevation sites were located at or above 5500 ft (1700m), low elevation sites were below 5500 ft (1700 m). Note that no low burn severity, high elevation sites were sampled during the study.

4.4 Watershed Models

4.4.1 WEPPcloud-Disturbed Modification

WEPPcloud-Disturbed was able to better predict annual peak flows using the Quinn (2018) modified parameters than with the default parameters (Figure 14 & Table 13).

Pearson's correlation coefficient improved from $r = 0.37$ ($p<0.05$) to $r = 0.66$ ($p<0.05$) and RMSE improved slightly, from 1.69 to 1.38.

The Nash-Sutcliffe efficiency (NSE) was greatly improved from -0.1 to 0.2 after modification. Modification shifted the model results from "insufficient" into the "sufficient" performance category (Foglia *et al.*, 2009).

Before modification, PBIAS was positive which indicated the model was primarily underpredicting observed peak flows (Table 14). After modification PBIAS becomes negative, indicating the model began to primarily overpredict peak flows.

Table 13: Observed peak annual streamflow versus default and modified WEPPcloud-Disturbed prediction.

		Observed		Predicted - *Default*		Predicted - *Modified*	
Site	Year	mm/day	in/day	mm/day	in/day	mm/day	in/day
Spruce 2	2018	68	2.7	40	1.6	104	4.1
	2019	36	1.4	8	0.3	40	1.6
	2020	27	1.1	11	0.4	92	3.6
Spruce 1	2018	71	2.8	95	3.7	106	4.2
	2020	41	1.6	79	3.1	86	3.4
Nome Creek	2018	74	2.9	89	3.5	101	4.0
	2019	99	3.9	53	2.1	34	1.3
	2020	65	2.5	76	3.0	81	3.2
Dunham East	2018	82	3.2	36	1.4	36	1.4
	2019	54	2.1	36	1.4	36	1.4
	2020	54	2.1	29	1.1	29	1.1
Dunham West	2018	98	3.8	132	5.2	129	5.1
	2019	39	1.5	83	3.3	84	3.3
	2020	39	1.5	81	3.2	81	3.2
Swamp Main	2019	12	0.5	9	0.3	30	1.2
	2020	14	0.6	38	1.5	69	2.7
Swamp Upper	2019	22	0.9	11	0.4	11	0.4
	2020	30	1.2	19	0.8	19	0.8
East Bemish Lower	2018	12	0.5	7	0.3	7	0.3
	2019	12	0.5	26	1.0	28	1.1
	2020	10	0.4	15	0.6	18	0.7
East Bemish Mid	2018	10	0.4	7	0.3	14	0.6
	2019	9	0.4	72	2.8	41	1.6
	2020	10	0.4	23	0.9	32	1.2
East Bemish Upper	2018	29	1.2	7	0.3	32	1.3
	2019	29	1.2	35	1.4	37	1.5
	2020	29	1.2	24	1.0	27	1.0
West Bemish 1	2018	159	6.3	12	0.5	93	3.7
	2019	177	7.0	87	3.4	204	8.0
	2020	80	3.2	31	1.2	162	6.4
West Bemish 2	2018	83	3.3	7	0.3	28	1.1
	2019	84	3.3	36	1.4	44	1.7
	2020	68	2.7	53	2.1	55	2.2

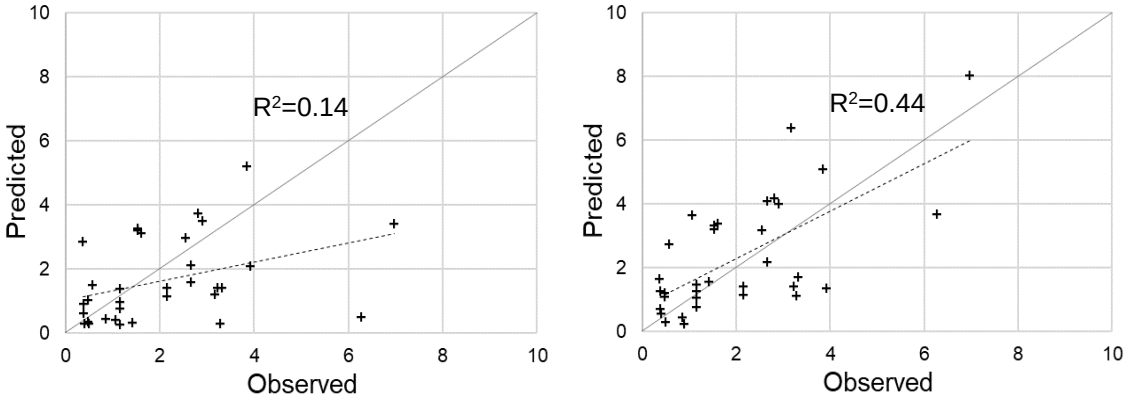

Figure 14: Observed vs Predicted discharge plots for WEPPcloud-Disturbed default values (left) and modified (right).

Table 14: Performance of WEPPcloud-Disturbed for annual peak flows.

Uncalibrated				Calibrated			
Pearson's	RMSE	NSE	PBIAS	Pearson's	RMSE	NSE	PBIAS
0.37	1.69	-0.12	21	0.66	1.38	0.19	-14

Another important result of modifying K_{eff} is that the model responds more realistically to rainfall-generated runoff events as well as to spring snowmelt events. While the default model does capture spring runoff, it does not respond at all to the summer rainfall events observed during the study. After modifying the hydraulic conductivity, the model does show a spike in runoff during spring snowmelt, but it also responds to rainfall events during the dry summer months (Figure 15 & Figure 16).

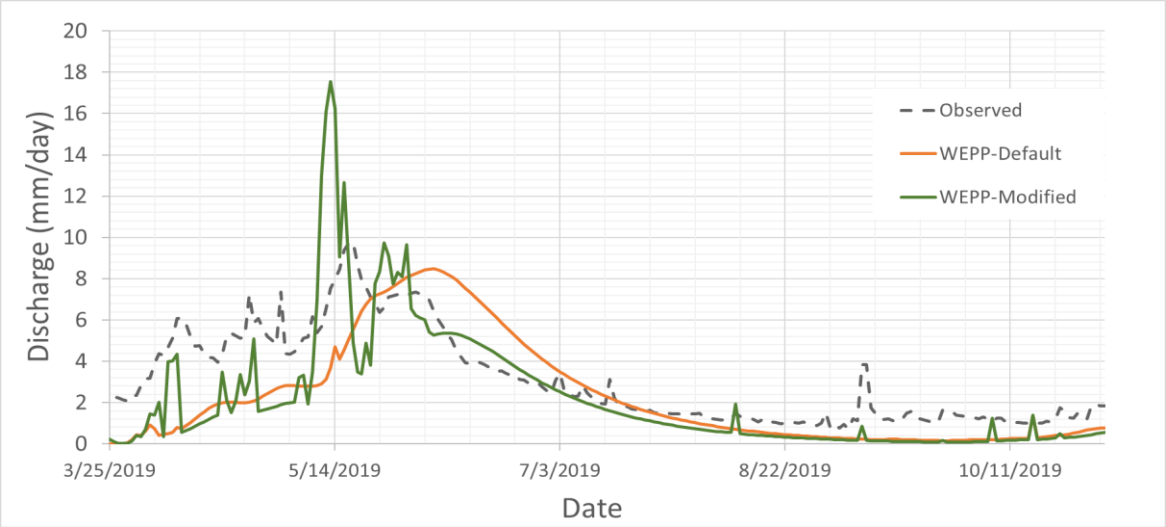

Figure 15: Hydrograph comparing observed streamflow at Swamp Creek with default WEPPcloud-Disturbed and WEPPcloud-Disturbed after modifying K_{eff}.

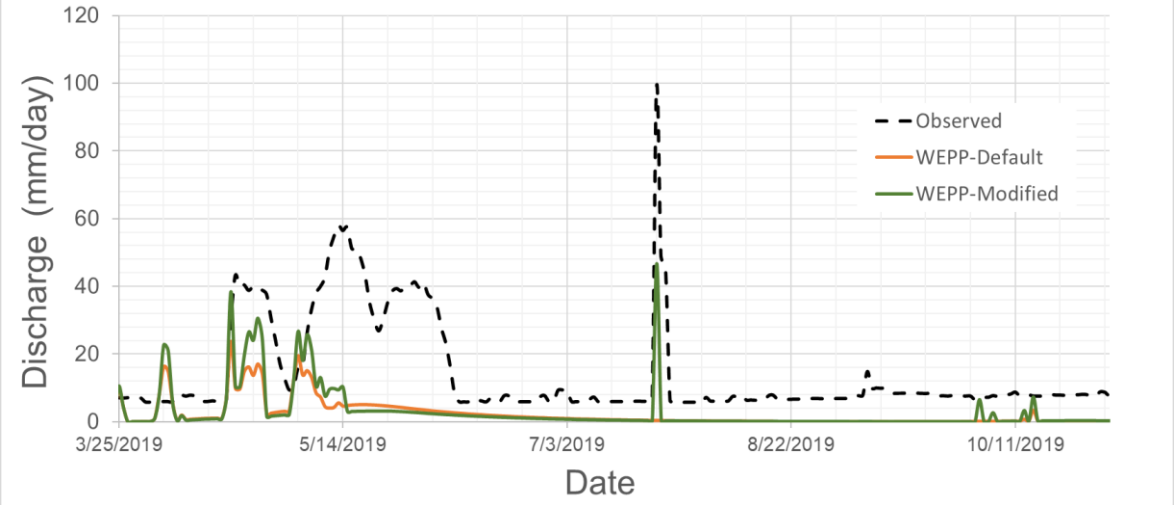

Figure 16: Hydrograph comparing observed streamflow at Nome Creek with default WEPPcloud-Disturbed and WEPPcloud-Disturbed after modifying K_{eff}.

4.4.2 Return Period Analysis

Values for the 2, 5, 10, and 25-year annual peak flow return interval at each watershed were calculated with each model (FireHydro, StreamStats, WEPPcloud-PEP, and WEPPcloud-Disturbed with modified K_{eff}). A summary of the output is presented in Table 15, with detailed output found in Table A3-Table A6.

In the pre-fire (i.e. unburned) condition WEPPcloud-PEP predicted much larger peak flows than the other three models, averaging between 4.3-6.8 in/day (110-172 mm/day) (Figure A7). The smallest pre-fire values were predicted by WEPPcloud-Disturbed at 0.2-0.7 in/day (6-18 mm/day), while FireHydro and StreamStats predicted values between 0.2-2.0 in/day (4-52 mm/day).

In the post-fire condition FireHydro and WEPPcloud-PEP predicted the largest average peak flows of between 3.5-10.4 in/day (89-265 mm/day) (Figure A8). WEPPcloud-Disturbed predicted post-fire flows between 2.2-3.4 in/day (57-86 mm/day), and StreamStats predicted the lowest flows of 1.0-3.2 in/day (24-81 mm/day).

Table 15: Average pre and post-fire peak flow predictions. These values are the average of the 2, 5, 10, and 25-year return intervals predicted by each model. See Table A3-Table A6 for more detailed output.

	FireHydro				StreamStats				WEPPcloud-PEP				WEPPcloud-Disturbed			
	Pre		Post		Pre		Post		Pre		Post		Pre		Post	
Fire	in/day	mm/day	in/day	mm/day	in/day	mm/day	in/day	mm/day	in/day	mm/day	in/day	mm/day	in/day	mm/day	in/day	mm/day
Rice Ridge	0.4	9	5.3	134	1.1	27	1.9	47	5.9	151	6.4	162	0.4	9	3.3	85
Liberty	1.9	48	10.4	265	2.0	52	3.2	81	6.8	172	7.5	191	0.7	18	3.2	81
Sheep Gap	1.1	28	5.7	144	0.7	18	1.3	32	4.7	119	7.2	182	0.3	8	3.0	76
Lolo Peak	0.2	4	5.2	132	0.8	20	1.4	35	5.4	138	5.9	150	0.3	8	2.2	57
Sunrise	0.6	15	3.5	89	0.6	16	1.0	24	4.3	110	8.5	217	0.2	6	3.4	86

Used as is, these models are each unique from one another. They use different equations, processes, and variables which ultimately results in the notable variability of their outputs and makes it difficult to directly compare one model to the other. But because the same burn scenarios are applied across each model run, we can compare how sensitive the models are to wildfire by using the relative difference in peak flow prediction between the unburned and burned scenarios. A summary of the average increase is presented in Table 16.

At 14 of the 18 study sites FireHydro was most sensitive to the burned condition, with peak flows increasing by up to 10-12 in/day (254-305 mm/day), or 6000% at some locations (Figure A9). This level of sensitivity to burning resulted in FireHydro simulating the largest post-fire peak flow of all models compared in this study.

WEPPcloud-Disturbed was also quite sensitive, though not to the same degree as FireHydro. At one location, Dunham West, the model predicted a 3000% increase in peak flow, while the remaining sites increased by <2000%. Even with flows increasing by sometimes 10-15x, their magnitude was still less than those predicted by FireHydro or WEPPcloud-PEP.

StreamStats predicted the overall lowest change in peak flow, between 9-100%. Because the StreamStats output was simply modified relative to the percent area burned at moderate and high severity, those two values will be equivalent. Meaning, if a watershed was burned at 50% moderate + high severity, the flow will increase by 50%. If the watershed was burned at 100% moderate + high severity, the flow will increase by 100%. With the modifier used in this study, flow will never increase by more than 100%.

Finally, WEPPcloud-PEP was by far the least sensitive to burning, often increasing by <10%. Still, the magnitude of WEPPcloud-PEP's flow predictions are among the highest of all four models indicating that it is likely overpredicting peak flow, especially for pre-fire conditions.

Table 16: Average percent (%) increase in peak flow from pre to post-fire. This is the average of each individual watershed within the given fire.

	FireHydro	**StreamStats**	**WEPPcloud-PEP**	**WEPPcloud-Disturbed**
Fire	**% increase**	**% increase**	**% increase**	**% increase**
Rice Ridge	2390%	63%	7%	1182%
Liberty	806%	56%	10%	359%
Sheep Gap	867%	76%	45%	863%
Lolo Peak	4311%	77%	8%	587%
Sunrise	550%	52%	79%	1442%

5 Discussion

5.1.1 Precipitation

The precipitation data recorded over three years of study suggests there are differences in rainfall/storm characteristics across the region. While understanding precipitation patterns is difficult, as it involves the complex interaction of atmospheric and topographic factors, we know that topography can have a significant impact on both regional (Buytaert *et al.*, 2006; Rotunno and Houze, 2007) and smaller catchment scales (Kirshbaum *et al.*, 2007; Colle, 2008).

A total of 15 rainfall events were recorded that met or exceeded a 2-year precipitation event. The average storm recorded was 20 hrs, and most study areas recorded at least one storm that met or exceeded that duration. Rice Ridge-Dunham Creek and Liberty were the only areas where no storm events exceeded 20 hrs. Even though the only >2-year storm recorded at Liberty had a 14 hr duration, the same event was captured at other study sites with durations greater than 20 hrs. This suggests that the 8 September 2019 storm was indeed a large frontal long-duration rainfall event that impacted a large portion of the other study areas as well.

Rice Ridge-Dunham Creek was the only area where no multi-hour rainfall events were recorded. In fact, three of the four most significant high intensity, short duration rainfall events that were recorded during the study occurred at Dunham Creek. The fourth significant event occurred at Lolo Peak. This study area also produced the single highest rainfall intensity recorded on 23 July 2019.

The Rice Ridge-Dunham Creek area is unique in that it is the eastern-most study area, and it is surrounded by high mountain peaks and ridges. Though the Swamp Creek area is just 6 mi (10 km) from Dunham Creek it’s topography is much different, opening into the large Seeley Lake valley to the west (Figure 17). Kirshbaum et al., (2007) found that topographic features such as mountains and ridgelines oriented with certain perpendicular relationships to an atmospheric flow pattern can “trigger” the growth of convective storms. It is possible that the windward topography at Dunham Creek is such that it does trigger orographic uplift when atmospheric conditions are right, thus increasing the probability of concentrated storms.

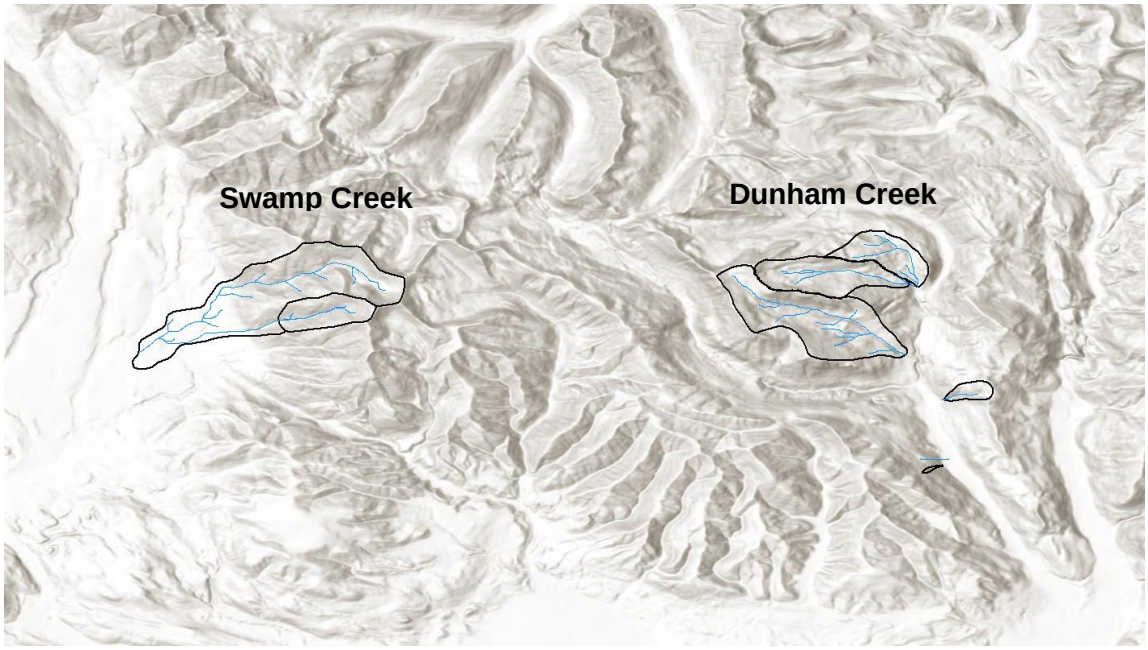

Figure 17: Topography of the Rice Ridge-Swamp Creek and Dunham Creek study areas. Black outlines denote study watershed boundaries. The distance between Swamp Creek and Dunham Creek is roughly 7 miles (11.5 km).

While short-duration (≤30-min) rainfall intensity seems to be the most important factor triggering runoff-generated debris flows in the first three years following wildfire, the intensity threshold beyond which a rainfall event may produce debris flows is difficult to identify and can vary greatly from region to region (Thomas *et al.*, 2021). Soil type, vegetation cover, antecedent soil moisture, time since burning, and the intensity characteristics of a given storm also impact whether large peak flows or debris flows will occur during a rainfall event.

After fires in 1984 and again in 2000, debris flows were recorded in this region following short duration rainfall events (Parrett, 1987; Parrett *et al.*, 2004). The debris flow event in July 2019 illustrates that this region is certainly capable of generating high intensity, destructive rainfall. While debris flow events may be relatively rare, the potential consequences of a high-intensity convective rainfall event can be significant in burned areas of Western Montana.

5.1.2 Peak Flows

Past research has shown that streamflow in this region tends to be snowmelt dominated (Pederson *et al.*, 2011), and we observed similar trends during this study. Although peak

flows caused by snowmelt can be well over 100% of the pre-fire flows (Seibert *et al.*, 2010; Niemeyer *et al.*, 2020), the effect on rainfall generated runoff can be much more significant, increasing by several orders of magnitude (Moody and Martin, 2001; Springer and Hawkins, 2005).

The largest unit peak flows were observed in the smallest watersheds suggesting that smaller watersheds respond more dramatically to rainfall events, especially under burned conditions (Gartner *et al.*, 2004; Neary *et al.*, 2005; Stoof *et al.*, 2012). It may also be representative of the fact that most runoff-generating rainfall events were relatively small in geographic size, thus a greater proportion of smaller watersheds would produce runoff compared to a larger watershed.

Few rainfall events generated measurable peak flows in any of our watersheds. While it is possible that these events were simply not significant enough to produce runoff, it is also possible that the resolution of our crest gauges was too low to capture and record them. Many of our gauges were installed during peak flow in 2018, near the edge of the active channel. After spring runoff, the water level would drop below the bottom of the crest gauge. Once this occurred, we were unable to capture any fluctuations in streamflow through much of the summer, unless the water level rose at least to the level of the crest gauge. It is likely that small fluctuations in streamflow did occur from these smaller summer storms, but the flow never got high enough to register on the crest gauge.

5.1.3 Groundcover

We collected ground cover data to compare results to the Soil Burn Severity (SBS) maps generated post-fire. Our field observations of ground cover generally agree with Parsons et al. (2010), which provides rough guidelines as to expected groundcover based on burn severity class (Table 17). Because our first measurement was taken nearly a year after burning, we would expect groundcover to be higher after even just one spring/summer of recovery. So, for example, we measured 40% ground cover at high severity sites. This is a reasonable estimate through one season of recovery, even though high severity sites might have only 20% immediately after burning.

Table 17: Expected groundcover based on burn severity class from Parsons et al. (2010). These are assumed immediately after the fire.

	Low Severity	Moderate Severity	High Severity
Ground Cover (%)	>50	20-50	<20

A distinct trend was noted at moderate burn severity sites between those with a North-East vs South-West aspect. Sites with a South-West aspect had significantly higher ground cover than those with a North-East aspect. In fact, sites burned at a moderate severity with a South-West aspect are much more similar to the sites burned at low severity, while those with a North-East aspect are similar to the average high burn severity site. This pattern is present across all three years of study.

Previous studies using satellite imagery to estimate post-fire burn severity have found groundcover was bimodally distributed in the first year post-fire, with low severity and moderate severity sites comparable to one another while high severity sites were distinctly different (Lewis *et al.*, 2017; Quintano *et al.*, 2017). This pattern was observed for those sites with a South-West aspect, but the pattern was essentially reversed for sites with a North-East aspect, and can be seen clearly in either Figure 12. Instead of low and moderate severities looking similar, it is the moderate and high severity sites that look similar while the low severity sites are distinctly different.

While the consequences of overestimating burn severity may result in applying unnecessary treatments and thus not wisely utilizing limited mitigation funding, the consequences of underestimating burn severity could be much more severe. For example, managers on the Lolo National Forest noted that burn severity in the Spruce 1 watershed (where the 2019 debris flow occurred) was likely underestimated, and resulted in a much more significant hydrologic response than was predicted during the initial BAER modeling (Walters *et al.*, 2019). Over half of the area in this watershed is made up of hillslopes with a north aspect (Figure A5) which, based on our cover observations, may have resulted in them being marked as moderate burn severity when high burn severity was more representative. Had this watershed been marked with a high burn severity instead of moderate, managers may have elected to treat it which could have mitigated the effects of the debris flow.

5.1.4 WEPPcloud-Disturbed Modification

The results of this analysis support findings from Quinn (2018), noting that effective hydraulic conductivity (K_{eff}) is a key parameter in predicting post-fire streamflow, and that WEPP requires a significant reduction of K_{eff} in order to represent certain post-fire runoff characteristics.

After calibrating the full suite of parameters (bulk density, effective hydraulic conductivity, anisotropy, field capacity, wilting point, organic matter, interrill erodibility, and rill erodibility) Quinn (2018) found the model predicted peak flow with an average NSE of 0.5 over 3 years of study. We were able to show that by simply modifying K_{eff} was enough to increase NSE from -0.1 to 0.2. With a larger dataset that allowed us to conduct a full calibration at these field sites, the model's predictive ability would likely increase further. These results suggest that WEPPcloud-Disturbed relies heavily on hydraulic conductivity as an input parameter that drives runoff generation and, at this time, using the modified values may be necessary to produce reasonable results when modeling post-fire streamflow.

5.1.5 Return Period Analysis

FireHydro (Curve Number method), StreamStats (USGS Regression method), and the WEPPcloud interfaces are each unique in their predictive ability and scope of application. It is critical that users have a certain level of background knowledge in order to understand these differences and to know when each tool should be used. Though their outputs look similar (a list of 2,5,10, and 25-year peak flows), the scenarios they are meant to represent are not necessarily identical. The comparison presented here highlights some notable differences between the models and how those differences should guide the interpretation of their results.

5.1.5.1 FireHydro

The Runoff Curve Number methodology implemented by FireHydro is well established as a way to predict direct runoff from rainfall events, but it makes several generalizations about watershed conditions that are important to understand. By assuming that the watershed is a uniform shape, slope, and burn severity, it neglects the importance of critical source areas on runoff generation (Boll et al., 2015). Even in unburned conditions, it is unlikely that the

entirety of a watershed contributes an equal amount of surface runoff at the outlet. Even within its stated maximum watershed size of 2000 acres (800 hectares), there can be significant variability in burn severity, hydrophobicity, slope steepness, etc. (Robichaud, 2000; Sheridan *et al.*, 2007; Moody *et al.*, 2013). This level of hydrologic simplification may be reasonable if the watershed is very small with considerable homogeneity in burn severity, but this is not the case in many post-fire scenarios.

FireHydro also uses a unit peak discharge method for precipitation inputs which essentially assumes a “worst case scenario” rainfall event, where the storm duration is equal to the watersheds time of concentration (the time it takes for a water molecule to travel from the hydrologically furthest point of the watershed to the outlet) and that the event occurs evenly across the entire watershed. This results in the highest possible peak flow for a given rainfall intensity. We know that high intensity rainfall events in this region tend to be quite short in duration (<30 minutes), so this may not be a reasonable assumption for many mid-size to large-size watersheds where the time of concentration can exceed 1 hour.

Lastly, selecting a proper curve number remains fraught with uncertainty. Though many forest managers have created guidelines for post-fire curve number selection, it is unclear how accurate or widely applicable the guidelines are as few site-specific studies have been published. The Curve Number method is useful in urban and agricultural areas, but it is often inaccurate in both unburned (Hawkins, 1993; Ponce and Hawkins, 1996; McCutcheon, 2003; Springer and Hawkins, 2005; Tedela *et al.*, 2012) and burned forest watersheds (Chen *et al.*, 2013; Soulis, 2018). Therefore, relying on the Curve Number method will likely result in inaccurate peak flow predictions without significant calibration at individual watersheds.

These issues become apparent when comparing the return period predictions made by FireHydro (Table A3-Table A6) to our observed annual peak flows. Keeping in mind that FireHydro only predicts rainfall-generated peak flows, the predictions were generally much higher than anything measured in the field during peak spring runoff, and were certainly higher than what was observed during most rainfall events. Ultimately, post-fire managers must decide whether this approach is suitable, relative to the complexity of conditions in their burned scenario.

5.1.5.2 StreamStats

The regression equations used in the Montana StreamStats application are well documented (USGS, 2016a), though little has been published on its applicability in the post-fire environment. The method relies on many of the same assumptions presented above meaning it does not address the complexity of variable burned conditions, and it relies on the user to select an appropriate scaling factor to represent post-fire hydrologic changes. The use of a 2x modifier for moderate and high burn severity means that the post-fire flow will only ever be 100% larger than the pre-fire flow, even in the most severe burned conditions. This “ceiling” on the magnitude of increase results in StreamStats being among the least responsive models to burning.

The two most sensitive parameters for StreamStats’ predictions are annual precipitation and watershed size (Sando *et al.*, 2018). This means that either annual variability or shifts in long term precipitation trends could result in significant model error, especially in smaller watersheds such as those in this study. If the basin characteristics of a given watershed vary significantly from those used the regression development, the results are likely to be unreliable (McCarthy *et al.*, 2016b). For example, the 53 basins used to generate the equations representing the sites in this study (Western hydrologic region) had areas between 6.4 mi^2 [16.4 km^2] and 2516 mi^2 [6516 km^2], much larger than the watersheds analyzed in this study. For many of the smaller mountain stream crossings that are frequently impacted by fire, modeling with StreamStats may not be the best option.

It is also important to recognize that the output values from StreamStats represent an entirely different set of peak-flow scenarios than FireHydro. While FireHydro only predicts rainfall-generated runoff, StreamStats simply predicts annual peak flow, whether that flow is generated by rainfall or snowmelt. So, because streamflow in this region is dominated by spring snowmelt, the peak flows predicted by StreamStats should be interpreted a spring runoff, not as rainfall-generated runoff. If managers’ primary concern is high-intensity summer rainfall events, then StreamStats would be inappropriate to use for peak flow predictions. If users are interested in changes in the overall annual streamflow regime, and if the watershed is of the appropriate size, StreamStats may be an effective tool to make rough hydrologic predictions.

5.1.5.3 WEPPcloud-PEP and WEPPcloud-Disturbed

Even though WEPPcloud-PEP and WEPPcloud-Disturbed employ the same base WEPP model processes, they use different input parameters which results in notably different simulated outputs. WEPPcloud-PEP uses an older WEPP soil file format (version 2006.2) that assumes a single soil layer with a standardized 15 in (400 mm) soil depth for all burned conditions. This limits both soil-water storage and losses to groundwater seepage which results in unrealistically elevated volumes of runoff and lateral flow that cause massive spikes in peak streamflow (Figure 18). In this simulation, the majority of runoff occurs very early in the spring, ending by late February or early march. Though earlier snowmelt is expected after wildfire (Seibert *et al.*, 2010; Gould *et al.*, 2016), the change should shift only by days or weeks, not months. Ultimately WEPPcloud-PEP did not appropriately represent the saturation-excess runoff scenarios that occur during spring.

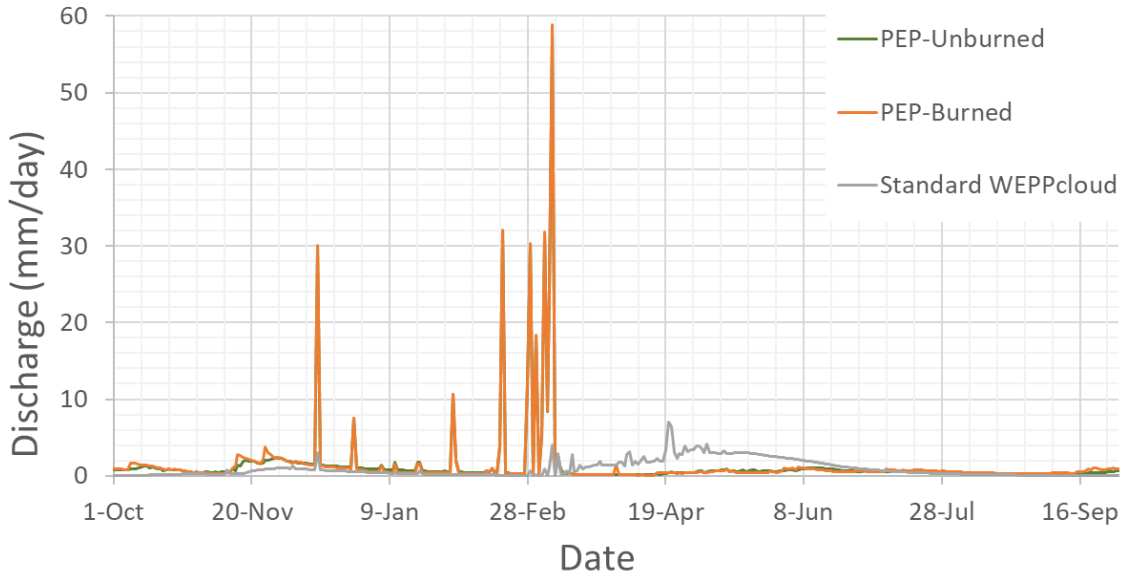

Figure 18: Example hydrograph comparing both a burned and unburned scenario ran with WEPPcloud-PEP with a standard (i.e. unburned) WEPPcloud run. WEPPcloud has been validated for use in snow-dominated watersheds by Srivastava et al., (2017). *Note that the green line (PEP-Unburned) tracks perfectly with the orange line (PEP-Burned) during the highest spikes indicating that there is very little difference between the burned and unburned scenarios.

Contrasting WEPPcloud-PEP, WEPPcloud-Disturbed uses the standard SSURGO soil input parameters and simply modifies the values for saturated hydraulic conductivity, rill erodibility, and interrill erodibility, all of which are altered by wildfire. Another critical difference is that WEPPcloud-PEP reduces soil depth on all burned hillslopes to 15 in (400

mm), while WEPPcloud-Disturbed does not alter the depth of burned soils. The resulting peak flow predictions from WEPPcloud-Disturbed (Table A3-Table A6) are more representative of the peak flows observed during this study.

While streamflow during spring runoff is still noticeably flashy, the magnitude of the peaks predicted by Disturbed is much less than WEPPcloud-PEP (Figure 19). The overall duration of snowmelt is shorter than the unburned scenario while still extending through mid to late spring, which would be expected under burned conditions.

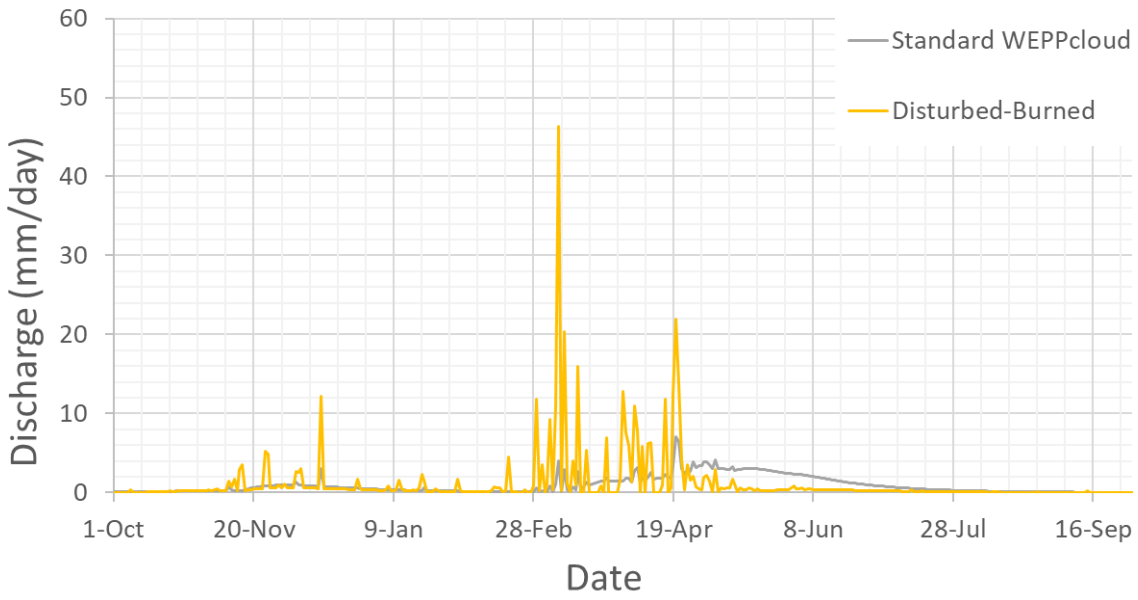

Figure 19: This is the same example hydrograph scenario from Figure 18, but comparing the unburned WEPPcloud output with a burned scenario from WEPPcloud-Disturbed. *Note that output from Standard WEPPcloud is identical to the output from running WEPPcloud-Disturbed in an unburned condition.

It is important to recognize that this study only modified hydraulic conductivity for the first-year post-fire; it was not adjusted to represent the successional hydrologic recovery of the watershed in years two and three of the study. Therefore, the model tending to overpredict observed peak flows (PBIAS=-14) is expected. Further research with more complete streamflow datasets is necessary to quantify the annual hydrologic recovery of these types of small, high elevation watersheds which would lead to a more thorough calibration of WEPPcloud-Disturbed.

Numerous studies have validated WEPP for modeling streamflow in forested watersheds (Covert *et al.*, 2005; Pieri *et al.*, 2007; Dun *et al.*, 2009; Brooks *et al.*, 2016; Srivastava *et al.*, 2017, 2020) but few have done this for post-fire conditions (Quinn, 2018). The results from this study indicate that WEPPcloud-Disturbed is able to predict post-fire peak flows with at least sufficient accuracy (NSE=0.2) with the simple modification/calibration of effective hydraulic conductivity.

6 Conclusion

After 5 wildfires in 2017, peak streamflow was monitored for three years at 17 culverts in burned watersheds spread throughout the Lolo National Forest in Western Montana. We found that peak annual flow occurred during spring runoff in all cases except for one short duration, high intensity rainfall event that caused large peak flows and debris flows in 3 watersheds. While other rainfall events were recorded throughout the study area, none were significant enough to generate large, measurable peak flows. We also found that short duration, high intensity convective rainfall events occurred most frequently in the eastern portion of the study area, whereas long duration, low intensity events were more common to the West. Because of this, it might make sense for managers to prioritize the eastern portion of the forest for post-fire treatments if faced with a restrictive budget or other resources.

Groundcover measurements suggested that aspect had an impact on burn severity. Within sites defined by the SBS map as moderate burn severity, we found that North-East facing hillslopes had significantly less vegetation cover than hillslopes facing South-West. This may be a result of greater pre-fire vegetation and fuel density on North-East hillslopes which lead to higher burn severity than the less vegetated South-West slopes.

We then compared streamflow predictions from four different hydrologic models. FireHydro and StreamStats are empirically based models that either oversimplify watershed conditions, have constraints on applicable watershed characteristics such as basin size, or are unable to predict runoff from spring snowmelt. They physically based WEPPcloud-PEP model uses simplified soil and landuse parameters which result in an inability to predict streamflow during certain conditions such spring snowmelt. WEPPcloud-Disturbed on the other hand uses more detailed and representative SSURGO soil parameters to represent burned conditions. Without modification, the default values provide accurate results during spring snowmelt though they do not accurately represent infiltration excess runoff, but by further reducing the effective hydrologic conductivity the model can predict runoff from both rainfall and snowmelt events. These results suggest that WEPPcloud-Disturbed likely represents the most useful and efficient method for conducting hydraulic analyses and making post-fire treatment prescriptions.

7 Fire Effects on Fish Populations

As wildfires continue to increase in size, severity, and frequency (Westerling *et al.*, 2006; Dennison *et al.*, 2014; Parks and Abatzoglou, 2020) post-fire mitigation efforts have become increasingly widespread and, critically, much more expensive (Robichaud *et al.*, 2014). Post-fire treatments implemented by the U.S. Forest Service Burned Area Emergency Response (BAER) program focus primarily on mitigating issues of increased runoff, erosion, flooding, and debris flows, all of which may result in damaged forest infrastructure (i.e. roads, buildings, etc.) and can limit access to public lands. Of course, these are not the only values that are at risk after a wildfire. Severe aquatic habitat degradation often occurs in burned-over riparian zones resulting from lost vegetation cover, decreased water quality, changes in flow regime, among other factors. BAER treatments often neglect to directly address degraded fish habitat, focusing more on land and road treatments (Robichaud *et al.*, 2014). Because of this, there is great need for the integration of post-fire land management and aquatic habitat restoration strategies.

Wildfire has been shown to have both direct and indirect impacts on fish populations. Direct impacts such as increased stream temperature and changes in water chemistry can directly cause fish mortality during and immediately following wildfire (Minshall *et al.*, 1989; McMahon and DeCalesta, 1990; Hitt, 2003). The indirect effects of wildfire include changes in hydrologic flow regime, increased erosion and sediment transport, altered channel substrate size and quality, and changes in woody debris and riparian vegetation cover (Amaranthus *et al.*, 1989; Megahan, 1991; Bozek and Young, 1994; Benda *et al.*, 2003; Burton, 2005)

In the Northern Rocky Mountain region, many fish species of interest such as Westslope Cutthroat Trout (*Oncorhynchus clarkii lewisi*), Yellowstone Cutthroat Trout (*Oncorhynchus clarkii bouvieri*), Bull Trout (*Salvelinus confluentus*), and Steelhead (*Oncorhynchus mykiss*) are able to sustain populations in fire prone environments under natural disturbance regimes (Thorpe, 1994; Willson, 1997). In fact, these species may rely on fire as a natural disturbance that maintains the general health of their aquatic ecosystem. The short-term effect of wildfire is often observed fish mortality due to increased stream temperature both during and after the fire (Gresswell, 1999; Isaak *et al.*, 2010) as well as elevated erosion and sediment loading during large runoff and debris flow events (Bozek and Young, 1994; Brown

et al., 2001; Benda *et al.*, 2003) The long term effect on the other hand is thought to be positive. Increased runoff, erosion, and mass wasting events supply the stream with large woody debris and sediment that leads to greater stream heterogeneity and ultimately provides a more complex, diverse, and healthy habitat (Brown, 1989; Reeves *et al.*, 1995; Rieman and Clayton, 1997; Gresswell, 1999; Benda *et al.*, 2003; Bisson *et al.*, 2003; Kirkland *et al.*, 2017).

7.1.1 Habitat Connectivity and Life History

Rieman et al. (1997) found that Bull Trout and Rainbow Trout may have been entirely extirpated from some streams immediately following wildfires in the 1990s due to a combination of the aforementioned effects. In this study, both species of fish were able to recolonize the defaunated stream reaches within 1-year post-fire. In some cases, fish densities became more abundant than they had been before the fire, though the increase was primarily in populations of younger fish. The rapid recovery was attributed to high levels of connectivity between areas of high severity burn and adjacent areas of low severity or unburned conditions, as well as connectivity to suitable habitat much further downstream or in separate tributaries. The unburned areas acted as refugia, allowing the fish to escape and survive until conditions recovered (i.e. reduced levels of suspended sediment, recovered riparian vegetation and shading, etc.) and they were able to move back into the heavily impacted streams. Had fish barriers existed between the downstream region where the adult fish were living and the headwaters spawning grounds, the Bull Trout may not have been able to successfully re-establish in this system.

There is also evidence (Novak and White, 1989; Sheldon and Meffe, 1995; Rieman and Clayton, 1997; Sloat *et al.*, 2014) that fish populations, especially in regions prone extreme disturbance (like wildfire) maintain non-residential, or migratory life histories. Rieman et al. (1997) observed a rapid recovery of young Bull Trout in in a stream reach that was presumed defaunated a year earlier. After spotting 5 large (>400 mm) Bull Trout just downstream, the authors concluded that these were non-resident adult fish had moved out of the system prior to it burning but had returned shortly after to spawn, thus repopulating the stream. This is an example of how fish species have adapted to survive in a fire prone landscape.

The above study is an example of successful recovery because of suitable habitat connectivity before the fire, but there are also examples of recoveries that were unsuccessful due to insufficient habitat connectivity. Following wildfires in the late 1980s and early 1990s (Divide Fire, 1989; Bonner Fire, 1995; Lookout Fire, 1996) populations of Gila Trout (*Oncorhynchus* gilae) were completely eliminated from several remaining strongholds in the Southwestern U.S. (Propst *et al.*, 1992; Propst and Stefferud, 1997; Brown *et al.*, 2001). These extirpations occurred where the trout populations were isolated in relatively small area of designated wilderness on federal land. When the watersheds burned, BAER teams took action to protect trail systems from accelerated erosion to prevent “deterioration of water quality” in trout streams (USFS, 1997). This alone was not enough. The trout were unable to escape either the direct impacts of stream temperature increases, or the indirect impact of sediment and wildfire ash pulses resulting from monsoonal rains. Brown et al. (2001) found that increasing stream length (i.e. habitat connectivity to refugia) could have increased the chances of survival for these fish populations.

Generally, forest management practices such as logging, livestock grazing, agriculture, and urban-type development have led to stream conditions that cut-off potential fish habitat through the construction of barriers such as impassable culverts, or that isolate fish populations above barriers in habitat fragments too small to support them (Hilderbrand and Kershner, 2000). It is this type habitat isolation that may can lead to fish recovery issues following wildfire.

7.1.2 Natural Fire Regime

A second finding of the Gila Trout study was that changes to the natural fire regime may have played an even more important role in the observed extirpation. Where the natural fire regime in this region had been one of relatively frequent and cool-burning fires, human intervention increased the potential for more catastrophic, high severity crown fires. Ultimately it was this type of wildfire that lead to the Gila Trout being eliminated from the burned areas. Brown et al. (2001) found that reducing the risk of catastrophic wildfire by even a small amount could lead to substantial reductions in the risk of fish extirpation. Unfortunately, reducing the risk of catastrophe is unlikely considering the observed increases in the scale and severity of wildfire over the past 2 decades (Westerling *et al.*, 2006; Littell *et al.*, 2010; Dennison *et al.*, 2014)

7.1.3 Post-Fire Management

Current post-fire assessment and treatment strategies used by the Burned Area Emergency Response (BAER) program focus on mitigating the negative effects of wildfire on human life and safety, property, natural resources, and cultural and heritage resources (Table 18). BAER treatments are broken into four categories:1) Land Treatments, 2) Channel Treatments, 3) Road and Trail Treatments, and 4) Public Protection and Safety Treatments (Napper, 2006). Prescription of these treatments is based on an assessment of the fire's effect on watershed function and "whether these effects will threaten life, safety, or property, or cause degradation to natural or cultural resources" (Napper, 2006). During the assessment, a BAER team evaluates 21 different items in order to identify the values at risk as a result of the wildfire (Table 19).

Table 18: Critical Values listed in the Burned Area Emergency Response Interim Directive (USFS, 2018)

Critical Values to be Considered During Burned-Area Emergency Response

CRITICAL VALUES
HUMAN LIFE AND SAFETY
Human life and safety on National Forest System (NFS) lands.
PROPERTY
Buildings, water systems, utility systems, road and trail prisms, dams, wells or other significant investments on NFS lands.
NATURAL RESOURCES
Water used for municipal, domestic, hydropower, or agricultural supply or waters with special Federal or State designations on NFS lands.
Soil productivity and hydrologic function on NFS lands.
Critical habitat or suitable occupied habitat for federally listed threatened or endangered terrestrial, aquatic animal, or plant species on NFS lands.
Native or naturalized communities on NFS lands where invasive species or noxious weeds are absent or present in only minor amounts.
CULTURAL AND HERITAGE RESOURCES
Cultural resources which are listed on or potentially eligible for the National Register of Historic Places, Traditional Cultural Properties, or Indian Sacred Sites on NFS lands.

Table 19: List of assessment items used by BAER teams to identify Values at Risk, taken from Napper (2006).

- Amount and distribution of high- and moderate-burn severity within each watershed.
- Presence and extent of water-repellent soils.
- Presence and extent of effective soil cover.
- Potential needle-cast from existing vegetation.
- Vegetative recovery timeframe and potential for noxious and invasive plant spread.
- Flood-prone areas and downstream effects.
- Debris-prone areas and downstream effects.
- Flood-source areas and downstream effects.
- Potential for stream diversion at trail and road crossings.
- Channel stability and riparian vegetation conditions.
- Potential for increased erosion or sedimentation.
- Potential for water quality deterioration.
- Barriers to natural water flow (e.g., fencing, stockponds, dams).
- Physical hazards at campgrounds, trailheads, and facilities.
- Capacity and condition of structures at stream crossings.
- Condition of road infrastructure including signs, guardrails, and road delineators.
- Potential hazardous materials contamination created or exposed by the fire.
- Downstream values outside the fire perimeter that may be at risk.
- Potential impacts on road and trail prisms to increased erosion and runoff from adjacent hillslopes.
- Access needs on routes throughout the burned area to facilities, residences, and campgrounds.

Note that while “Critical habitat or suitable occupied habitat for federally listed threatened or endangered terrestrial, aquatic animal, or plant species on NFS lands” is listed as a critical value, there are no assessment items that directly address a fires impact on fish/aquatic-animal habitat. Still, Robichaud et al. (2014) found that 40% of BAER projects between 1972-2009 cited “threatened and endangered (T and E) species” as a risk to be mitigated using BAER funds (Table 20). It is unclear what proportion of the T and E species of concern in the BAER reports were either plants or animals, but it is likely that the 40% is a combination of the two. The authors do note that protection of Bull Trout likely contributed, in part, to the frequent selection of water quality as a treatment justification in Regions 1, 4, and 6.

Table 20: Table 3 from Robichaud et al. (2014) showing the proportion of Burned Area Reports that selected each value at risk category as justification for post-fire treatment expenditures by both

	Values-at-risk category				
	Life (%)	Property (%)	T and E species (%)	Water quality (%)	Soil productivity (%)
Decade					
1970s	3	41	1	39	24
1980s	2	36	6	40	31
1990s	16	45	19	44	42
2000s	42	61	25	40	63
Region					
1	48	**28**	39	**61**	24
2	43	4	35	55	17
3	42	11	25	40	23
4	**58**	**29**	36	**63**	**36**
5	**59**	16	**45**	45	**32**
6	**56**	**26**	**59**	**64**	**31**
Mean	51	19	40	55	27

There seems to be a disconnect between the Critical Values outlined in the BAER directive and the treatment options/actions available to BAER teams. By design, the BAER treatment options, their descriptions, or their emergency stabilization objectives rarely identify habitat stabilization as a primary goal of the treatment. In fact, the treatment's impact on "sensitive aquatic species" is mentioned in only 2 of the 36 treatment options outlined in the Burned Area Emergency Response Treatments Catalog (Napper, 2006). This means that rather than being able to prescribe a treatment with the specific purpose of maintaining suitable fish habitat (e.g. upgrading a culvert to allow fish passage), BAER teams may include a fish habitat treatment as a more general "water quality" treatment.

Because BAER expenditures have slowly risen over the past 3-4 decades (Robichaud *et al.*, 2014), some BAER teams have found it difficult to secure funding for fish habitat-specific post-fire treatments. If this problem persists, BAER teams may still be able to find funding opportunities from third party/private entities whose mission is to maintain or improve fish habitat through this type of mitigation work.

7.1.4 Funding Opportunities for Post-Fire Rehabilitation

A variety of groups, in both the private and public sector, sustain programs that provide funding for fish habitat restoration projects across the country. For example, in 2015, Trout Unlimited (TU) established the Coldwater Conservation Fund (CCF) with the mission of "supporting scientific research, on-the ground projects, and other high-priority work of Trout Unlimited that might not otherwise be funded". Conservation funding has been the primary way that TU has worked to achieve their mission of "conserving, protecting, and restoring

North America's coldwater fisheries and their watersheds" (TU, 2020). Historically they have done this through both private fundraising as well as leveraging federal resources towards what they believe are important conservation projects. The CCF provides a private, unrestricted source of funding for TU projects. Since it's creation, the CCF has granted over $1.2M worth of funding for conservation-related issues "ranging from venture-capital style project startups to emergency funding for urgent needs or late-breaking opportunities".

A brief analysis of CCF project summaries from 2015-2019 indicates that CCF has provided grants to a wide array of projects from reintroducing native brook trout to the Delaware River, to dam removal projects in Western Montana, to developing an mobile application that allows users to conduct their own basic surveys of stream impairment (TU, 2015, 2016, 2017, 2018, 2019). Only one project in the last 5 years has been related to habitat degradation caused by wildfire. In 2019, a project was proposed that would aid in the large-scale restoration of the Upper Eel River in Northern California. This stretch of river provides important habitat for the Northern California Coast Steelhead, which is listed as threatened under the Endangered Species Act (HHS, 2014). In 2018, the Mendocino Wildfire Complex burned this area at moderate to high severity and, as was addressed above, the BAER program was unable to address the fire impacts on river and stream habitat. In this case, the CCF provided $20,000 to develop a restoration plan for this watershed. While this type of funding is important in the long-term recovery of the watershed, it is not the type of immediate funding that would be necessary to work with a BAER project and the BAER timeframe. Funding proposals for Trout Unlimited can take anywhere from six to eighteen months to process.

If organizations like TU (CCF) provided a quickly accessible funding source, BAER teams could supplement the resources provided by the federal government with these private grants. With these funds, BAER teams could more effectively address their mandate while also working to mitigate the degradation of critical stream habitat, and more quickly begin the habitat restoration process.

7.1.5 Recommendations

If a BAER team is unable to secure funding through the BAER program for post-fire fish habitat treatments, then outside agencies should be contacted for assistance. Below is a list

of entities, both public and private, that may be suitable to fund some portion of a fish habitat related post-fire mitigation project (Table 21).

Many of these agencies require a relatively lengthy (6-18 month) application process. This timeline may be suitable for BAER Emergency Stabilization treatments that must be within 1 year of fire containment (USFS, 2018a), however it may be suitable to acquire funding for Burned-Area Restoration treatments which have a window of 3 years post-fire to be implemented (USFS, 2018a).

A few of these entities have been involved in post-fire emergency and restoration treatments. Namely, Trout Unlimited (TU) and the National Fish and Wildlife Federation (NFWF) have both provided funding directly to U.S. National Forests for post-fire fish habitat management (see TU/CCF discussion above, and see existing partnerships between NFWF and the U.S. Forest Service: (https://www.nfwf.org/partnerships/federal-state-partners/usda-forest-service). U.S. Forest Service managers should check to see if their region is already involved in a partnership with NFWF as this may provide a more efficient and timely mechanism for funding acquisition.

Many of the organizations listed in Table 21 explicitly state that providing “emergency funding” is one of their goals. What they may not understand that, in the BAER program, “emergency funding” comes with a very short timeline of implementation, often and ideally just a couple of months. Not only does a quick response result in a more effective overall treatment, it is also mandated under the Burned Area Emergency Response program (USFS, 2018a). They may be unaware that by not providing a “fast track” option for emergency funding, they are limiting the possibility of their involvement in important post-fire mitigation and rehabilitation work.

In an emergency funding situation, the 2500-8 Burned Area Reports and associated specialist reports are quite thorough and could be used as initial application documentation. Supplementary information may be required to finish the application. In this way, a BAER team would quickly and relatively easily apply for funding that can be incorporated into their general treatment plan. Working together with Forest Service (i.e. BAER) managers, these entities can begin planning and organizing a pool of post-fire emergency funds.

Table 21: Third-party entites with potential funding for post-fire rehabilitation projects. This list is not exhaustive but provides a starting point for BAER teams searching for supplemental funding opportunities. (Accessed December 2022)

National Scale Funding Entities

Organization Name	Webpage	Phone Number	Email
Trout Unlimited	https://www.tu.org/get-involved/volunteer-tacklebox/fundraising-resources/grants-corporate-fundraising/applying-for-grants/	(703) 284-9426	-
National Fish Passage Program	https://www.fws.gov/fisheries/fish-passage/fish-passage-coordinators-and-resources.html	-	michael_bailey@fws.gov
National Fish and Wildlife Foundation	https://www.nfwf.org/become-partner	(202) 857-0166	-
U.S. Fish and Wildlife Service	https://www.fws.gov/grants/	-	fwsgrants@fws.gov
The Fund for Wild Nature	https://fundwildnature.org/	(858) 367-9453	fwn@fundwildnature.org

Region-Specific Funding Entities

Organization Name	Webpage	Phone Number	Email
Local State Fish & Wildlife Departments	-	-	-
Fish America Foundation	https://www.fishamerica.org/	(703) 519-9691	fafgrants@asafishing.org
Western Native Trout Initiative	https://westernnativetrout.org/	-	tthompson@westernnativetrout.org
The Partners for Fish and Wildlife Program	https://www.fws.gov/pacific/ecoservices/habcon/partners/index.html	Varies by State/Region	Varies by State/Region
NOAA Fisheries	https://www.fisheries.noaa.gov/funding-opportunities	Varies by State/Region	Varies by State/Region
Montana Future Fisheries Improvement Program	http://fwp.mt.gov/fishAndWildlife/habitat/fish/futureFisheries/eligibility.html	(406) 444-2432	mmcgree@mt.gov
RiversEdge West	https://riversedgewest.org/funding	(970) 256-7400	Kjespersen@riversedgewest.org
Eastern Brook Trout Joint Venture	https://easternbrooktrout.org/funding-opportunities	-	ebtjv.coordinator@gmail.com

References

Adams MS, Fromm R, Lechner V. 2016. High-resolution debris flow volume mapping with unmanned aerial systems (UAS) and photogrammetric techniques. *International Archives of the Photogrammetry, Remote Sensing and Spatial Information Sciences - ISPRS Archives*: 749–755 DOI: 10.5194/isprsarchives-XLI-B1-749-2016

Amaranthus M, Jubas H, Arthur D. 1989. Stream shading , summer streamflow and maximum water temperature following intense wildfire in headwater streams. In *Proceedings of the Symposium on Fire and Watershed Management*US Department of Agriculture, Forest Service, Pacific Southwest Research Station: Albany, CA; 75–78. Available at: https://www.fs.usda.gov/treesearch/pubs/26927

Anderson H. 1976. Fire effects on water supply, floods, and sedimentation. *Proceedings of the Tall Timbers fire ecology conference*: 249–260

Arkell RE, Richards F. 1986. Short duration rainfall relations for the Western United States. *Conference on Climate and Watermanagement*: 136–141

Arno SF. 1980. Forest fire history in the Northern Rockies. *Journal of Forestry*: 460–465

Benda LE, Miller DJ, Bigelow P, Andras K. 2003. Effects of post-wildfire erosion on channel environments, Boise River, Idaho. *Forest Ecology and Management* **178** (2): 105–119 DOI: 10.1016/S0378-1127(03)00056-2

Best DW, Kelsey HM, Hagans DK, Alpert M. 1995. Role of fluvial hillslope erosion and road construction in the sediment budget of Garret Creek, Humboldt County, California (KM Nolan, HM Kelsey, and DC Marron, eds). *U.S. Geological Survey Professional Paper 1454-M*: M1–M9

Bisson PA, Rieman BE, Luce C, Hessburg PF, Lee DC, Kershner JL, Reeves GH, Gresswell RE. 2003. Fire and aquatic ecosystems of the western USA: current knowledge and key questions. *Forest Ecology and Management* **178** (1–2): 213–229 DOI: 10.1016/S0378-1127(03)00063-X

Boll J, Brooks ES, Crabtree B, Dun S, Steenhuis TS. 2015. Variable source area hydrology modeling with the water erosion prediction project model. *Journal of the American Water Resources Association* **51** (2): 330–342 DOI: 10.1111/1752-1688.12294

Bozek MA, Young MK. 1994. Fish mortality resulting from delayed effects of fire in the Greater Yellowstone ecosystem. *Great Basin Naturalist* **54** (1): 91–95 DOI: 10.2307/41712815

Brooks ES, Dobre M, Elliot WJ, Wu JQ, Boll J. 2016. Watershed-scale evaluation of the Water Erosion Prediction Project (WEPP) model in the Lake Tahoe basin. *Journal of Hydrology* **533**: 389–402 DOI: 10.1016/j.jhydrol.2015.12.004

Brown DK, Echelle AA, Propst DL, Brooks JE, Fisher WL. 2001. Catastrophic wildfire and number of populations as factors influencing risk of extinction for Gila trout (Oncorhynchus gilae). *Western North American Naturalist* **61** (2): 139–148

Brown JK. 1989. Effect of Fire on Aquatic Systems. In *Wild Trout IV Symposium*Yellowstone National Park, Mammoth, WY; 106–110.

Brown PM, Kaufmann MR, Shepperd WD. 1999. Long-term, landscape patterns of past fire events in a montane ponderosa pine forest of central Colorado. *Landscape Ecology* **14** (6): 513–532 DOI: 10.1023/A:1008137005355

Burton TA. 2005. Fish and stream habitat risks from uncharacteristic wildfire: Observations from 17 years of fire-related disturbances on the Boise National Forest, Idaho. *Forest Ecology and Management* **211** (1–2): 140–149 DOI: 10.1016/j.foreco.2005.02.063

Buytaert W, Celleri R, Willems P, Bièvre B De, Wyseure G. 2006. Spatial and temporal rainfall variability in mountainous areas: A case study from the south Ecuadorian Andes. *Journal of Hydrology* **329** (3–4): 413–421 DOI: 10.1016/j.jhydrol.2006.02.031

Byrd TC, Furbish DJ, Warburton J. 2000. Estimating depth-averaged velocities in rough -channels. *Earth Surface Processes and Landforms* **25** (2): 167–173 DOI: 10.1002/(sici)1096-9837(200002)25:2<167::aid-esp66>3.3.co;2-7

Cannon SH. 2001. Debris-flow generation from recently burned watersheds. *Environmental & Engineering Geoscience* **7** (4): 321–341

Cannon SH, Gartner JE, Rupert MG, Michael JA, Rea AH, Parrett C. 2010. Predicting the probability and volume of postwildfire debris flows in the intermountain Western United States. *Geological Society of America Bulletin* **122** (1–2): 127–144 DOI: 10.1130/B26459.1

Cerda A, Robichaud PR. 2009. Fire Effects on Soil Infiltration. In *Fire Effects on Soils and Restoration Strategies*, Cerda A, , Robichaud PR (eds).Science Publishers: Enfield, NH; 81–103.

Cerrelli GA. 2005. FIRE HYDRO: A simplified method for predicting peak discharges to assist in the design of flood protection measures for western wildfires. *Managing Watersheds for Human and Natural Impacts*: 1–7 DOI: 10.1061/40763(178)80

Chambers JC, Brown RW. 1983. Methods for vegetation sampling and analysis on revegetated mined lands. US Department of Agriculture, Forest Service, Intermountain Forest and Range Experiment Station, Ogden, UT. DOI: 10.5962/bhl.title.99993

Chandramohan T, Venkatesh B, Balchand AN. 2015. Evaluation of three soil erosion models for small watersheds. *Aquatic Procedia* **4**: 1227–1234 DOI: 10.1016/j.aqpro.2015.02.156

Chen L, Berli M, Chief K. 2013. Examining modeling approaches for the rainfall-runoff process in wildfire-affected watersheds: Using San Dimas Experimental Forest. *JAWRA Journal of the American Water Resources Association* **49** (4): 851–866 DOI: 10.1111/jawr.12043

Chu TW, Shirmohammadi A. 2004. Evaluation of the SWAT model's hydrology component in the Piedmont physiographic region of Maryland. *Transactions of the ASAE* **47** (4): 1057–1073 DOI: 10.13031/2013.16579

Colle BA. 2008. Two-dimensional idealized simulations of the impact of multiple windward ridges on orographic precipitation. *Journal of the Atmospheric Sciences* **65** (2): 509–523 DOI: 10.1175/2007JAS2305.1

Collins BM, Roller GB. 2013. Early forest dynamics in stand-replacing fire patches in the Northern Sierra Nevada, California, USA. *Landscape Ecology* **28** (9): 1801–1813 DOI: 10.1007/s10980-013-9923-8

Covert SA, Robichaud PR, Elliot WJ, Link TE. 2005. Evaluation of runoff prediction from WEPP-based erosion models for harvested and burned forest watersheds. *Transactions of the ASAE* **48** (3): 1091–1100 DOI: 10.13031/2013.18519

DeBano LF. 1981. Water repellent soils: a state-of-the-art. *General Technical Report PSW-46*: 22 Available at: https://www.fs.fed.us/psw/publications/documents/psw_gtr046/psw_gtr046.pdf [Accessed 15 August 2019]

DeBano LF, Osborn JF, Krammes JS, Letey J. 1967. Soil wettability and wetting agents: our current knowledge of the problem. *U.S. Forest Serv. Res. Paper PSW-RP-43*: 13 Available at: https://www.fs.usda.gov/treesearch/pubs/28757 [Accessed 14 August 2019]

Dennison PE, Brewer SC, Arnold JD, Moritz MA. 2014. Large wildfire trends in the Western United States, 1984-2011. *Geophysical Research Letters* **41** (8): 2928–2933 DOI: 10.1002/2014GL059576

Dobre M, Srivastava A, Lew R, Deval C, Brooks ES, Elliot WJ, Robichaud PR. 2022. WEPPcloud: An online watershed-scale hydrologic modeling tool. Part II. Model performance assessment and applications to forest management and wildfires. *Journal of Hydrology*: 127776 DOI: 10.1016/j.jhydrol.2022.127776

Doerr SH, Shakesby RA, Blake WH, Chafer CJ, Humphreys GS, Wallbrink PJ. 2006. Effects of differing wildfire severities on soil wettability and implications for hydrological response. *Journal of Hydrology* **319** (1–4): 295–311 DOI: 10.1016/j.jhydrol.2005.06.038

Doerr SH, Shakesby RA, MacDonald LH. 2009. Soil water repellency: A key factor in post-fire erosion. In *Fire Effects on Soils and Restoration Strategies*, Cerda A, , Robichaud PR (eds).CRC Press; 28. DOI: 10.1201/9781439843338

Dun S, Wu JQ, Elliot WJ, Robichaud PR, Flanagan DC, Frankenberger JR, Brown RE, Xu AC. 2009. Adapting the Water Erosion Prediction Project (WEPP) model for forest applications. *Journal of Hydrology* **366** (1–4): 46–54 DOI: 10.1016/j.jhydrol.2008.12.019

Elliot WJ. 2013. Erosion processes and prediction with wepp technology in forests in the Northwestern U.S. *Transactions of the ASABE* **56** (2): 563–579

Elliot WJ, Hall DE. 1997. Water Erosion Prediction Project (WEPP) Forest Applications. US Forest Service, Rocky Mountain Forest and Range Experiment Station, Fort Collins, CO. DOI: http://dx.doi.org/10.15446/rbct.n39.52888

Elliot WJ, Foltz RB, Luce CH. 1995. Validation of Water Erosion Prediction Project (WEPP) model for low-volume forest roads. *Sixth International Conference on Low-Volume Roads*: 178–186

Flanagan DC, Ascough JC, Nearing MA, Laflen JM. 2001. The Water Erosion Prediction Project (WEPP) model. *Landscape Erosion and Evolution Modeling*: 145–199 DOI: 10.1007/978-1-4615-0575-4_7

Flanagan DC, Frankenberger JR, Ascough JC. 2012. WEPP: Model use, calibration, and validation. *Transactions of the ASABE* **55** (4): 1463–1477 DOI: 10.13031/2013.42254

Flanagan DC, Gilley JE, Franti TG. 2007. Water Erosion Prediction Project (WEPP): Development History, Model Capabilities, and Future Enhancements. *Transactions of the ASABE* **50** (5): 1603–1612 DOI: 10.13031/2013.23968

Foglia L, Hill MC, Mehl SW, Burlando P. 2009. Sensitivity analysis, calibration, and testing of a distributed hydrological model using error-based weighting and one objective function. *Water Resources Research* **45** (6) DOI: 10.1029/2008WR007255

Foltz RB, Robichaud PR, Rhee H. 2009. A Synthesis of Post-Fire Raod Treatments for BAER Teams: Methods, Treatment Effectiveness, and Decisionmaking Tools for Rehabilitation. US Department of Agriculture, Forest Service, Rocky Mountain Research Station, Fort Collins, CO.

Friday J. 1965. The Operation and Maintenance of a Crest-Stage Gaging Station. US Geological Survey, Surface Water Branch, Portland, OR. Available at: http://pubs.er.usgs.gov/publication/ofr6645

Furniss MJ, Ledwith TS, Love MA, McFadin BC, Flanagan SA. 1998. Response of road-stream crossings to large flood events in Washington, Oregon, and Northern California. US Department of Agriculture, Technology & Development Program, San Dimas, CA.

Garbrecht J, Martz LW. 1999. TOPAZ: An automated digital landscape analysis tool for topographic evaluation, drainage identification, watershed segmentation, and subcatchment parameterization. US Department of Agriculture, Grazinglands Research Laboratory, El Reno, OK.

Gartner JE, Bigio ER, Cannon SH. 2004. Compilation of post-wildfire runoff data from the western United States. *Open-File Report 2004-1085* Available at: https://pubs.usgs.gov/of/2004/1085/ofr-04-1085.html

Gould GK, Liu M, Barber ME, Cherkauer KA, Robichaud PR, Adam JC. 2016. The effects of climate change and extreme wildfire events on runoff erosion over a mountain watershed. *Journal of Hydrology* **536**: 74–91 DOI: 10.1016/j.jhydrol.2016.02.025

Gresswell RE. 1999. Fire and aquatic ecosystems in forested biomes of North America. *Transactions of the American Fisheries Society* **128** (2): 193–221 DOI: 10.1577/1548-8659(1999)128<0193:FAAEIF>2.0.CO;2

Gupta HV, Sorooshian S, Yapo PO. 1999. Status of automatic calibration for hydrologic models: Comparison with multilevel expert calibration. *Journal of Hydrologic Engineering* **4** (2): 135–143 DOI: 10.1061/(ASCE)1084-0699(1999)4:2(135)

Gusman JA, Teal MJ, Todesco D, Bandurraga M. 2009. Estimating sediment/debris bulking factors. In *33rd Annual: International Association for Hydraulic Research Biennial Conference*Vancouver, B.C, Canada; 83–91.

Hallema DW, Sun G, Bladon KD, Norman SP, Caldwell P V., Liu Y, McNulty SG. 2017. Regional patterns of postwildfire streamflow response in the Western United States: The importance of scale-specific connectivity. *Hydrological Processes* **31** (14): 2582–2598 DOI: 10.1002/hyp.11208

Hanson CL, Pierson FB, Johnson GL. 2004. Dual-gauge system for measuring precipitation: Historical development and use. *Journal of Hydrologic Engineering* **9** (5): 350–359 DOI: 10.1061/(ASCE)1084-0699(2004)9:5(350)

Hardesty J, Myers R, Fulks W. 2005. Fire, Ecosystems, and People: A preliminary assessment of fire as a global conservation issue. *The George Wright Forum* **22** (4): 78–87

Hawkins RH. 1993. Asymptotic Determination of Runoff Curve Numbers from Data. *Journal of Irrigation and Drainage Engineering* **119** (2): 334–345 DOI: 10.1061/(ASCE)0733-9437(1993)119:2(334)

Hawkins RH, Barreto-Munoz A. 2016. Wildcat5 for Windows , a rainfall-runoff hydrograph model : user manual and documentation. US Department of Agriculture, Forest Service, Rocky Mountain Research Station, Fort Collins, CO.

HHS. 2014. Endangered and Threatened Wildlife; Final Rule To Revise the Code of Federal Regulations for Species Under the Jurisdiction of the National Marine Fisheries Service. In *Federal Register, Vol. 79 No. 71*National Marine Fisheries Service, National Oceanic and Atmospheric Administration, Department of Commerce; 20802–20817. DOI: 10.1016/0196-335x(80)90058-8

Hilderbrand RH, Kershner JL. 2000. Conserving inland cutthroat trout in small streams: How much stream is enough? *North American Journal of Fisheries Management* **20** (2): 513–520 DOI: 10.1577/1548-8675(2000)020<0513:CICTIS>2.3.CO;2

Hitt NP. 2003. Immediate effects of wildfire on stream temperature. *Journal of Freshwater Ecology* **18** (1): 171–173 DOI: 10.1080/02705060.2003.9663964

Hongve D. 1987. A revised procedure for discharge measurement by means of the salt dilution method. *Hydrological Processes* **1** (3): 267–270 DOI: 10.1002/hyp.3360010305

Isaak DJ, Luce CH, Rieman BE, Nagel DE, Peterson E, Horan DL, Parkes S, Chandler GL. 2010. Effects of climate change and wildfire on stream temperatures and salmonid thermal habitat in a mountain river network. *Ecological Applications* **20** (5): 1350–1371 DOI: 10.1890/09-0822

Iverson RM. 1997. The physics of debris flows. *Reviews of Geophysics* **35** (3): 245–296 DOI: 10.1029/97RG00426

Kawamoto K, Moldrup P, Komatsu T, de Jonge LW, Oda M. 2007. Water Repellency of Aggregate Size Fractions of a Volcanic Ash Soil. *Soil Science Society of America Journal* **71** (6): 1658–1666 DOI: 10.2136/sssaj2006.0284

Kean JW, Staley DM. 2021. Forecasting the Frequency and Magnitude of Postfire Debris Flows Across Southern California. *Earth's Future* **9** (3): 1–19 DOI: 10.1029/2020EF001735

Kean JW, McGuire LA, Rengers FK, Smith JB, Staley DM. 2016. Amplification of postwildfire peak flow by debris. *Geophysical Research Letters* **43** (16): 8545–8553 DOI: 10.1002/2016GL069661

Keeley JE. 2009. Fire intensity, fire severity and burn severity: a brief review and suggested usage. *International Journal of Wildland Fire* **18** (1): 116 DOI: 10.1071/WF07049

Key CH, Benson NC. 2006. Landscape Assessment. In *FIREMON: Fire Effects Monitoring and Inventory System*219–273.

Kilpatrick FA, Cobb ED. 1985. Techniques of water-resources investigations of the United States Geological Survey: Measurement of discharge using tracers. US Department of the Interior, US Geological Survey, Reston, VA.

Kirkland J, Flitcroft RL, Reeves GH, Hessburg PF, Falke JA, Benda LE, Miller DJ, Dunham JB. 2017. Adaptation To wildfire: a fish story. US Department of Agriculture, Forest Service, Pacific Northwest Research Station, Portland, OR.

Kirshbaum DJ, Bryan GH, Rotunno R, Durran DR. 2007. The triggering of orographic rainbands by small-scale topography. *Journal of the Atmospheric Sciences* **64** (5): 1530–1549 DOI: 10.1175/JAS3924.1

Larsen IJ, MacDonald LH, Brown E, Rough D, Welsh MJ, Pietraszek JH, Libohova Z, Dios Benavides-Solorio J, Schaffrath K. 2009. Causes of post-fire runoff and erosion: water repellency, cover, or soil sealing? *Soil Science Society of America Journal* **73** (4): 1393–1407 DOI: 10.2136/sssaj2007.0432

Lew R, Dobre M, Srivastava A, Brooks ES, Elliot WJ, Robichaud PR, Flanagan DC. 2022. WEPPcloud: An online watershed-scale hydrologic modeling tool. Part I. Model description. *Journal of Hydrology*: 51 DOI: 10.1016/j.jhydrol.2022.127603

Lewis SA, Hudak AT, Robichaud PR, Morgan P, Satterberg KL, Strand EK, Smith AMS, Zamudio JA, Lentile LB. 2017. Indicators of burn severity at extended temporal scales: a decade of ecosystem response in mixed-conifer forests of western Montana. *International Journal of Wildland Fire* **26** (9): 755–771 DOI: 10.1071/WF17019

Lewis SA, Robichaud PR, Frazier BE, Wu JQ, Laes DYM. 2008. Using hyperspectral imagery to predict post-wildfire soil water repellency. *Geomorphology* **95** (3–4): 192–205 DOI: 10.1016/j.geomorph.2007.06.002

Littell JS, Oneil EE, McKenzie D, Hicke JA, Lutz JA, Norheim RA, Elsner MM. 2010. Forest ecosystems, disturbance, and climatic change in Washington State, USA. *Climatic Change* **102** (1–2): 129–158 DOI: 10.1007/s10584-010-9858-x

Lutes DC, Keane RE, Caratti JF, Key CH, Benson NC, Sutherland S, Gangi LJ. 2006. *FIREMON: Fire effects monitoring and inventory system.* US Department of Agriculture, Forest Service, Rocky Mountain Research Station: Fort Collins, CO.

McCarthy PM, Dutton DM, Sando SK, Sando R. 2016a. Chapter A: Montana StreamStats—A method for retrieving basin and streamflow characteristics in Montana. US Department of the Interior, US Geological Survey, Reston, VA.

McCarthy PM, Sando R, Sando SK, Dutton DM. 2016b. Chapter G: Methods for Estimating Streamflow Characteristics at Ungaged Sites in Western Montana Based on Data through Water Year 2009. US Department of the Interior, US Geological Survey, Reston, VA.

McCutcheon SC. 2003. Hydrologic evaluation of the curve number method for forest management in West Virginia. West Virginia Division of Forestry, Charleston, WV.

McGuire LA, Rengers FK, Kean JW, Staley DM. 2017. Debris flow initiation by runoff in a recently burned basin: Is grain-by-grain sediment bulking or en masse failure to blame? *Geophysical Research Letters* **44** (14): 7310–7319 DOI: 10.1002/2017GL074243

McMahon TE, DeCalesta DS. 1990. Effects of fire on fish and wildlife. In *Natural and Prescribed Fire in Pacific Northwest Forests*, Walstad JD, , Radosevich SR, , Sandberg D V. (eds).Oregon State University Press: Corvallis, OR; 233–250.

Megahan WF. 1991. Erosion and site productivity in western-montane forest ecosystems. In *Proceedings of the Symposium on Management and Productivity of Western-Montane Forest Soils*Boise, ID; 146–150.

Miller JF, Frederick RH, Tracey RJ. 1973. Precipitation-frequency atlas of the Western United States. Volume 1: Montana. US Department of Commerce, National Oceanic and Atmospheric Administration, National Weather Service, Washington, DC.

Minshall GW, Brock JT, Varley JD. 1989. Wildfires and Yellowstone's Stream Ecosystems. *BioScience* **39** (10): 707–715 DOI: 10.2307/1311002

Moody JA, Martin DA. 2001. Initial hydrologic and geomorphic response following a wildfire in the Colorado Front Range. *Earth Surface Processes and Landforms* **26** (10): 1049–1070 DOI: 10.1002/esp.253

Moody JA, Shakesby RA, Robichaud PR, Cannon SH, Martin DA. 2013. Current research issues related to post-wildfire runoff and erosion processes. *Earth-Science Reviews* **122**: 10–37 DOI: 10.1016/j.earscirev.2013.03.004

Moriasi DN, Arnold JG, Van Liew MW, Bingner RL, Harmel RD. 2007. Model evaluation guidelines for systematic quantification of accuracy in watershed simulations. *American Society of Agricultural and Biological Engineers* **50** (3): 885–900

Myers RL. 2006. Living with fire— Sustaining ecosystems & livelihoods through integrated fire management. The Nature Conservancy, Global Fire Initiative, Tallahassee, FL. Available at: https://www.academia.edu/31525166/Living_with_Fire_Sustaining_Ecosystems_and_Livelihoods_Through_Integrated_Fire_Management_Global_Fire_Initiative

Napper C. 2006. *Burned area emergency response treatments catalog*. US Department of Agriculture, Forest Service: Washington, DC.

Nash JE, Sutcliffe J V. 1970. River flow forecasting through conceptual models part I - A discussion of principles. *Journal of Hydrology* **10** (3): 282–290 DOI: 10.1016/0022-1694(70)90255-6

Neary DG, Gottfried GJ, Debano LF, Tecle A. 2003. Impacts of Fire on Watershed Resources. *Journal of the Arizona-Nevada Academy of Science* **35** (1): 23–41

Neary DG, Koestner KA, Youberg A. 2010. Hydrologic impacts of high severity wildfire : learning from the past and preparing for the future. *24th Annual Symposium of the Arizona Hydrological Society; Watersheds near and far: Response to changes in climate and landscape*: 8

Neary DG, Ryan KC, DeBano LF. 2005. Wildland fire in ecosystems: effects of fire on soils and water. US Department of Agriculture, Forest Service, Rocky Mountain Research Station, Ogden, UT. DOI: 10.2737/RMRS-GTR-42-V4

Nicks AD, Lane LJ, Gander GA. 1995. The water erosion prediction project (WEPP) technical documentation, Chapter 2: Weather generator. US Department of Agriculture, Forest Service, Rocky Mountain Research Station, Fort Collins, CO.

Niemeyer RJ, Bladon KD, Woodsmith RD. 2020. Long-term hydrologic recovery after wildfire and post-fire forest management in the interior Pacific Northwest. *Hydrological Processes* **34** (5): 1182–1197 DOI: 10.1002/hyp.13665

Nitsche M, Rickenmann D, Kirchner JW, Turowski JM, Badoux A. 2012. Macroroughness and variations in reach-averaged flow resistance in steep mountain streams. *Water Resources Research* **48** (12): 1–16 DOI: 10.1029/2012WR012091

Novak MA, White RG. 1989. Impact of a fire and flood on the trout population of Beaver Creek, Upper Missouri Basin, Montana. In *Proceedings of Wild Trout IV*, Trout Unlimited (ed.).Arlington, VA; 120–127.

Odion DC, Hanson CT, Arsenault A, Baker WL, DellaSala DA, Hutto RL, Klenner W, Moritz MA, Sherriff RL, Veblen TT, et al. 2014. Examining historical and current mixed-severity fire regimes in ponderosa pine and mixed-conifer forests of western North America. *PLoS ONE* **9** (2) DOI: 10.1371/journal.pone.0087852

Ostrem G. 1964. A method of measuring water discharge in turbulent streams. *Geography Bulletin* (21): 21–43

Parise M, Cannon SH. 2012. Wildfire impacts on the processes that generate debris flows in burned watersheds. *Natural Hazards* **61** (1): 217–227 DOI: 10.1007/s11069-011-9769-9

Parks SA, Abatzoglou JT. 2020. Warmer and drier fire seasons contribute to increases in area burned at high severity in western US forests from 1985-2017. *Geophysical Research Letters* **2**: 229–235 DOI: 10.1029/2020GL089858

Parrett C. 1987. Fire-Related Debris Flows in the Beaver Creek Drainage, Lewis and Clark County, Montana. US Department of the Interior, US Geological Survey, Reston, VA.

Parrett C, Cannon SH, Pierce KL. 2004. Wildfire-related floods and debris flows in Montana in 2000 and 2001. US Department of the Interior, US Geological Survey, Reston, VA.

Parsons A, Robichaud PR, Lewis SA, Napper C, Clark JT. 2010. Field guide for mapping post-fire soil burn severity. US Department of Agriculture, Forest Service, Rocky Mountain Research Station, Fort Collins, CO. DOI: 10.2737/RMRS-GTR-243

Pederson GT, Gray ST, Ault T, Marsh W, Fagre DB, Bunn AG, Woodhouse CA, Graumlich LJ. 2011. Climatic controls on the snowmelt hydrology of the Northern Rocky Mountains. *Journal of Climate* **24** (6): 1666–1687 DOI: 10.1175/2010JCLI3729.1

Pieri L, Bittelli M, Wu JQ, Dun S, Flanagan DC, Pisa PR, Ventura F, Salvatorelli F. 2007. Using the Water Erosion Prediction Project (WEPP) model to simulate field-observed runoff and erosion in the Apennines mountain range, Italy. *Journal of Hydrology* **336** (1–2): 84–97 DOI: 10.1016/j.jhydrol.2006.12.014

Ponce VM, Hawkins RH. 1996. Runoff Curve Number: has it reached maturity? *Journal of Hydrologic Engineering* **1** (1): 11–19 DOI: 10.1061/(ASCE)1084-0699(1996)1:1(11)

Propst DL, Stefferud JA. 1997. Population dynamics of Gila trout in the Gila River drainage of the south-western United States. *Journal of Fish Biology* **51** (6): 1137–1154 DOI: 10.1111/j.1095-8649.1997.tb01132.x

Propst DL, Stefferud JA, Turner PR. 1992. Conservation and Status of Gila Trout, Oncorhynchus gilae. *The Southwestern Naturalist* **37** (2): 117–125 DOI: 10.2307/3671659

Quinn DS. 2018. Simulation of post-fire watershed hydrology anderosion responses with the physically-based WEPP model. University of Idaho, Water Resources Department, Moscow, ID. Available at: https://www.lib.uidaho.edu/digital/etd/items/quinn_idaho_0089n_11453.html

Quintano C, Fernandez-Manso A, Roberts DA. 2017. Burn severity mapping from Landsat MESMA fraction images and land surface temperature. *Remote Sensing of Environment* **190**: 83–95 DOI: 10.1016/j.rse.2016.12.009

Raines GL, Johnson BR. 1996. Digital representation of the Montana state geologic map: a contribution to the Interior Columbia River Basin Ecosystem Management Project. US Department of the Interior, US Geological Survey, Reston, VA.

Rantz SE. 1982a. Measurement and Computation of Streamflow: Volume 1. Measurement of Stage and Discharge. US Department of the Interior, US Geological Survey, Reston, VA.

Rantz SE. 1982b. *Measurement and Computation of Streamflow: Volume 2. Computation of Discharge.* US Department of the Interior, US Geological Survey: Reston, VA.

Reeves GH, Benda LE, Burnett KM, Bisson PA, Sedell JR. 1995. A disturbance-based ecosystem approach to maintaining and restoring freshwater habitats of evolutionarily significant units of anadromous salmonids in the Pacific Northwest. In *American Fisheries Society Symposium 17*334–349.

Rengers FK, McGuire LA, Kean JW, Staley DM, Hobley DEJ. 2016. Model simulations of flood and debris flow timing in steep catchments after wildfire. *Water Resources Research* **52** (8): 6041–6061 DOI: 10.1002/2015WR018176

Rieman BE, Clayton J. 1997. Wildfire and Native Fish: Issues of Forest Health and Conservation of Sensitive Species. *Fisheries* **22** (11): 6–15 DOI: 10.1577/1548-8446(1997)022<0006:wanfio>2.0.co;2

Rieman BE, Lee DC, Chandler GL, Myers D. 1995. Does wildfire threaten extinction for salmonids? Responses of Redband Trout and Bull Trout following recent large fires on the Boise National Forest. In *Proceedings of Fire Effects on Rare and Endangered Species and Habitats Conference*Coeur d'Alene, ID; 47–57.

Robichaud PR. 2000. Fire effects on infiltration rates after prescribed fire in Northern Rocky Mountain forests, USA. *Journal of Hydrology* **231**–**232**: 220–229 DOI: 10.1016/S0022-1694(00)00196-7

Robichaud PR, Ashmun LE. 2013. Tools to aid post-wildfire assessment and erosion-mitigation treatment decisions. *International Journal of Wildland Fire* **22** (1): 95–105 DOI: 10.1071/WF11162

Robichaud PR, Elliot WJ, Pierson FB, Hall DE, Moffet CA. 2007. Predicting postfire erosion and mitigation effectiveness with a web-based probabilistic erosion model. *Catena* **71** (2): 229–241 DOI: 10.1016/j.catena.2007.03.003

Robichaud PR, Lewis SA, Ashmun LE. 2008. New procedure for sampling infiltration to assess post-fire soil water repellency. US Department of Agriculture, Forest Service, Rocky Mountain Research Station, Fort Collins, CO. DOI: 10.2737/RMRS-RN-33

Robichaud PR, Rhee H, Lewis SA. 2014. A synthesis of post-fire Burned Area Reports from 1972 to 2009 for western US Forest Service lands: trends in wildfire characteristics and post-fire stabilisation treatments and expenditures. *International Journal of Wildland Fire* **23** (7): 929 DOI: 10.1071/WF13192

Robichaud PR, Wagenbrenner JW, Pierson FB, Spaeth KE, Ashmun LE, Moffet CA. 2016. Infiltration and interrill erosion rates after a wildfire in Western Montana, USA. *CATENA* **142**: 77–88 DOI: 10.1016/j.catena.2016.01.027

Rotunno R, Houze RA. 2007. Lessons on orographic precipitation from the Mesoscale Alpine Programme. *Quarterly Journal of the Royal Meteorological Society* **133** (625): 811–830 DOI: 10.1002/qj.67

Rust AJ, Saxe S, McCray J, Rhoades CC, Hogue TS. 2019. Evaluating the factors responsible for post-fire water quality response in forests of the western USA. *International Journal of Wildland Fire* **28** (10): 769 DOI: 10.1071/WF18191

Sando R, Sando S, McCarthy PM, Dutton DM. 2018. Methods for estimating peak-flow frequencies at ungaged sites in Montana based on data through Water Year 2011. US Department of the Interior, US Geological Survey, Reston, VA. DOI: 10.3133/sir20155019F

Sappa G, Ferranti F, Pecchia GM. 2015. Validation of salt dilution method for discharge measurements in the upper valley of Aniene River (Central Italy). *Recent Advances in Environment, Ecosystems and Development* (October 2015): 42–48

Saxe S, Hogue TS, Hay L. 2016. Characterization of post-fire streamflow response across Western U.S. Watersheds. *Hydrology and Earth System Sciences Discussions* (October): 1–18 DOI: 10.5194/hess-2016-533

Schwab GO, Fangmeir DD, Elliot WJ, Frevert RK. 1992. Intensity, duration, and frequency of rainfall. In *Soil and Water Conservation Engineering, 4th Edition*John Wiley and Sons Inc.: New York, NY; 26–32.

Seibert J, McDonnell JJ, Woodsmith RD. 2010. Effects of wildfire on catchment runoff response: a modelling approach to detect changes in snow-dominated forested catchments. *Hydrology Research* **41** (5): 378–390 DOI: 10.2166/nh.2010.036

Sheldon AL, Meffe GK. 1995. Short-term recolonization by fishes of experimentally defaunated pools of a coastal plain. *Copeia* **1995** (4): 828–837

Sheridan GJ, Lane PNJ, Noske PJ. 2007. Quantification of hillslope runoff and erosion processes before and after wildfire in a wet Eucalyptus forest. *Journal of Hydrology* **343** (1–2): 12–28 DOI: 10.1016/j.jhydrol.2007.06.005

Slaymaker O. 1988. The distinctive attributes of debris torrents. *Hydrological Sciences Journal* **33** (6): 567–573 DOI: 10.1080/02626668809491290

Sloat MR, Fraser DJ, Dunham JB, Falke JA, Jordan CE, McMillan JR, Ohms HA. 2014. Ecological and evolutionary patterns of freshwater maturation in Pacific and Atlantic salmonines. *Reviews in Fish Biology and Fisheries* **24** (3): 689–707 DOI: 10.1007/s11160-014-9344-z

Soulis KX. 2018. Estimation of SCS Curve Number variation following forest fires. *Hydrological Sciences Journal* **63** (9): 1332–1346 DOI: 10.1080/02626667.2018.1501482

Springer EP, Hawkins RH. 2005. Curve number and peakflow responses following the Cerro Grande fire on a small watershed. In *American Society of Civil Engineers Watershed Management 2005 Symposium*Williamsburg, VA; 12. Available at: https://permalink.lanl.gov/object/tr?what=info:lanl-repo/lareport/LA-UR-05-0552

Srivastava A, Brooks ES, Dobre M, Elliot WJ, Wu JQ, Flanagan DC, Gravelle JA, Link TE. 2020. Modeling forest management effects on water and sediment yield from nested, paired watersheds in the interior Pacific Northwest, USA using WEPP. *Science of The Total Environment* **701** DOI: 10.1016/j.scitotenv.2019.134877

Srivastava A, Wu JQ, Elliot WJ, Brooks ES, Flanagan DC. 2017. Modeling streamflow in a snow-dominated forest watershed using the water erosion prediction project (WEPP) model. *Transactions of the ASABE* **60** (4): 1171–1187 DOI: 10.13031/trans.12035

Staley DM, Gartner JE, Kean JW. 2015. Objective definition of rainfall intensity-duration thresholds for post-fire flash floods and debris flows in the area burned by the Waldo Canyon Fire, Colorado, USA. In *Engineering Geology for Society and Territory - Volume 2*Springer International Publishing: New York, NY; 621–624.

Staley DM, Negri JA, Kean JW, Laber JL, Tillery AC, Youberg AM. 2016. Updated logistic regression equations for the calculation of post-fire debris-flow likelihood in the Western United States. US Department of the Interior, US Geological Survey, Reston, VA. DOI: 10.3133/ofr20161106

Staley DM, Tillery AC, Kean JW, McGuire LA, Pauling HE, Rengers FK, Smith JB. 2018. Estimating post-fire debris-flow hazards prior to wildfire using a statistical analysis of historical distributions of fire severity from remote sensing data. *International Journal of Wildland Fire* **27** (9): 595–608 DOI: 10.1071/WF17122

Stoof CR, Vervoort RW, Iwema J, van den Elsen E, Ferreira AJD, Ritsema CJ. 2012. Hydrological response of a small catchment burned by experimental fire. *Hydrology and Earth System Sciences* **16** (2): 267–285 DOI: 10.5194/hess-16-267-2012

Story M, Johnson S, Stuart B, Hickenbottom J, Thatcher R, Swartz S. 2006. BAER specialist report: hydrology and roads, Derby Fire. US Department of Agriculture, Forest Service, Northern Region, Gallatin National Forest, Bozeman, MT.

Tedela NH, McCutcheon SC, Rasmussen TC, Hawkins RH, Swank WT, Campbell JL, Adams MB, Jackson CR, Tollner EW. 2012. Runoff Curve Numbers for 10 small forested watersheds in the mountains of the Eastern United States. *Journal of Hydrologic Engineering* **17** (11): 1188–1198 DOI: 10.1061/(ASCE)HE.1943-5584.0000436

Thomas MA, Rengers FK, Kean JW, McGuire LA, Staley DM, Barnhart KR, Ebel BA. 2021. Postwildfire Soil-Hydraulic Recovery and the Persistence of Debris Flow Hazards. *Journal of Geophysical Research: Earth Surface* **126** (6): 1–25 DOI: 10.1029/2021JF006091

Thorpe JE. 1994. Performance thresholds and life-history flexibility in salmonids. *Conservation Biology* **8** (3): 877–879 DOI: 10.1046/j.1523-1739.1994.08030863-8.x

TU. 2015. 2015 Coldwater Conservation Fund Summary of Funded Projects. Trout Unlimited, Coldwater Conservation Fund, Arlington, VA. Available at: https://www.tu.org/wp-content/uploads/2020/05/CCF-Projects-2015.pdf [Accessed 20 July 2020]

TU. 2016. 2016 Coldwater Conservation Fund Summary of Funded Projects. Trout Unlimited, Coldwater Conservation Fund, Arlington, VA. Available at: https://www.tu.org/wp-content/uploads/2020/05/CCF-Projects-2016.pdf [Accessed 20 July 2020]

TU. 2017. 2017 Coldwater Conservation Fund Summary of Funded Projects. Trout Unlimited, Coldwater Conservation Fund, Arlington, VA. Available at: https://www.tu.org/wp-content/uploads/2020/05/CCF-Projects-2017.pdf [Accessed 20 July 2020]

TU. 2018. 2018 Coldwater Conservation Fund Summary of Funded Projects. Trout Unlimited, Coldwater Conservation Fund, Arlington, VA. Available at: https://www.tu.org/wp-content/uploads/2020/05/CCF-Projects-2018.pdf [Accessed 20 July 2020]

TU. 2019. 2019 Coldwater Conservation Fund Summary of Funded Projects. Trout Unlimited, Coldwater Conservation Fund, Arlington, VA. Available at: https://www.tu.org/wp-content/uploads/2020/05/CCF-Proposals-2019.pdf [Accessed 20 July 2020]

TU. 2020. Trout Unlimited Strategic Plan: 2015-2020. Trout Unlimited, Arlington, VA. Available at: https://doi.org/10.1016/j.solener.2019.02.027%0Ahttps://www.golder.com/insights/block-caving-a-viable-alternative/%0A???

Tucker CJ. 1979. Red and photographic infrared linear combinations for monitoring vegetation. *Remote Sensing of Environment* **8**: 127–150

Turnipseed DP, Sauer VB. 2010. Discharge measurements at gaging stations. In *U.S. Geological Survey Techniques and Methods Book 3, Chapter A8*US Department of the Interior, US Geological Survey: Reston, VA; 87. Available at: https://pubs.usgs.gov/tm/tm3-a8/tm3a8.pdf

USDA-NRCS. 1986. Urban Hydrology for Small Watersheds. US Department of Agriculture, Natural Resources Conservation Service, Washington DC. Available at: http://scholar.google.com/scholar?hl=en&btnG=Search&q=intitle:Urban+Hydrology+for+Small+watersheds#1

USDA-NRCS. 1989. Runoff Curve Number Computation. US Department of Agriculture, Natural Resources Conservation Service, Washington, DC. Available at: https://www.wcc.nrcs.usda.gov/ftpref/wntsc/H&H/training/runoff-curve-numbers1.pdf

USDA-NRCS. 1991. National Engineering Field Handbook. Chapter 2: Hydrology. US Department of Agriculture, Natural Resources Conservation Service, Washington, DC.

USDA-NRCS. 1995. WEPP User Summary: USDA-Water Erosion Prediction Project. US Department of Agriculture, Agricultural Research Service, National Soil Erosion Research Laboratory, West Lafayette, IN.

USDA-NRCS. 2016. Hydrologic analyses of post-wldfire conditions. US Department of Agriculture, Natural Resources Conservation Service, Washington, DC.

USDA-NRCS. 2020. Web Soil Survey online web application. US Department of Agriculture, Natural Resources Conservation Service, Washington, DC. Available at: http://websoilsurvey.sc.egov.usda.gov/

USFS. 1997. *Lookout Fire: Burned Area Report*. US Department of Agriculture, Forest Service, Southwestern Region, Gila National Forest: Silver City, NM.

USFS. 2016. Bitterroot-Lolo VMap: Version 16. US Department of Agriculture, Forest Service, Northern Region, Engineering, Geospatial Group, Missoula, MT. Available at: https://www.fs.usda.gov/detailfull/r1/landmanagement/gis/?cid=stelprdb5331054&width=full

USFS. 2017a. Lolo Peak Fire: Burned Area Report. US Department of Agriculture, Forest Service, Northern Region, Lolo National Forest, Missoula, MT.

USFS. 2017b. *Highway 200/Moose Peak Fire: Burned Area Report*. US Department of Agriculture, Forest Service, Northern Region, Lolo National Forest: Missoula, MT.

USFS. 2017c. *Liberty Fire: Burned Area Report*. US Department of Agriculture, Forest Service, Northern Region, Lolo National Forest: MIssoula, MT.

USFS. 2017d. Sunrise Fire: Burned Area Report. US Department of Agriculture, Forest Service, Northern Region, Lolo National Forest, Missoula, MT.

USFS. 2018a. Burned Area Emergency Response - Interim Directive FSM 2500. US Department of Agriculture, Forest Service, Washington, DC. Available at: https://www.fs.fed.us/naturalresources/watershed/pubs/wo_id_2520-2018-1.docx

USFS. 2018b. Rice Ridge Fire: Burned Area Report. US Department of Agriculture, Forest Service, Northern Region, Lolo National Forest, Missoula, MT.

USGS. 2016a. Montana StreamStats online application. US Department of the Interior, US Geological Survey, Reston, VA. Available at: https://streamstats.usgs.gov/ss/

USGS. 2016b. The StreamStats program Available at: http://streamstats.usgs.gov [Accessed 11 January 2018]

VanDine DF. 1985. Debris flows and debris torrents in the Southern Canadian cordillera. *Canadian Geotechnical Journal* **22**: 44–68

Wagenbrenner JW, MacDonald LH, Coats RN, Robichaud PR, Brown RE. 2015. Effects of post-fire salvage logging and a skid trail treatment on ground cover, soils, and sediment production in the interior western United States. *Forest Ecology and Management* **335**: 176–193 DOI: 10.1016/j.foreco.2014.09.016

Walters D, DeWire D, Krenzelok J, Herbine L. 2019. Rice Ridge 2019 Debris Flows. US Department of Agriculture, Forest Service, Northern Region, Lolo National Forest, Missoula, MT.

Wang L, Wu JQ, Elliot WJ, Dun S, Lapin S, Fiedler FR, Flanagan DC. 2010. Implementation of channel-routing routines in the Water Erosion Prediction Project (WEPP) model. In *Proceedings of the 2009 SIAM Conference on "Mathematics for Industry"*Society for Industrial and Applied Mathematics: Philadelphia, PA; 120–127. DOI: 10.1137/1.9781611973303.14

Westerling AL, Hidalgo HG, Cayan DR, Swetnam TW. 2006. Warming and earlier spring increase Western U.S. forest wildfire activity. *Science* **313** (5789): 940–943 DOI: 10.1126/science.1128834

Wilcox AC, Wohl EE. 2007. Field measurements of three-dimensional hydraulics in a step-pool channel. *Geomorphology* **83**: 215–231 DOI: 10.1016/j.geomorph.2006.02.017

Willson MF. 1997. *Variation in salmonid life histories: patterns and perspectives*. US Department of Agriculture, Forest Service, Pacific Northwest Research Station: Portland, OR.

Appendix A: Tables Figures, cont'd

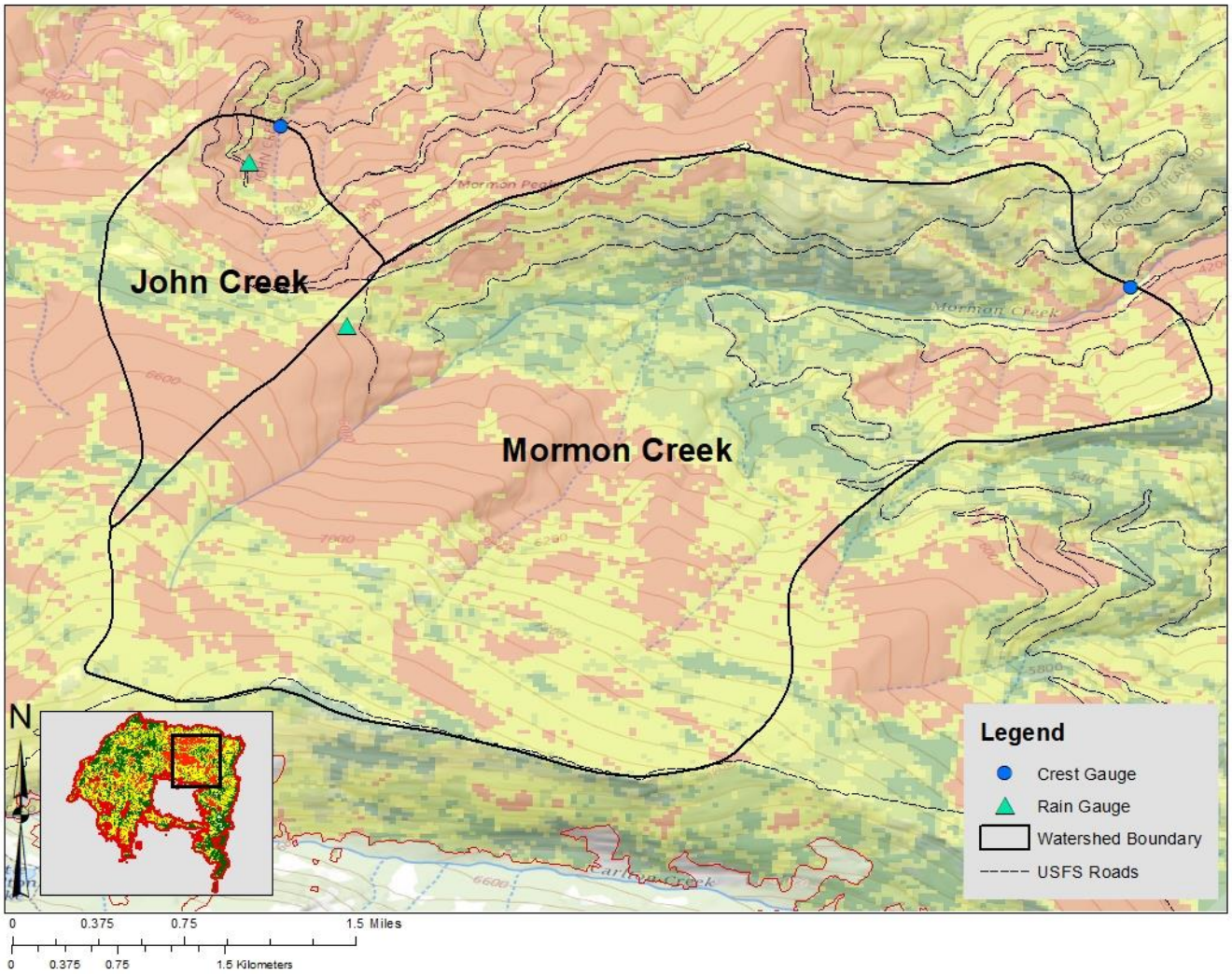

Figure A1: Study watersheds at the Lolo Peak Fire. Mormon Creek was instrumented, and flow data was recorded by managers at the Lolo National Forest.

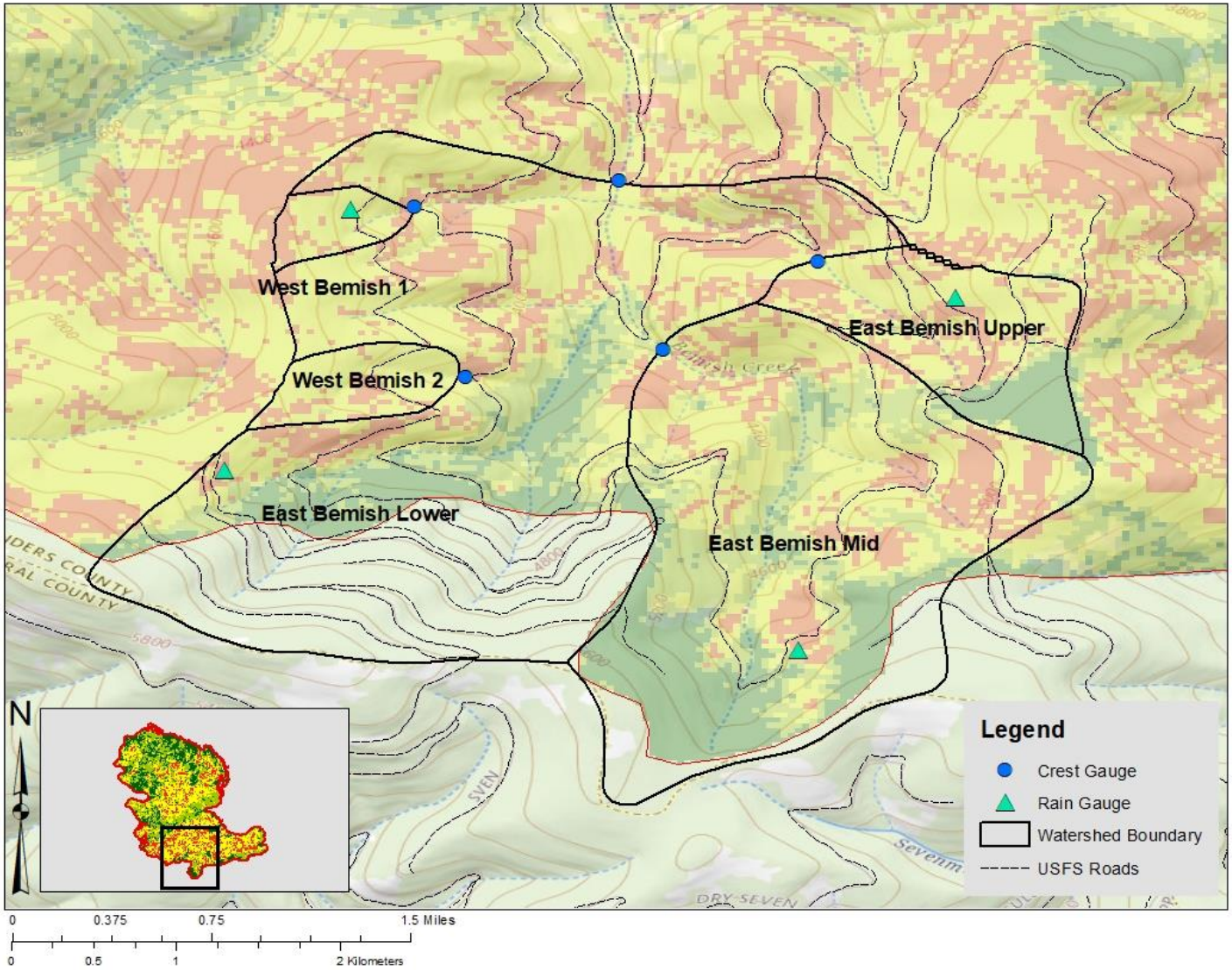

Figure A2: Study watersheds at the Sheep Gap Fire. Note that East Bemish Mid, East Bemish Upper, West Bemish 1, and West Bemish 2 are nested within the East Bemish Lower watershed.

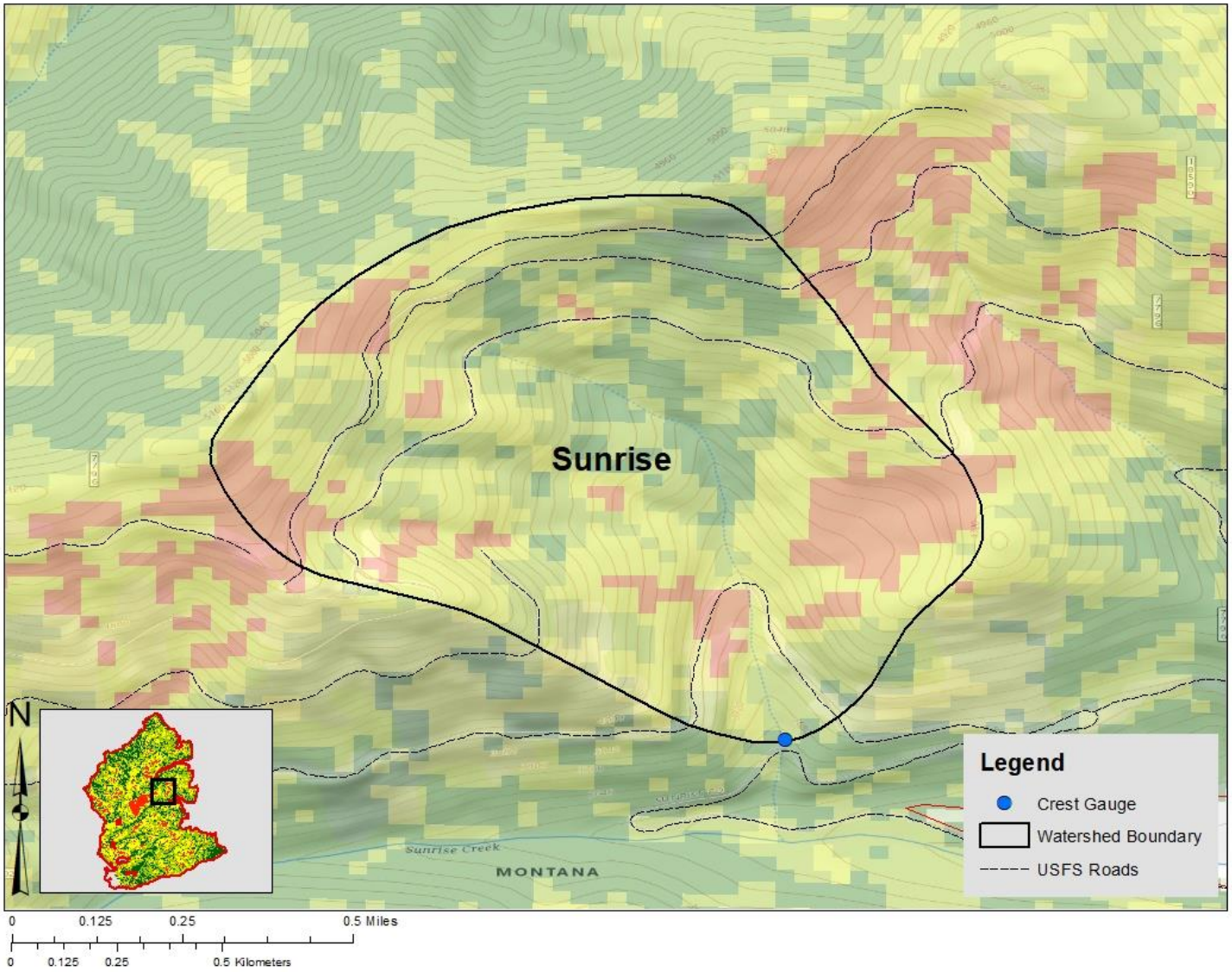

Figure A3: Study watersheds at the Sunrise Fire.

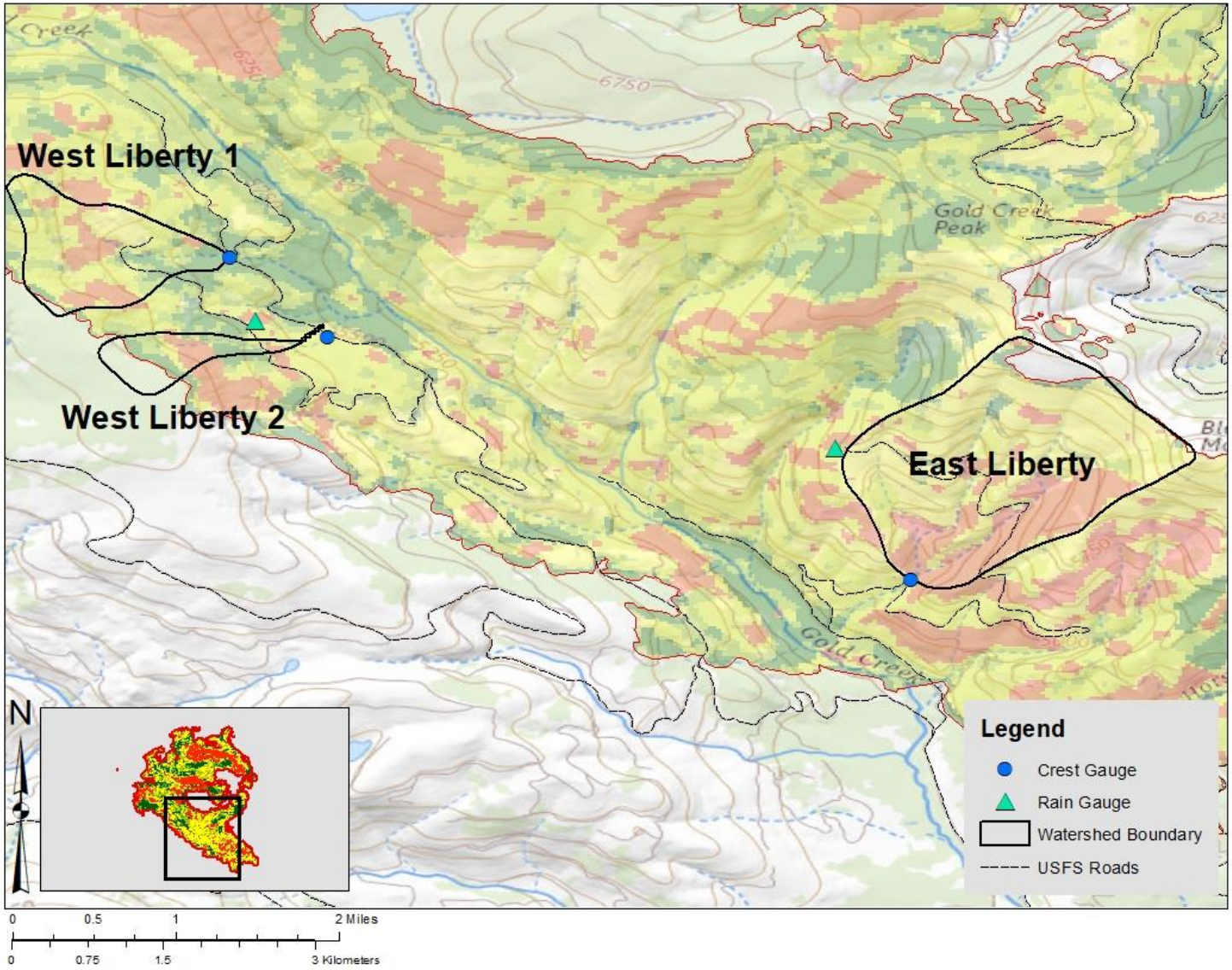

Figure A4: Study watersheds at the Liberty Fire.

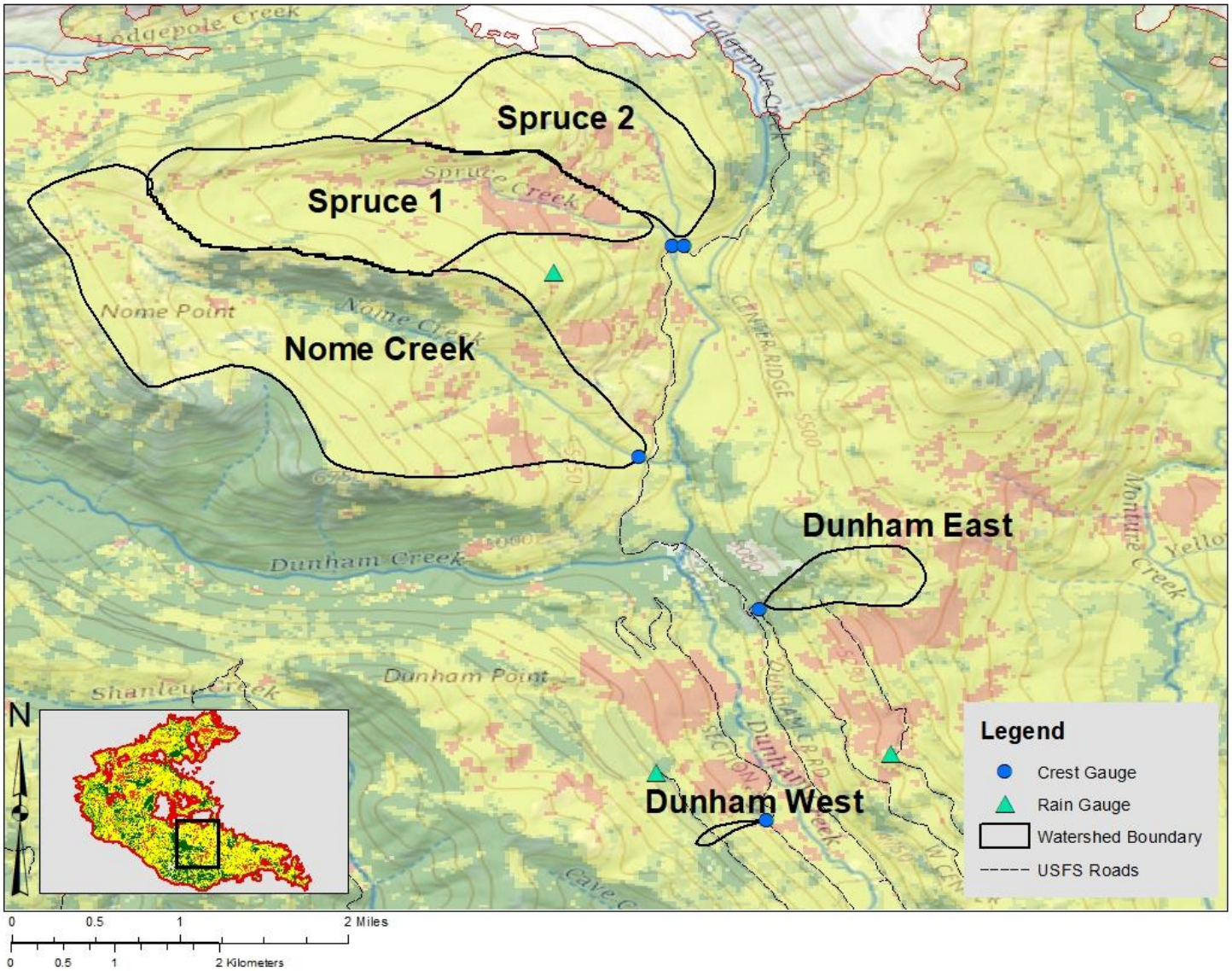

Figure A5: Study watersheds at the Rice Ridge Fire – Dunham Creek.

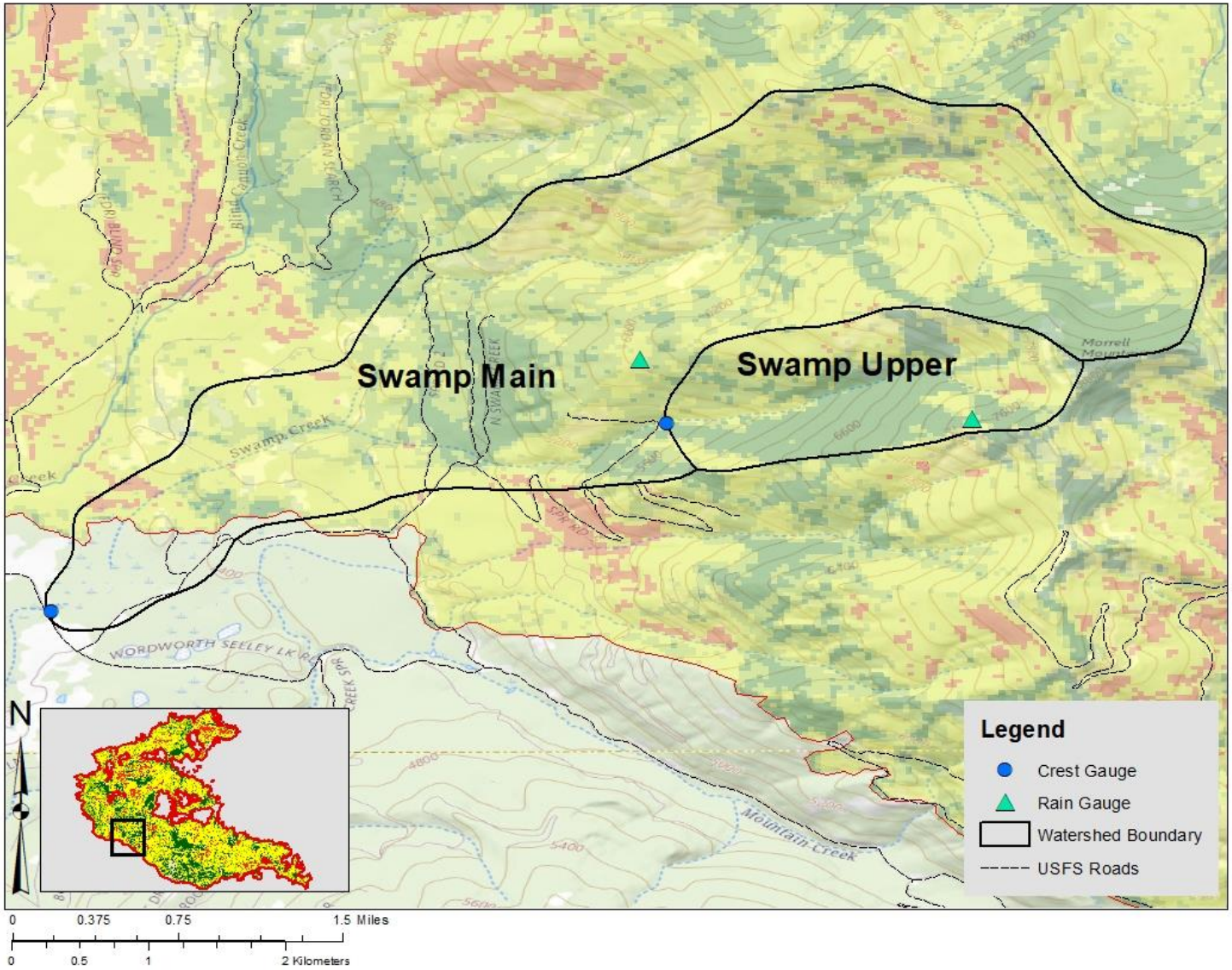

Figure A6: Study watershed at the Rice Ridge Fire – Swamp Creek.

Table A1: 6-hr and 24-hr precipitation return intervals, from (Miller *et al.*, 1973).

		24-hr		6-hr	
Fire	Return Period	in	mm	in	mm
Rice Ridge	2-year	1.9	48	1	25
	5-year	2.2	56	1.3	33
	10-year	2.7	69	1.5	38
	25-year	3	76	1.6	41
	50-year	3.4	86	1.9	48
	100-year	3.8	97	2.1	53
Lolo Peak	2-year	1.7	43	0.8	20
	5-year	1.8	46	1.1	28
	10-year	2.2	56	1.3	33
	25-year	2.6	66	1.5	38
	50-year	3	76	1.6	41
	100-year	3.4	86	2	51
Sheep Gap	2-year	1.4	36	0.9	23
	5-year	1.7	43	1.1	28
	10-year	2	51	1.3	33
	25-year	2.6	66	1.7	43
	50-year	2.8	71	1.8	46
	100-year	3.2	81	2.1	53
Liberty	2-year	1.9	48	1.2	30
	5-year	2.4	61	1.5	38
	10-year	2.8	71	1.8	46
	25-year	3.2	81	2.1	53
	50-year	3.6	91	2.4	61
	100-year	4	102	2.6	66
Sunrise	2-year	2.2	56	1.1	28
	5-year	2.6	66	1.3	33
	10-year	3	76	1.5	38
	25-year	3.6	91	1.8	46
	50-year	3.9	99	2	51
	100-year	4.3	109	2.2	56

Table A2: Short duration rainfall intensity return intervals. These were calculated using the values in Table A1 and methods from Miller et al. (1973) and Arkell & Richards (1986).

	Lolo Peak Fire				Sheep Gap Fire				Rice Ridge Fire				Liberty Fire			
Return	10 min		30 min		10 min		30 min		10 min		30 min		10 min		30 min	
Interval	in/hr	mm/hr	in/hr	mm/hr	in/hr	mm/hr	in/hr	mm/hr	in/hr	mm/hr	in/hr	mm/hr	in/hr	mm/hr	in/hr	mm/hr
2 year	1.5	39	0.7	19	1.6	41	0.8	20	1.6	39	0.8	19	2.2	55	1.1	27
5 year	1.7	43	0.8	21	2.6	65	1.3	32	2.4	61	1.2	30	2.7	69	1.3	34
10 year	2.4	61	1.2	30	2.9	74	1.4	36	2.6	65	1.3	32	3.4	87	1.7	43
25 year	2.7	69	1.3	34	3.4	86	1.7	43	3.1	77	1.5	38	4.1	103	2.0	51
50 year	3.4	85	1.7	43	4.0	102	2.0	51	3.4	85	1.7	43	4.4	111	2.2	55
100 year	3.9	98	2.0	50	4.3	109	2.2	56	3.9	99	2.0	50	5.0	128	2.6	65

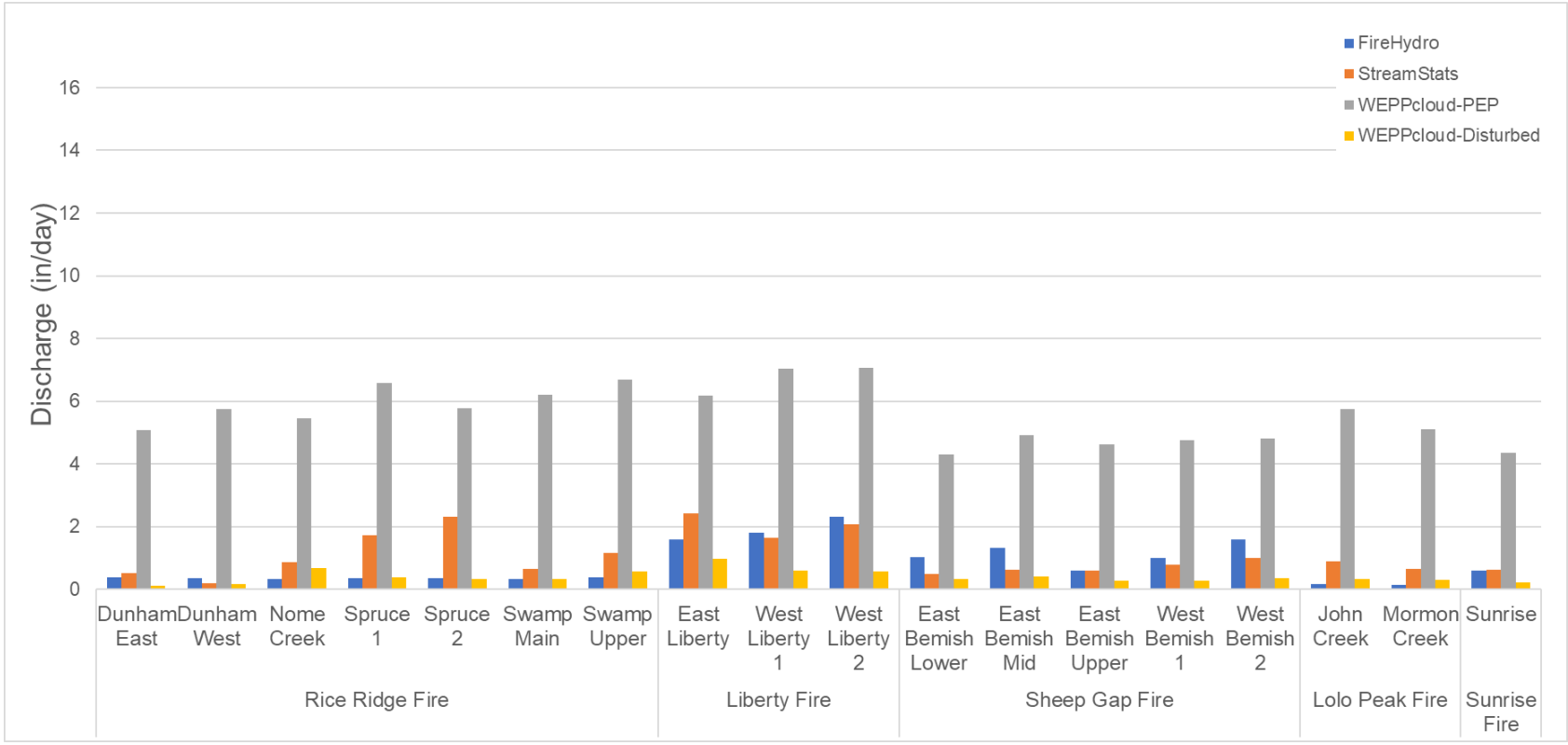

Figure A7: Pre-Fire peak flow predictions. This is the average of the 2, 5, 10, and 25-year flow prediction at each site. Values are normalized by watershed area. This uses the default (i.e. uncalibrated) WEPPcloud-Disturbed soil values.

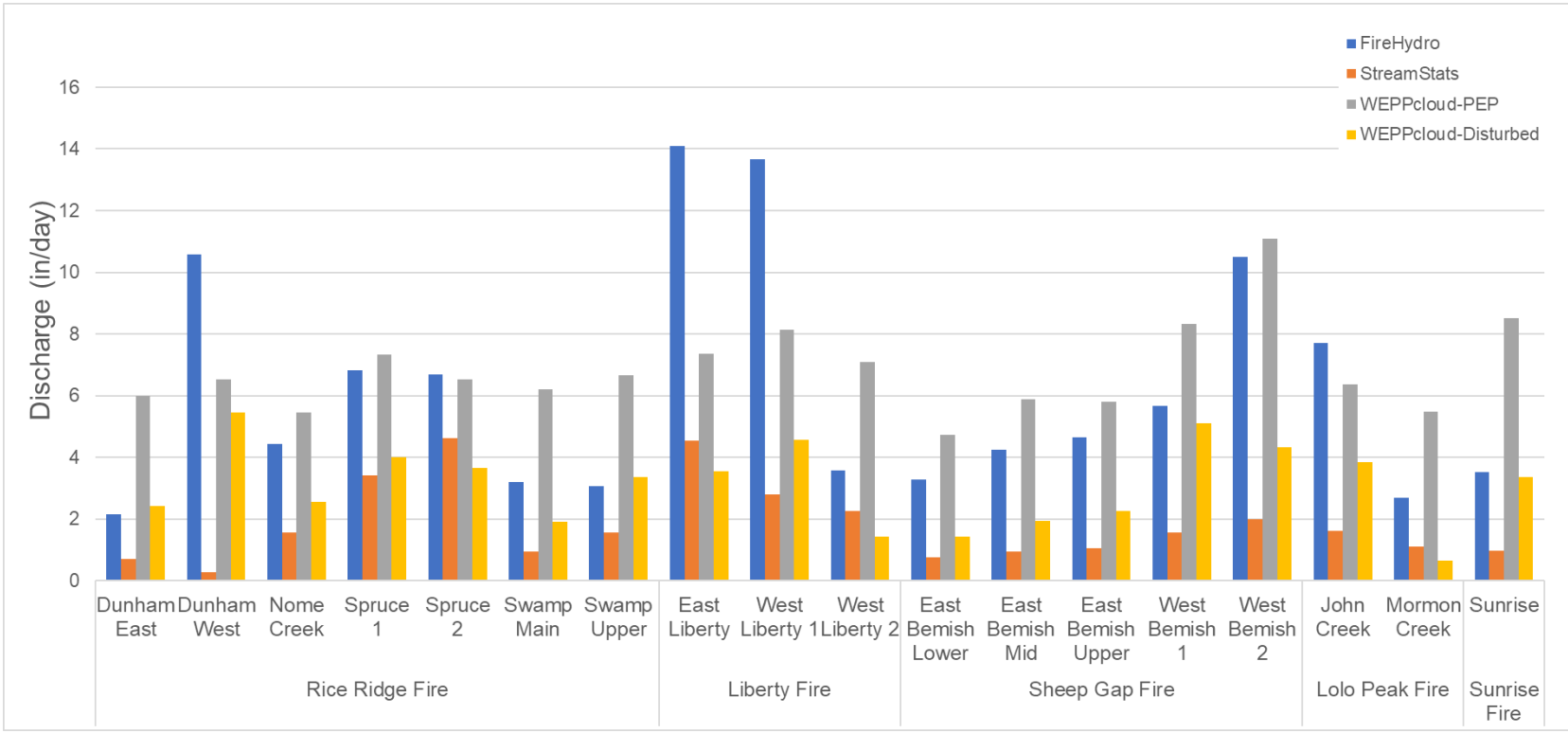

Figure A8: Post-Fire peak flow predictions. This is the average of the 2, 5, 10, and 25-year flow prediction at each site. Values are normalized by watershed area. This uses the default (i.e. uncalibrated) WEPPcloud-Disturbed soil values.

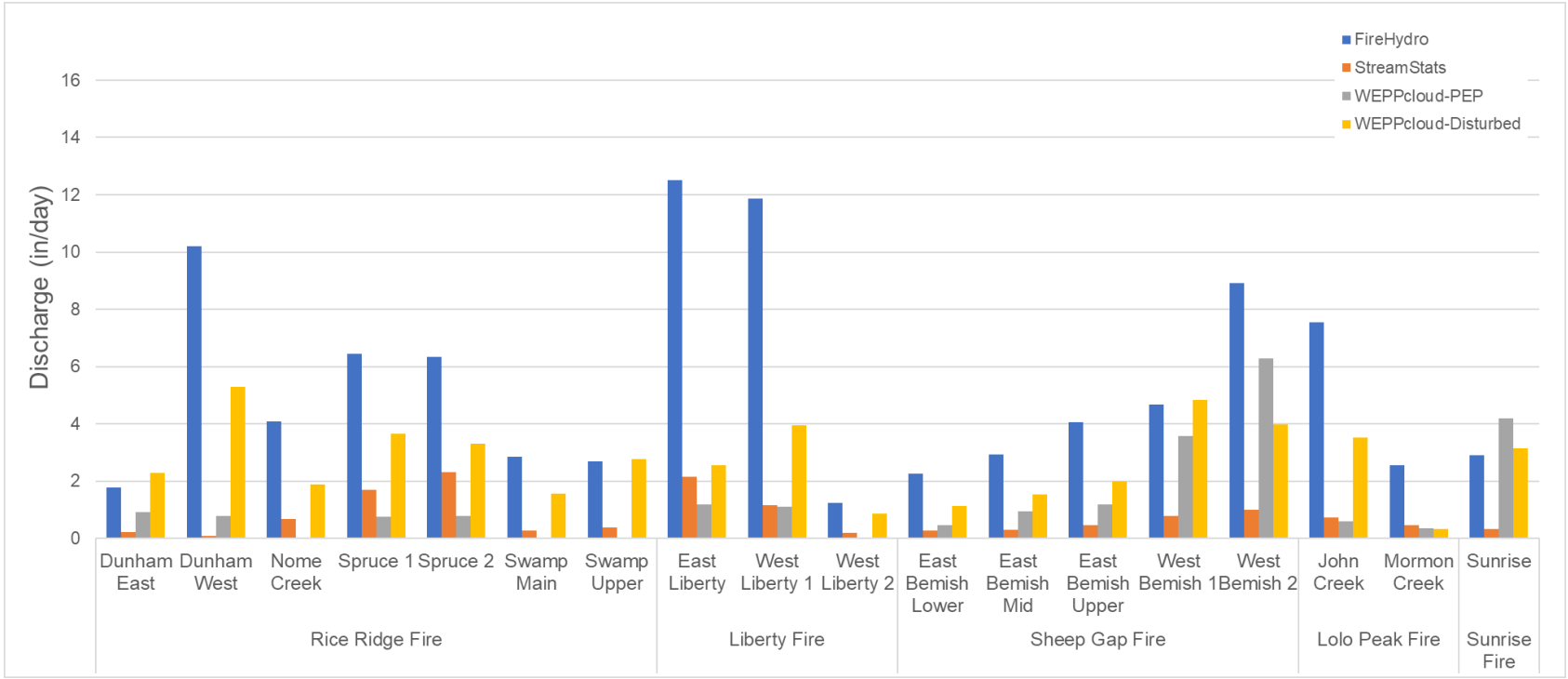

Figure A9: Average increase in peak flow predictions from pre to post-fire. This is the average of the 2, 5, 10, and 25-year flow prediction at each site. Values are normalized by watershed area. This uses the default (i.e. uncalibrated) WEPPcloud-Disturbed soil values.

Table A3: Return period Pre and Post-fire peak flow predictions for study locations at the Rice Ridge Fire. Peak flow values are normalized by watershed area. All are in units of inches/day.

Rice Ridge Fire		RCN (FireHydro)				USGS-Regression (StreamStats)				WEPPcloud-PEP				WEPPcloud-Disturbed			
Site	**Return Period (yrs)**	**Pre**	**Post**	**Increase**	**Avg. Increase**	**Pre**	**Post**	**Increase**	**Avg. Increase**	**Pre**	**Post**	**Increase**	**Avg. Increase**	**Pre**	**Post**	**Increase**	**Avg. Increase**
Spruce 2	2	0.1	3.5	3.5	6.3	0.6	1.3	0.6	2.3	4.5	4.7	0.2	0.8	0.2	2.8	2.6	3.3
	5	0.2	5.2	5.0		1.5	3.0	1.5		5.5	6.1	0.5		0.3	3.4	3.1	
	10	0.4	8.0	7.6		2.4	4.9	2.4		6.1	6.7	0.6		0.3	3.9	3.5	
	25	0.7	9.9	9.2		4.7	9.4	4.7		6.9	8.7	1.8		0.4	4.4	4.0	
Spruce 1	2	0.1	3.6	3.6	6.4	0.6	1.3	0.6	1.7	4.8	4.9	0.1	0.7	0.3	3.1	2.8	3.6
	5	0.2	5.3	5.1		1.2	2.4	1.2		6.2	6.2	0.0		0.4	3.8	3.5	
	10	0.4	8.2	7.8		1.9	3.7	1.8		6.7	7.8	1.0		0.4	4.2	3.8	
	25	0.8	10.1	9.4		3.2	6.3	3.1		8.6	10.4	1.9		0.4	4.9	4.5	
Nome Creek	2	0.1	2.1	2.0	4.1	0.5	0.8	0.4	0.7	4.3	4.3	0.0	0.0	0.5	2.0	1.5	1.9
	5	0.2	3.2	3.1		0.7	1.3	0.6		5.1	5.1	-0.1		0.6	2.5	1.8	
	10	0.4	5.5	5.1		1.0	1.8	0.8		5.7	5.7	0.0		0.7	2.8	2.1	
	25	0.7	6.9	6.2		1.3	2.3	1.0		6.7	6.7	0.0		0.8	3.0	2.1	
Dunham East	2	0.0	0.4	0.4	1.8	0.2	0.2	0.1	0.2	3.8	4.0	0.2	0.9	0.1	1.4	1.3	2.3
	5	0.2	0.9	0.6		0.4	0.5	0.2		4.8	5.2	0.3		0.1	2.0	1.9	
	10	0.4	2.8	2.4		0.6	0.8	0.2		5.5	5.9	0.3		0.1	2.7	2.6	
	25	0.9	4.5	3.7		0.9	1.2	0.4		6.2	8.9	2.8		0.2	3.5	3.4	
Dunham West	2	0.1	6.0	5.9	10.2	0.1	0.1	0.0	0.1	3.9	4.0	0.2	0.8	0.1	3.1	3.0	5.3
	5	0.1	7.9	7.9		0.1	0.2	0.1		4.8	5.8	1.1		0.1	5.0	4.9	
	10	0.7	12.6	11.9		0.2	0.3	0.1		6.2	7.1	0.9		0.2	6.2	6.0	
	25	0.7	15.9	15.2		0.3	0.5	0.2		8.2	9.1	0.9		0.2	7.5	7.3	
Swamp Upper	2	0.1	0.8	0.7	2.7	0.6	0.8	0.2	0.4	5.4	5.4	0.0	0.0	0.5	2.6	2.1	2.8
	5	0.2	1.8	1.6		1.0	1.3	0.3		6.3	6.2	0.0		0.6	3.2	2.7	
	10	0.5	4.0	3.6		1.3	1.8	0.4		6.9	6.9	0.1		0.6	3.5	2.9	
	25	0.9	5.7	4.9		1.7	2.3	0.6		8.1	8.0	-0.1		0.6	4.1	3.5	
Swamp Main	2	0.1	1.3	1.2	2.9	0.4	0.5	0.2	0.3	4.5	4.5	0.0	0.0	0.3	1.6	1.3	1.6
	5	0.2	2.2	2.0		0.6	0.8	0.2		5.6	5.6	0.0		0.3	1.8	1.5	
	10	0.4	4.0	3.6		0.8	1.1	0.3		7.0	7.0	0.0		0.3	1.9	1.6	
	25	0.7	5.3	4.6		1.0	1.4	0.4		7.7	7.7	-0.1		0.4	2.3	1.9	

Table A4: Return period Pre and Post-fire peak flow predictions for study locations at the Liberty Fire. Peak flow values are normalized by watershed area. All are in units of inches/day.

Liberty Fire		RCN (FireHydro)				USGS-Regression (StreamStats)				WEPPcloud-PEP				WEPPcloud-Disturbed			
Site	**Return Period (yrs)**	**Pre**	**Post**	**Increase**	**Avg. Increase**	**Pre**	**Post**	**Increase**	**Avg. Increase**	**Pre**	**Post**	**Increase**	**Avg. Increase**	**Pre**	**Post**	**Increase**	**Avg. Increase**
East Liberty	2	0.3	7.2	6.9	12.5	1.3	2.4	1.1	2.1	4.9	4.9	0.0	1.2	0.7	2.7	2.0	2.6
	5	0.9	12.0	11.1		2.1	3.9	1.8		5.7	5.8	0.1		0.9	3.3	2.4	
	10	1.8	16.3	14.5		2.8	5.2	2.5		6.3	6.8	0.5		1.0	3.8	2.8	
	25	3.4	20.9	17.5		3.5	6.6	3.1		7.9	11.9	4.1		1.3	4.4	3.1	
West Liberty 1	2	0.3	6.7	6.3	11.9	0.9	1.6	0.6	1.2	5.5	5.6	0.1	1.1	0.5	3.7	3.1	4.0
	5	1.0	11.5	10.5		1.4	2.4	1.0		6.8	7.2	0.3		0.6	4.3	3.7	
	10	2.0	15.9	13.9		1.9	3.2	1.3		7.4	8.2	0.8		0.6	4.6	4.0	
	25	3.9	20.6	16.7		2.4	4.0	1.6		8.4	11.6	3.2		0.6	5.6	5.0	
West Liberty 2	2	0.5	0.7	0.2	1.2	1.1	1.2	0.1	0.2	5.5	5.4	0.0	0.0	0.5	0.9	0.4	0.9
	5	1.2	1.9	0.7		1.8	1.9	0.2		6.5	6.5	0.0		0.6	1.2	0.7	
	10	2.6	4.3	1.7		2.4	2.6	0.2		7.4	7.5	0.1		0.6	1.5	0.9	
	25	5.0	7.4	2.4		3.0	3.3	0.3		8.9	8.9	0.0		0.6	2.0	1.4	

Table A5: Return period Pre and Post-fire peak flow predictions for study locations at the Sheep Gap Fire. Peak flow values are normalized by watershed area. All are in units of inches/day.

Sheep Gap Fire		RCN (FireHydro)				USGS-Regression (StreamStats)				WEPPcloud-PEP				WEPPcloud-Disturbed			
Site	**Return Period (yrs)**	**Pre**	**Post**	**Increase**	**Avg. Increase**	**Pre**	**Post**	**Increase**	**Avg. Increase**	**Pre**	**Post**	**Increase**	**Avg. Increase**	**Pre**	**Post**	**Increase**	**Avg. Increase**
East Bemish Lower	2	0.1	0.8	0.6	2.3	0.3	0.4	0.1	0.3	3.2	3.3	0.0	0.5	0.3	1.2	0.9	1.1
	5	0.4	1.9	1.5		0.4	0.6	0.2		4.1	4.2	0.1		0.3	1.4	1.1	
	10	0.8	3.4	2.6		0.6	0.9	0.3		4.7	5.0	0.2		0.3	1.5	1.2	
	25	2.8	7.1	4.3		0.7	1.1	0.4		5.1	6.5	1.4		0.4	1.6	1.3	
East Bemish Mid	2	0.2	1.0	0.8	2.9	0.3	0.5	0.1	0.3	3.7	3.8	0.1	1.0	0.3	1.6	1.3	1.5
	5	0.5	2.4	1.9		0.5	0.8	0.3		4.5	5.0	0.5		0.4	1.9	1.5	
	10	1.0	4.4	3.4		0.7	1.1	0.4		5.1	5.7	0.6		0.4	2.0	1.6	
	25	3.6	9.2	5.6		1.0	1.4	0.5		6.4	9.0	2.6		0.5	2.3	1.8	
East Bemish Upper	2	0.1	1.0	0.8	4.0	0.2	0.4	0.2	0.5	3.5	3.6	0.1	1.2	0.2	1.8	1.6	2.0
	5	0.1	2.5	2.4		0.5	0.8	0.4		4.4	4.6	0.2		0.3	2.2	1.9	
	10	0.5	4.8	4.3		0.7	1.2	0.5		4.8	5.6	0.8		0.3	2.5	2.2	
	25	1.7	10.4	8.7		1.0	1.7	0.8		5.7	9.3	3.6		0.3	2.6	2.3	
West Bemish 1	2	0.1	1.1	1.1	4.7	0.3	0.6	0.3	0.8	3.7	3.7	0.0	3.6	0.2	3.0	2.7	4.8
	5	0.1	2.8	2.7		0.6	1.2	0.6		4.6	5.0	0.4		0.3	4.4	4.1	
	10	0.6	5.5	5.0		0.9	1.8	0.9		5.0	5.9	0.9		0.3	5.9	5.6	
	25	3.3	13.3	10.0		1.3	2.6	1.3		5.8	18.7	13.0		0.3	7.1	6.8	
West Bemish 2	2	0.4	2.5	2.1	8.9	0.4	0.8	0.4	1.0	3.7	3.8	0.0	6.3	0.3	2.9	2.6	4.0
	5	0.7	5.3	4.6		0.8	1.6	0.8		4.5	5.4	0.9		0.3	3.4	3.1	
	10	1.1	9.1	8.1		1.2	2.3	1.2		5.2	11.6	6.4		0.4	4.4	4.1	
	25	4.2	25.2	21.0		1.6	3.2	1.6		5.8	23.6	17.8		0.4	6.5	6.1	

Table A6: Return period Pre and Post-fire peak flow predictions for study locations at the Lolo Peak and Sunrise Fires. Peak flow values are normalized by watershed area. All are in units of inches/day.

Lolo Peak Fire		**RCN (FireHydro)**				**USGS-Regression (StreamStats)**				**WEPPcloud-PEP**				**WEPPcloud-Disturbed**			
Site	**Return Period (yrs)**	**Pre**	**Post**	**Increase**	**Avg. Increase**	**Pre**	**Post**	**Increase**	**Avg. Increase**	**Pre**	**Post**	**Increase**	**Avg. Increase**	**Pre**	**Post**	**Increase**	**Avg. Increase**
John Creek	2	0.0	2.6	2.6	7.5	0.4	0.8	0.4	0.7	4.3	4.4	0.1	0.6	0.3	2.9	2.6	3.5
	5	0.0	6.3	6.2		0.7	1.4	0.6		5.2	5.6	0.4		0.3	3.5	3.2	
	10	0.2	9.3	9.1		1.0	1.9	0.9		6.5	6.9	0.5		0.3	4.0	3.6	
	25	0.4	12.6	12.2		1.3	2.5	1.1		7.1	8.5	1.5		0.4	5.0	4.6	
Mormon Creek	2	0.0	0.7	0.7	2.6	0.4	0.6	0.3	0.5	3.7	3.7	0.0	0.4	0.2	0.4	0.2	0.3
	5	0.1	1.8	1.8		0.6	1.0	0.4		4.6	4.6	0.0		0.3	0.6	0.3	
	10	0.2	3.3	3.1		0.7	1.3	0.5		5.6	5.9	0.3		0.3	0.7	0.4	
	25	0.3	4.9	4.6		0.9	1.6	0.7		6.4	7.6	1.1		0.4	0.8	0.4	
Sunrise Fire																	
Sunrise	2	0.1	6.0	5.9	8.2	1.5	3.0	1.5	3.7	3.2	3.2	0.0	4.2	0.2	2.2	2.1	3.2
	5	0.5	7.6	7.0		3.0	6.0	3.0		4.0	5.0	1.0		0.2	3.0	2.8	
	10	0.5	9.7	9.2		4.3	8.7	4.3		4.5	7.2	2.8		0.2	3.6	3.4	
	25	1.6	12.4	10.8		6.0	11.9	6.0		5.7	18.6	13.0		0.3	4.7	4.4	